# SECONDARY AEROSPACE BATTERIES AND BATTERY MATERIALS

## A BIBLIOGRAPHY



JULY 1976

NATIONAL AERONAUTICS AND SPACE ADMINISTRATION

# SECONDARY AEROSPACE BATTERIES AND BATTERY MATERIALS

## A BIBLIOGRAPHY (1969–1974)

P. McDermott, G. Halpert, S. Ekpanyaskun, and P. Nche

*Prepared by Goddard Space Flight Center*

*Scientific and Technical Information Office*
NATIONAL AERONAUTICS AND SPACE ADMINISTRATION
JULY 1976
*Washington, D.C.*

For sale by the National Technical Information Service
Springfield, Virginia 22161
Price – $6.25

## CONTENTS

Page
Intentionally
Left Blank

## PREFACE

This annotated bibliography on the subject of secondary aerospace battery materials and related physical and electrochemical processes was compiled from references to journal articles published between 1969 and 1974. A total of 332 citations are arranged in chronological order under journal titles. Indices by system and component, techniques and processes, and author are included.

Page
Intentionally
Left Blank

# INTRODUCTION

This bibliography is a survey of relevant literature in the field of secondary batteries covering a period from 1969 to 1974. It follows a similar work (SP-7027) which was published in 1969 by G. Halpert and W. H. Webster of the Goddard Space Flight Center (GSFC). The first volume covered the period from 1923 to 1968.

In this volume, the same general format was adopted with the following exception. Foreign language journals are grouped in sections according to language or region with the abbreviated journal titles printed with the abstract as they appear in Chemical Abstracts. Patents and government reports are not included in this publication.

The authors of this bibliography include G. Halpert, GSFC, and P. McDermott, S. Ekpanyaskun, and P. Nche of Coppin State College, Baltimore, Maryland. The latter three authors were supported in this work by a grant from the National Aeronautics and Space Administration (NASA).

This document consists of five parts:

Part 1—Index by system and component. Includes both electrochemical system and system components; e.g., nickel-cadmium systems, nickel electrodes, and separators

Part 2—Index by techniques and processes used in the investigations; e.g., analytical, thermal, metallurgical, and kinetic

Part 3—Listing of publications. A listing of the 13 most important electrochemical journals, four general foreign categories, and dissertations in order of appearance in this bibliography

Part 4—Citations and abstracts. Journal titles are arranged in alphabetical order, with the citations and abstracts for the articles in each journal arranged under the journal title in chronological sequence. The main entry for each citation is the name of the author, which is followed by the volume number of the journal and the page number on which the cited article begins.

Part 5—Index by author

# PART I
# INDEX BY SYSTEM AND COMPONENT

Page Intentionally Left Blank

## INDEX BY SYSTEM AND COMPONENT

**Secondary Systems**

Nickel-Cadmium



Nickel-Hydrogen



Nickel-Zinc



Silver-Cadmium



Silver-Zinc



**Component**

Cadmium



Cadmium Electrode

## INDEX BY SYSTEM AND COMPONENT (Continued)

## INDEX BY SYSTEM AND COMPONENT (Continued)

Page
Intentionally
Left Blank

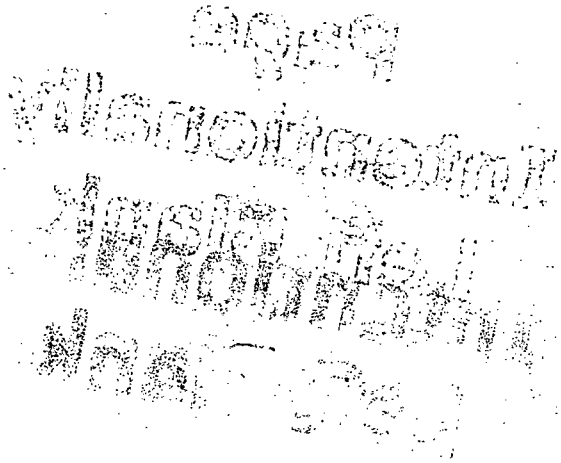

## PART II
## INDEX BY TECHNIQUES AND PROCESSES

Page Intentionally Left Blank

## INDEX BY TECHNIQUES AND PROCESSES

Page
Intentionally
Left Blank

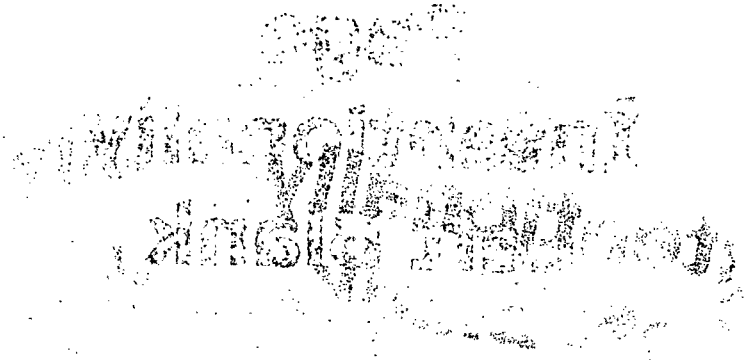

# PART III
# LISTING OF PUBLICATIONS

Page
Intentionally
Left Blank

## LISTING OF PUBLICATIONS

Page
Intentionally
Left Blank

# PART IV
# CITATIONS AND ABSTRACTS

Page Intentionally Left Blank

100. **Gillibrand, M. I., Langrish, L., and Lomax, G. R.** **1, 9, (1971)**

**Reaction in the Silver Zinc Cell**

An adiabatic calorimeter was used to measure the thermodynamics of the Ag-Zn cell. The charge and discharge reactions take place in two stages involving the production of argentous oxide and argentic oxide, respectively. No thermal evidence was found to suggest the existence of a higher oxide of Ag. The cell reations were: (1) $2Ag + ZnO \rightleftharpoons Ag_2O + Zn$, $\Delta H = 158.7$ kJ/F; and (2) $Ag_2O + ZnO \rightleftharpoons Ag_2O_2 + Zn$, $\Delta H = 176.1$ kJ/F. If the cell was left on open circuit for a long period, or the positive electrodes heated, reaction (2) was suppressed, and the discharge took place by reaction (1), without any reduction in capacity.

101. **Armstrong, R. D., Sperrin, A. D., Tye, F. L., and West, G. D.** **2, 265, (1972)**

**Mechanism of Discharge of Sintered Plate Cadmium Electrodes**

Sintered-plate Cd electrodes were studied in alkaline solution using potentiostatic and galvanostatic techniques. In many ways, the behavior is similar to that of a flat Cd electrode. A pseudo steady-state current is found caused by the dissolution of Cd as $Cd(OH)_4^{2-}$. At more anodic potentials, passivation occurs because of the solid-state formation of $Cd(OH)_2$. This model can account for the results obtained on galvanostatic discharge.

102. **Buder, E.** **2, 301, (1972)**

**Oxygen Evolution During Recharging of Positive Nickel Oxide Sinter Electrodes**

Oxygen evolution during anodic oxidation of positive Ni-oxide electrodes is of theoretical and practical interest for both open and sealed storage batteries. The gas volume produced on positive sinter electrodes during the charging operation was plotted as a function of time. The influence of the anodic current and/or of the electrolyte temperature on the charging efficiency is discussed. The results permit the deduction of the optimum combination of charging parameters that are characterized by minimum parasitic oxygen formation.

A small but continuous gas formation can be observed after the electrode is charged to ~50 percent capacity by using charging currents of the order of the 1-hour rate at ambient temperature. At higher temperatures, the beginning of gassing is shifted toward lower charge levels (e.g., at 40 degrees, it already begins at a charge of ~ 17%). Furthermore, the gas volume, which is evolved during charging to identical levels, increases with increasing temperatures and decreasing current density. The described phenomenon can, at least in part, be explained by the decomposition of higher Ni oxides. The decomposition rate depends on charging time, charging current, and temperature.

103. Selånger, P. 4, 249, (1974)

**Analysis of Porous Alkaline Cd-Electrodes**
**I. Anodic High Rate Transients**

Galvanostatic anodic high-rate transients in porous Cd-electrodes are analyzed. A one-dimensional electrode model is developed. The model includes effects of variation in electrolyte composition and reaction surface activity. Overpotential transients are computed and compared with experimental transients. Failure in low-porosity electrodes with great surface activity is usually caused by the blockage of pores at low rates. At high rates, the discharge depth is limited by pure mass-transfer limitations. The reaction activity group $i_0 S$ is estimated from the experimental electrodes in conjunction with the model. Transition from pore blockage to pure mass-transfer limitations occurs between 100 and 200 mA $cm^{-2}$ for a medium porosity of 0.60.

104. Selånger, P. 4, 259, (1974)

**Analysis of Porous Alkaline Cd-Electrodes**
**II. Potential Recovery Transients After a Period of Discharge**

The recovery of the diffusion potential after a period of discharge is analyzed for porous Cd-electrodes. A composite process with discharge-idle time and discharge is simulated and compared with an experimental process. The general influence of porosity on charge capacity is examined in a charge-porosity diagram.

105. Selånger, P. 4, 263, (1974)

**Analysis of Porous Alkaline Cd-Electrodes**
**III. The Application of Charge Porosity Diagrams in Electrode Design**

A simple charge-porosity diagram is presented for the rapid estimation of charge capacity in battery electrodes. Porosity changes reflect differences in mole volumes of the reactants and reaction products. Each system has a specific sensitivity to porosity changes. This diagram can be a useful tool for the assessment of mass and current transport performance of electrodes that give insoluble reaction products. Alkaline Cd, Zn, and Fe electrolytes are compared.

200. Dignam, M. J., Barrett, H. M., and Nagy, G. D. 47, 4253, (1969)

## Anodic Behavior of Silver in Alkaline Solutions

Data covering a range of pH and temperature were obtained for the anodic oxidation of electropolished silver and the results were compared with electrodes that had undergone repeated oxidation and reduction cycles. The behavior of the electrode is usually complex, showing, for example, autopotential cycling under certain galvanostatic conditions ($\sim \mu A/cm^2$, 25°C, 0.7 N Na OH), the period of oscillation being about 0.5 hour. Several other hitherto unreported phenomena were also observed. The main conclusions reached are: (1) that two different mechanisms are involved in the anodic formation of $Ag_2O$ on silver electrodes in basic electrolytes resulting in two types of film; one mechanism involves a dissolution-precipitation process, the other possibly a direct interfacial reaction; (2) that the reduction of anodically formed $Ag_2O$ films either electrochemically or in hydrogen at 800°C, and leaves behind a highly porous layer of silver metal; and (3) that the limiting $Ag_2O$ film thickness is probably determined by a diffusion process occurring within the film.

201. Barradas, R.G., and McDonnell, D.B. 48, 2453, (1970)

## Conditions for the Electrochemical Formation of $Ag_2O_3$ on Silver in Aqueous KOH Solutions

New evidence is presented to substantiate the electrochemical formation, at certain temperatures, of $Ag_2O_3$ as a reasonably stable species under galvanostatic conditions in aqueous KOH electrolytes saturated with $Ag_2O$ and $O_2$. The experimental data offer a better understanding of the nature of the $Ag_2O/AgO$ transition peak.

## ELECTROANALYTICAL CHEMISTRY AND INTERFACIAL ELECTROCHEMISTRY

300. Giles, I. D., Harrison, J. A., and Thirsk, H. R. 22, 375, (1969)

### Anodic Dissolution of Silver and Formation of $Ag_2O$ in Hydroxide Solutions Using Single Crystal Electrodes in Faradaic Impedance Study

In spite of many measurements on the oxidation of silver in an alkaline solution, the primary electrochemical processes involved are still not certain. All previous work has been done on a rather macroscope scale that was mainly concerned with layers thicker than a few monolayers. The present objectives are to study the kinetics of oxidation of silver at flat, clean, single silver crystals, and to observe the formation of the first monolayer of $Ag_2O$.

301. Diggle, J. W., and Lovrecek, B. 24, 119, (1970)

### The Deposition of Zinc from Alkaline Solutions: A Capacitance Study

Although the application of capacitance measurements to studies of metal-solution interfaces as a function of potential are numerous, they have rarely been useful in the study of metal deposition because of complications arising from faradaic reactions. Graphical methods or complex instrumentation have usually been necessary to attain adequate separation. In this work, the electrical double layer (edl) capacitance of the electrodeposited zinc substrate was determined using a galvanostatic pulse technique. Preliminary investigations were concerned with the potential dependence of the edl capacitance of the initial zinc substrate to ascertain at which potential the edl capacitance should be determined. Following this, further deposition of zinc from alkaline zincate solutions was done and the change in edl capacitance (measured in the absence of $OH^-$ and zincate) was observed with respect to deposition time.

302. Giles, I. D., and Harrison, J. A. 24, 399, (1970)

### The Double Layer Region of Single Crystal Silver in Alkaline Solutions

In general, the chemical nature of metal surfaces is important in determining the reaction mechanism and the properties of the double layer. Mercury is well known to behave as the bare metal over a wide potential range, whereas platinum shows a much narrower

region where it is not covered with either adsorbed hydrogen or oxide. Other metals have been less well characterized. In the case of silver, the mechanism of oxygen reduction and the measurement of the point of zero charge are both complicated by the surface structure, and, in practice, depend on the prehistory of the electrode. This paper attempts to show that the effects are more serious and that the available potential range of silver in alkali metal containing solutions is more limited than was previously assumed.

303. **Armstrong, R. D., and Bulman, G. M.** 25, 121, (1970)

**The Anodic Dissolution of Zinc in Alkaline Solutions**

In an earlier communication, it was shown that the passivation of zinc amalgam in alkaline solutions is attributable to the formation of an anodic phase monolayer on the electrode surface. In this work, these measurements are extended to solid zinc and are compared with previous work on the zinc electrode.

The anodic dissolution of zinc in sodium hydroxide solutions ($3 \times 10^{-2}$ –2 M) has been studied using rotating disk electrodes. The dissolution of zinc in both the active and passive branches occurs with simultaneous zinc deposition. The deposition reaction is first-order in zincate. In the active branch, the anodic Tafelslope is 42 ±10 mV per decade after diffusion effects are eliminated. Passivity is attributable to the formation of an anodic phase monolayer on the electrode surface, which has a reversible potential ~100 mV more anodic than the Zn/ZnO electrode.

304. **Giles, I. D., and Harrison, J. A.** 27, 161, (1970)

**Potentiodynamic Sweep Measurements of the Anodic Oxidation of Silver in Alkaline Solutions**

It is well established that the oxidation of silver to $Ag_2O$ in alkaline solutions when investigated by the potentiodynamic sweep method is characterized by two peaks. The more anodic peak corresponds to the formation of $Ag_2O$, but the more cathodic one has been variously assigned. The objectives of this paper are to investigate the first stages of the oxidation of Ag to $Ag_2O$ in alkaline solutions using the sweep method and to assign the peaks by comparison with the results of some recent faradaic impedance work by the authors.

305. Armstrong, R. D., and West, G. D. 30, 385, (1971)

**The Anodic Behaviour of Cadmium in Alkaline Solution**

In spite of previous studies of the cadmium electrode in alkaline solutions, there is uncertainty concerning the following two points:

(1) The nature of dissolved cadmium species and the relationship of this species to the formation of the anodic film.

(2) The character of the anodic film and the mechanism whereby it is produced.

Cadmium hydroxide is known to dissolve in alkali to some extent; in 10 M KOH, the concentration of Cd species in equilibrium with $\beta$-$Cd(OH)_2$ is $\simeq 5 \times 10^{-5}$ M. Recent effort has centered on whether this species is largely $Cd(OH)_3^-$ or $Cd(OH)_4^{2-}$. The most satisfactory work in this connection showed that $Cd(OH)_4^{2-}$ is the predominant species at alkali concentrations $> 1$ M.

306. Hampson, N. A., and Latham, R. J. 32, 337, (1971)

**The Exchange Reaction at Polycrystalline Cadmium Electrodes in Measurements in Alkaline Electrolytes**

The majority of reported investigations of the Cd electrode in alkali have been concerned with the morphological aspects of the surface film that is nucleated and grown as the anodic reaction proceeds. Published data on the charge transfer reaction are limited in spite of the rapidly growing interest in the nickel-cadmium alkaline battery. A preliminary investigation showed that the exchange reaction in alkaline solution was likely to be a fast process, possibly because of the stabilizing effect of adsorption on the species involved in the charge-transfer process. It was decided to investigate the exchange process in ultrapure alkaline electrolytes using the a.c. impedance method and the double pulse galvanostatic technique of Gerischer and Krause. For a fast reaction, the latter technique was in this case preferred rather than the single impulse technique.

307. Armstrong, R. D., and Edmondson, K. 53, 371, (1974)

### The Impedance of Cadmium in Alkaline Solution

Cadmium in alkaline solution shows some active dissolution prior to passivation. Both active and passive regions have been studied extensively using potentiostatic and galvanostatic measurements, but few impedance measurements have been made in either region. In the active region, it is known that cadmium dissolves as a hydroxide complex, and the most satisfactory work showed the predominant species to be $Cd(OH)_4^{2-}$ at concentrations > 1 M of hydroxide. In the passive region, the presence of $\beta$-$Cd(OH)_2$ in the film is well established, and there is also evidence that $\gamma$-$Cd(OH)_2$ is simultaneously present to some extent.

308. Armstrong, R. D., and Bell, M. F. 55, 201, (1974)

### The Active Dissolution of Zinc in Alkaline Solution

On anodic polarization of zinc in alkaline solutions, the current initially shows an exponential increase with increase in potential. This is the region of active dissolution or simply the "active region." In this region, it has generally been found that the system obeys a Tafel relationship with a slope of approximately 40 mV per decade, which is consistent with an overall mechanism:

$$Zn(0) \rightleftharpoons Zn(I) \quad (1)$$

$$Zn(I) \rightleftharpoons Zn(II) \quad (2)$$

It seems unlikely that the Tafel slope can be explained by specific adsorption KOH ions or slow lattice incorporation because the same slope is found in solutions of concentration between 0.05 and 3 M.

It has been shown that the solution-soluble product is the zincate ion, $Zn(OH)_4^{2-}$. However, it is impossible to decide the state of complexation of the zinc intermediates on the basis of existing electrochemical kinetic measurements. These could also be either solution-soluble or adsorbed species.

The objective of this work was to clarify this situation, using both steady-state potentiostatic techniques and a.c. impedance measurements.

400. Dirkse, T. P., and Timmer, R. 116, 162, (1969)

### The Corrosion of Zinc in KOH Solutions

The corrosion rate of zinc in KOH solutions has been measured under a variety of conditions. Amalgamation and the presence of zincate ions that lower this rate of corrosion is different for nonamalgamated zinc. This temperature effect is also different for the two types of zinc electrodes.

401. Arouete, S., Blurton, K. F., and Oswin, H. G. 116, 167, (1969)

### Controlled Current Deposition of Zinc from Alkaline Solution

Electrodeposition of zinc onto foil electrodes from alkaline zincate solutions with direct current results in dendritic or black, porous, mossy deposits. Smoother deposits are obtained with a pulsed current source or periodic reversal of current. The nature of the deposit with pulsed charging depends on the current density, the amount of charge passing through the electrolytic cell, the on time, and the off time. The optimum values of these parameters are dependent on the cell geometry, and the differences between the apparatus used in the present study and a cell containing a secondary zinc electrode are discussed.

402. Gaines, L. 116, 61C, (1969)

### Secondary Silver-Zinc Battery Technology

A review of the current status of silver-zinc battery technology is presented as part of an attempt to organize, on a fundamental basis, the varied design improvements developed as a result of empirical studies. Past efforts to improve the secondary silver-zinc system have been devoted to: (a) stabilizing the zinc electrode structure, (b) controlling zinc dendrite growth, (c) increasing the utilization of the silver electrode, (d) improving separators, and (e) developing sealed batteries. Improvements that have been suggested in these areas are often mutually exclusive and interdependent. Clarification of the fundamental processes involved is necessary for the creation of an optimum battery configuration.

403. Naybour, R. D. 116, 520, (1969)

**The Effect of Electrolyte Flow on the Morphology of Zinc Electrodeposited from Aqueous Alkaline Solution Containing Zincate Ions**

The effect of flowing electrolyte on the morphology of zinc electrodeposited from aqueous alkaline solution has been investigated. Aqueous potassium hydroxide solution of 5.8N normally containing 19.1 g/dm$^3$ of dissolved zinc oxide was circulated through a flow tube at flow velocities up to 1.7 m/s, corresponding to Reynold's numbers of up to 13,500. The morphologies of zinc electrodeposits formed on a zinc substrate in the wall of the flow tube were examined over a range of current densities and Reynold's numbers. The results showed that flowing electrolyte under both turbulent flow and laminar flow conditions greatly modified the deposit morphologies. It was possible to construct a morphology, current density, and Reynold's number "phase diagram" to describe the effects of flowing electrolyte on deposit morphology.

404. Elder, J. P., and Jost, E. M. 116, 687, (1969)

**Statistical Studies of Rechargeable Battery Systems**

The application of the $2^n$ factorial experiment to the study of the factors influencing the behavior of hermetically sealed, rechargeable Ni-Cd cells is discussed. The characteristic cell parameters may be expressed as logarithmic functions of the pertinent charge/discharge conditions. Data-fitting is accomplished by means of a linear regression analysis. Both primary and factor interaction effects contribute to the behavior of the cells. The magnitudes of the effects are dependent on the cell operating conditions. The effects resulting from a cobalt addition to the positive electrode are primarily related to the kinetics of the charge and discharge reactions.

405. Wagner, O. C. 116, 693, (1969)

**Secondary Cadmium-Air Cells**

Cadmium-air cells have been developed that deliver 45 to 50 Wh/lb at the C/5 rate of discharge. The major failure modes of the cadmium-air system are: loss of capacity by the cadmium anode, shorting by cadmium penetration, poisoning of the air cathode by a soluble cadmium species, loss of electrocatalytic activity by the air cathode during prolonged cycling, and water loss by evaporation through the cathode pores and/or cell vent.

It has been determined that loss of capacity by the cadmium anode can be prevented by the addition of $Fe_2O_3$ or $TiO_2$ extender into the active structure and by the removal of $CO_2$ from the influent air stream. It was found that cadmium penetration through the separator wrap can be avoided by preventing carbonate buildup in the electrolyte and by placing a wettable, inert interseparator between the anode and main separator. Poisoning of the air cathode by soluble cadmium can be overcome by saturating the electrolyte with zincate or aluminate ions. Deactivation of the air cathode is a problem that requires further investigation, and drying out of the cadmium-air cell can be prevented by providing the cell with an electrolyte sump.

406. **Powers, R. W., and Breiter, M. W.** 116, 719, (1969)

### The Anodic Dissolution and Passivation of Zinc in Concentrated Potassium Hydroxide Solutions

In this study, mainly two sets of experiments were carried out to obtain a better understanding of the tendency of the alkaline zinc electrode to passivate. Either photomicrographs of the electrode surface were taken *in-situ* at different potentials during an anodic voltage sweep, or the two components of the electrode impedance were measured with a small signal of superimposed 1000-Hz a.c. The course of the passivation was found to depend strongly on the convective conditions in the electrolyte near the zinc electrode. The conditions for the formation of two different types of solid films have been defined, and their effects on the current-potential curve have been determined. Type-I film is white, loose, and flocculent. It forms in the absence of convection by precipitation from a supersaturated layer of zincate near the surface. When the conditions for supersaturation are nearly removed by stirring, the formation of the type-II film can be observed. The latter is more compact and appears to form directly at the surface rather than by precipitation. Its color can range from light gray to black, depending on the potential and time of formation. The type-II film is considered to be responsible for the transition from the active to the passive state of zinc in alkaline solution.

407. **Wales, C. P.** 116, 729, (1969)

### The Microstructure of Sintered Silver Electrodes I. During Discharges at the 1-Hour Rate

Silver electrodes that had been manufactured for Ag-Zn storage batteries were cycled in 35% KOH at 25°C. The electrodes were examined by optical microscopy. The

initial $Ag_2O$ formation during a discharge at the 1-hr rate usually occurred on the surfaces of AgO clumps at many scattered areas throughout the electrode. After discharge potential fell to the $Ag_2O$/Ag plateau, Ag formation occurred on the electrode surface and then gradually spread to the interior as a discharge was continued. When a slow (20-hr) discharge rate was used, however, Ag formed at both the surface and at the interior of an electrode simultaneously.

408. Elder, J. P. 116, 757, (1964)

**The Electrochemical Behavior of Zinc in Alkaline Media**

The electrochemical behavior of horizontally disposed planar zinc in 30% (6.9M) potassium hydroxide, alone and saturated with zinc oxide at 25°C, has been investigated in a controlled manner, using both galvanostatic and potentiostatic techniques. The anodic characteristics have been interpreted in terms of a kinetically controlled process preceding a diffusion step. The cathodic behavior of oxidized zinc has been interpreted in terms of a complex two-state process, involving the formation of a bound zinc hydroxide, followed by a reduction of both the adsorbed species and the soluble zincate to zinc metal.

409. Myers, R. A., and Marchello, J. M. 116, 790, (1969)

**Capacities of Zinc-Potassium Hydroxide Interfaces**

A galvanostatic pulse current technique was employed to measure the capacitance of flat and porous zinc electrodes in 32% KOH solution at 25°C. The data were obtained by operating near the hydrogen evolution potential. The electrode capacities were used to obtain the wet surface area of the zinc-KOH interface. Some exchange currents were obtained and average pore cross sections were calculated for porous zinc electrodes.

410. Alkire, R. C., Grens, E. A. II, and Tobias, C. W. 116, 809, (1969)

**Preparation of Uniform Pore Structures for Porous Electrode Studies**

In many experimental studies using porous materials, it is desirable to have highly regular pore structures where the local porosity and specific surface area are determinable to a much greater accuracy than would be possible with random pore configurations. In

these cases, knowledge of the pore geometry reduces the number of unknown parameters of the system, thereby permitting a more quantitative assessment of experimental results.

In connection with studies of anodic dissolution of porous metal electrodes, a technique has been developed for fabrication of porous structures possessing highly uniform porosity and having individual pores of nearly identical and uniform size and shape. These structures are formed from fine wires sintered in parallel close-packed configuration.

In principle, the method may be used to fabricate porous bodies from any material which may be sintered and which is available in wire form. A bundle of straight wires is assembled so that the wires lie in a hexagonal close-packed array. The bundle is then sintered under appropropriate conditions of temperature and duration. The resulting mass has parallel individual pores passing through it which correspond to the original void spaces between wires.

411. **Pizzini, S., Morlotti, R., and Wagner, V.** 116, 915, (1969)

### Study of the Lithium Oxide-Nickel Oxide System I. Thermodynamics of Dilute Solid Solutions

Emf measurements on suitable solid galvanic cells have been carried out to investigate the thermodynamics of solid solutions of $Li_2O$ in NiO. It was shown that in the range of the dilute solutions [0.15-7% (atomic percent) Li] $\alpha - Li_2SO_4$ is useful as an intermediate electrolyte. The following cell was operated:

$$Pt/NiO,Li_2O(\chi_2)//\alpha - Li_2SO_4//NiO,Li_2O(\chi_1)/Pt$$

at temperatures between 570 and 800°C. Results show that the mixture is ideal to 1.5% Li. Deviations from ideality at higher concentrations can be described with purely configurational energy terms.

412. **Tvarusko, A.** 116, 1070, (1969)

### The Decomposition of AgO in Alkaline Solutions

The gassing rate, $r$, of powder AgO samples, made by the chemical oxidation of $AgNO_3$, was measured in gassing pipettes. The mean $r$ of 52 AgO samples at 200 hr (AgO content $\geqslant 95\%$, $r_{200} \leqslant 35\mu l/day/g$) was 23.0 $\mu l/day/g$. Gassing rates at different times and in different solutions are correlated respectively. $r$ increased with increasing NaOH

concentration, temperature, and pelletizing pressure and with ball milling. In general, *r* of AgO samples made in the presence of transition elements (added as compounds) were larger than *r* of samples with nontransition elements. The effect of Co and Ni is especially catastrophic, Pb suppressed *r* of highly gassing AgO samples regardless of the method of addition.

413. **Argue, G. R., Recht, H. L., and Arcand, G. M.** 116, 1164, (1969)

**Effects of Gamma Radiation on the Behavior of Nickel and Cadmium Electrodes**

A number of workers have reported studies in which alkaline batteries were exposed to gamma radiation and have stated that doses as high as $10^8$ rads produced no discernible effects. However, some data have shown that nickel-cadmium batteries lost about 10% of their capacity when irradiated in a nuclear reactor. This loss fell within the requirements for this particular work. In no instance previous to the present work have alkaline-battery electrodes been studied as entities in experimental cells. Many of the materials (separators, cases, etc.) in a complete battery are known to be degraded by nuclear radiation. The present work was undertaken to study the effects of radiation on the electrodes in alkaline solutions without the possible interferences of these other materials.

414. **Andersen, T. N., Miner, B. A., Ghandehari, M. H., Brodd, R. J., and Eyring, H.** 116, 1342, (1969)

**The Effect of High Pressure on the Voltage and Current Output of Silver Oxide-Zinc and Mercury Oxide-Zinc Miniature Batteries**

The open-circuit voltage (emf) and the voltage under load of alkaline silver oxide-zinc and mercuric oxide-zinc miniature batteries have been measured at pressures up to 20 kbars. The emf of these batteries varies with pressure in the manner expected based on the thermodynamics of the cell reactions. Pressure affects the voltage of the discharging silver oxide batteries only by its effect on the emf. The voltage of the discharging mercuric oxide battery is lowered with increasing pressure by approximately 5 mV/kbar. This decrease in voltage is attributable both to an increase in the over-voltage at the HgO electrode and to the ohmic resistance. These pressure effects are discussed in terms of the postulated diffusion of hydroxyl ions through water channels in the reduced oxide and the influence of these channels on the number of oxide sites at which reduction may occur.

415. **Diggle, J. W., Despic, A. R., and Bockris, J. O'M.** 116, 1503, (1969)

**The Mechanism of the Dendritic Electrocrystallization of Zinc**

Measurements have been made of the growth rate of zinc dendrites in alkaline zincate solutions as a function of overpotential ($\eta$), concentration (c), and temperature (T). The tip radii have been measured by electron microscopy. At constant potential, an initiation time of between 5 and 100 minutes is observed, depending on $\eta$, c, and T. The dendrite grows linearly with time at a rate depending on $\eta$, c, and T. The total current to base and dendrite was independent of time until a time, $\tau_i > \tau_d$ (the time for initiation obtained from the growth rate vs. time relation). Thereafter, $i \alpha t^2$. A critical overpotential was determined, $-75$ mV $> \eta_{crit} > -85$ mV. Below this $\eta_{crit}$, sponge was formed. Dendrites were observed up to $\eta = -160$ mV; above this, the deposition was heavy sponge. At a given c, the growth rate of a given dendrite increased with $\eta$ according to an exponential law. The growing tip is parabolic, where $10^{-5} < r_{tip} < 10^{-4}$ cm. No twinning was observed.

416. **Wales, C. P.** 116, 1633, (1969)

**The Microstructure of Sintered Silver Electrodes**
**II. At the End of 1-Hour Rate Discharges**

A single discharge of an Ag electrode at the relatively fast 1-hr rate resulted in Ag particles smaller than those present in the unused sintered electrode. As an electrode was cycled in 35% KOH at 25°C, the active material tended to clump together, and void spaces became larger. At the same time, the average size of Ag particles gradually increased, although particle size remained small at the surface of a discharged electrode. These changes were accompanied by a gradual decrease in discharge capacity. The small Ag particles that formed during fast (1-hr) discharges could be oxidized more readily and more completely during a charge than the large Ag particles that formed during slow (20-hr) discharges. Therefore, the capacity decreased more slowly when an electrode was cycled using fast discharges.

417. **Powers, R. W.** 116, 1652, (1969)

**Anodic Films on Zinc and the Formation of Cobwebs**

When a zinc anode in a strongly alkaline electrolyte is observed under a microscope, two different films can be noted under appropriate conditions. Although both have been

identified as zinc oxide, type I is white and forms by precipitation from a supersaturated layer of electrolyte covering the electrode. Type II, on the other hand, appears to form directly on the electrode surface. Its color can range form light gray to black. During dissolution of the type-II film, entities appear which resemble spiderwebs under the microscope. These so-called cobwebs seem to form by the gathering together of the darkening agent in this film. They are mainly zinc, are electronically conducting, and can be oxidized. Cobwebs appear to have a relationship to the hydrogen evolution that occurs at potentials anodic to the zinc rest potential. In addition, they are important because, during subsequent electrodeposition, they accelerate the formation of spongy zinc at low cathodic potentials and of dendritic zinc at higher potentials.

418. **Overthrow, T. I., Miller, J. N., and Hampson, N. A.** 116, 1757, (1969)

**The Effect of $CO_2$ on the Viscosity of Alkaline Electrolytes**

Alkaline electrolytes are of general interest in many battery applications, including zinc cells, fuel cells, and others. Electrolytes are frequently based on KOH (4-10M) in which the OH- concentration may fall to about 3M at the end of discharge. $CO_2$ pickup is a problem in all cases. This note records a preliminary investigation of this effect.

419. **Silver, H. G., and Lekas, E.** 117, 5, (1970)

**The Products of the Anodic Oxidation of an Iron Electrode in Alkaline Solution**

X-ray diffraction patterns have been recorded of the surface of an activated iron electrode during anodic oxidation in 30% KOH. At the end of the first plateau (−0.8 V relative to an Hg/HgO reference electrode), only *a*-Fe and $Fe(OH)_2$ are detected. At the end of the second plateau (0.0 V), *a*-Fe and δ-FeO(OH) are detected on the first discharge. On subsequent discharges, a gradual conversion to *a*-Fe and $Fe_3O_4$ is observed. In 30% KOH saturated with LiOH, *a*-Fe and $Fe_3O_4$ are detected at the end of the second plateau on the first and subsequent cycles.

420. **Hull, M. N., Ellison, J. E., and Toni, J. E.** 117, 192, (1970)

**The Anodic Behavior of Zinc Electrodes in Potassium Hydroxide Electrolytes**

The electrochemical oxidation of zinc anodes in potassium hydroxide solutions of 0.5 to 5.0M has been studied under stationary and hydrodynamic conditions. Linear sweep voltammetry and rotating ring-disk electrode techniques were employed to elucidate the different processes involved in the electrode reaction. Two different surface films are formed on zinc anodes. The first of these causes a small retardation in the rate of dissolution of the electrode in the active region while the second causes passivation. Measurements with rotating ring-disk arrangements indicate that the "dissolution-precipitation" model for the formation of these films may not be correct. The majority of the current passed in those regions where the surface is covered by a film is utilized in direct electrochemical oxidation of the zinc to soluble products but not in processes associated with thickening of the surface layer.

421. **Okinaka, Y.** 117, 289, (1970)

**On the Oxidation-Reduction Mechanism of the Cadmium Metal-Cadmium Hydroxide Electrode**

Electrochemical oxidation-reduction processes of the $Cd/Cd(OH)_2$ electrode in concentrated alkaline solutions were investigated by using a rotating ring-disk electrode, as well as a stationary electrode. Results support the mechanism that the anodic oxidation of Cd to $Cd(OH)_2$ in the active potential range proceeds entirely through the dissolution-precipitation sequence, and that the cathodic reduction of $Cd(OH)_2$ takes place both through the solution phase and by a direct solid-state mechanism.

422. **Weininger, J. L., and Holub, F. F.** 117, 340, (1970)

**Ultrafine Porous Polymer Membranes as Battery Separators**

In nonaqueous galvanic systems based on organic solvents, it is important to keep soluble ions of the cathodic reactant from the anode. In solvent exchange, only an insufficient amount of organic solvent (e.g., propylene carbonate or dimethyl sulfoxide) replaces water in the ion-exchange resing. To obviate this problem and obtain a separator for organic electrolyte cells, an alternate method of ion exclusion is reported in this note.

423. MacArthur, D. M. 117, 422, (1970)

**The Hydrated Nickel Hydroxide Electrode Potential Sweep Experiments**

The mechanism of the hydrated nickel-hydroxide electrode, used in the nickel-cadmium battery, is a matter of considerable controversy. Potential sweep experiments were performed on film nickel-hydroxide electrodes in an effort to determine the oxidation-reduction mechanism. The existence of more than one reduced structure was confirmed and the structure known as *a*-nickel hydroxide was studied in detail. A model based on a reversible charge-transfer step with a rate-controlling diffusion process was used to analyze the data. The results were in good agreement with the model. The overall reaction for *a*-nickel hydroxide was found to be

$$2[3Ni(OH)_2 \cdot 2H_2O] + 6\,OH^- + 3/2KOH \rightleftharpoons 2[3NiOOH \cdot 7/2H_2O \cdot 3/4KOH] + 3H_2O + 6\epsilon^-$$

The rate-controlling process, which was assumed to be proton diffusion, was found to have a diffusion coefficient of approximately $2 \times 10^{-9}$ $cm^2$ $s^{-1}$. Evidence for the formation of a poorly conducting layer during discharge of the electrode was found, and capacity loss was attributed to this.

424. Memming, R., Mollers, F., and Neumann, G. 117, 451, (1970)

**Photoelectrochemical Processes on Silver-Silver Oxide Electrodes**

Oxidation and reduction processes of silver-silver oxide electrodes were studied, particularly the influence of light excitation of these processes. The experimental results have shown that light absorption by silver (I) oxide leads to an anodic oxidation to silver (II) oxide. The electrochemical reduction of silver (II) oxide formed during illumination is considerably inhibited. A possible mechanism explaining the photoelectrochemical processes and the inhibition is discussed.

425. **Miller, B.** 117, 491, (1970)

**Rotating Ring-Disk Study of the Silver Electrode in Alkaline Solution**

Rotating ring-disk electrodes have been used for observing the soluble products on charge and discharge of potential or current-controlled silver disks in 1.0 to 10.1M KOH and 1.0M NaOH. Limits on the solubility of higher valent silver species corresponding to AgO formation and the oxygen-evolution region are given. The relative surface concentration of Ag(I) for all disk conditions has been measured and related to existing solubility data, the polarization characteristics of silver, and the reaction mechanisms.

426. **Okinaka, Y., and Whitehurst, C. M.** 117, 583, (1970)

**Charge Acceptance of the Cadmium-Cadmium Hydroxide Electrode at Low Temperatures**

Premature hydrogen evolution occurs when a discharged cadmium-hydroxide electrode is brought to a low temperature and charged at a moderate rate. It was found that, in addition to various other known factors, the discharge rate and the temperature during discharge just prior to the temperature lowering greatly affect the charge acceptance in the first low-temperature charge. Light and electron microscopic examination and BET surface area measurement showed that the cadmium-hydroxide crystals formed at lower discharge rates and that, at higher temperatures, they are larger and more difficult to reduce. The results are interpreted on the basis of the mechanism involving a soluble intermediate species in both the charging and the discharging reactions. X-ray and electron diffraction analyses of the cadmium-hydroxide crystals formed on discharge in 6.9*N* KOH at temperatures below -18°C showed the presence of $\gamma$-$Cd(OH)_2$ in addition to the oridnary $\beta$-$Cd(OH)_2$. Electrodes containing $\gamma$-$Cd(OH)_2$ have a greater low-temperature charge acceptability than those containing $\beta$-$Cd(OH)_2$ alone.

427. **Mansfeld, F., and Gilman, S.** 117, 588, (1970)

**The Effect of Lead Ions on the Dissolution and Deposition Characteristics of a Zinc Single Crystal in 6*N* KOH**

Dissolution of the basal plane of single-crystal zinc and deposition of zinc on the same material in alkaline solutions in the presence of $10^{-4}$ M lead ion has been studied using *in-situ* microscopy and the scanning electron microscope (SEM). It was found that, in the

presence of lead ions, most of the surface was protected against dissolution when polarized as much as 100 mV positive to the rest potential. Dissolution occurs initially in the form of a limited number of hexagonal etch pits that grow in size and number with time. The pits appear to correspond to sites of macroscopic crystalline imperfection.

In the absence of Pb ions, deposition of Zn on the basal plane of a zinc crystal tends toward epitaxial growth at low overpotentials. In the presence of Pb ions, at both high and low overpotentials, Zn deposition tends to initiate mainly at the few sites not protected by the microscopically smooth Pb film. At high overpotentials, growth tends to be cylindrical and microcrystalline, rather than dendritic. It is shown that, under the present conditions, no increase in the cathodic current is to be expected with increase of time.

428. MacArthur, D. M. 117, 729, (1970)

**The Proton Diffusion Coefficient for the Nickel-Hydroxide Electrode**

The diffusion coefficient for protons moving in the hydrated nickel-hydroxide lattice has been determined using a potential-step technique. It was found to have a value of about $3.1 \times 10^{-10}$ $cm^2$ $s^{-1}$ during charging and $4.6 \times 10^{-11}$ $cm^2 s^{-1}$ during discharging for the nickel-cadmium battery. The temperature dependence of the coefficient has been determined, and it has been concluded that the proton moves in the lattice by thermal diffusion. The enthalpy of diffusion was found to be 2.2 kcal $deg^{-1}$ $mole^{-1}$ during charging and 2.3 kcal $deg^{-1}$ $mole^{-1}$ during discharging of the electrode.

429. Breiter, M. W. 117, 738, (1970)

**Film Formation and Reduction on Zinc Electrodes in Concentrated Potassium Hydroxide Solutions**

Anodic films were formed under potentiostatic conditions at three characteristic potentials in unstirred 6M KOH + 0.25M ZnO at 25°C on polycrystalline zinc electrodes arranged in either horizontal or vertical position. The film formation was followed as a function of time by determining the charge equivalent of the films by a method employing cathodic potential sweeps at 0.33 mV/s. At each of the potentials, film formation occurred more rapidly on the horizontal than on the vertical electrode. The efficiency of film formation decreased from values above 50% at 250 seconds to values around 20% on the horizontal electrodes. It stayed below 6% for the vertical electrodes.

430. Mansfeld, F., and Gilman, S. 117, 1154, (1970)

**The Effect of Tin and Tetraethylammonium Ions on the Characteristics of Zinc Deposition on a Zinc Single Crystal in Aqueous KOH**

The authors report the effect of lead ions added to the electrolyte on the dissolution and deposition characteristics of a zinc single crystal. The deposit obtained at −200 mV polarization (all potentials refer to the rest potential of pure zinc in the same solution) is converted by the addition of Pb ions from classical dendrites, with side branches to compact cylinders with rounded tops consisting of many small crystallites. It was shown that lead blocks most of the sites active for dissolution and deposition of zinc. Growth is nucleated preferentially at sites of macroscopic defects in the crystal, where impurity segregation is also expected. In the present communication, the effect of tin and tetraethylammonium ions on the morphology of zinc deposits at −200 mV is discussed. As a dendrite-inhibiting additive for secondary zinc battery applications, Sn offers the advantage over Pb in that the oxidation potential of Sn is not much higher than that of Zn, as shown by thermodynamic data and potentiostatic polarization curves in 6*N* KOH. On discharge, both Zn and Sn may therefore ionize simultaneously, making Sn ions available for the recharge process.

431. Mao, G. W., Polcyn, D. S., and Tieder, R. E. 117, 1319, (1970)

**Development of a Controlled Porosity Silver Electrode**

Silver electrodes that require no supporting grid and have a porosity graded structure were fabricated by combining silver powder of uniform mesh size with a plasticizer and pore-forming additives. The proportions of these materials were selected to give a uniform doughlike mixture that was rolled and then sintered. Porosity control was achieved by controlled decomposition of the plasticizer and pore-forming additives. Multilayered graded porosity electrodes were assembled by a combination of sintering and compaction. Performance data, based on cycling tests and coulombic efficiencies, demonstrated that these electrodes are comparable to conventional silver electrodes and that the absence of the grid is not a limiting factor.

432. Mansfeld, F., and Gilman, S. 117, 1328, (1970)

**The Effect of Several Electrode and Electrolyte Additives on the Corrosion and Polarization Behavior of the Alkaline Zinc Electrode**

The corrosion behavior of zinc in 6*N* KOH at 25°C was investigated by measuring the rate of hydrogen evolution ($r_{H_2}$) at the corrosion potential. Anodic and cathodic potentiostatic polarization curves as a function of alloying and additions to the electrolyte were obtained. It was found that the corrosion and polarization behavior of 99.999% zinc can be explained by mixed-potential theory, assuming that the reactions were $Zn + 4\ OH^- \rightleftharpoons Zn(OH)_4^{2-} + 2e^-$ and $H_2O + e^- \rightleftharpoons \frac{1}{2}H_2 + OH^-$. Good agreement between theoretical curves obtained by computer solution of the kinetic equations corresponding to the above reactions and actual polarization measurements was obtained in the absence and presence of zincate. Theoretical and experimental corrosion rates also agreed well. Binary Zn-Pb alloys [0.1 to 1.0% (weight percent)] and Zn-Al alloys (0.2 to 0.8%) made from high-purity metals had $r_{H_2}$-values which were lower than those for zinc although $r_{H_2}$-values of commercial zinc alloys were much higher than those of zinc, probably because of the presence of low overvoltage impurities such as Cu, Ni, or Fe. Addition of $10^{-3}$M copper, tin, or lead ions to the electrolyte also influenced $r_{H_2}$, which in the presence of metal ions noble to zinc is no longer equivalent to the corrosion rate. The strong increase of $r_{H_2}$ in the presence of Cu ions is explained by the low hydrogen overvoltage of Cu, and the decrease of $r_{H_2}$ in the presence of Pb ions is explained by the high hydrogen overvoltage of Pb. Anions such as $Cl^-$ or $Br^-$ do not affect $r_{H_2}$. In the presence of thiourea, $r_{H_2}$ increases steadily, but $S^{2-}$ leads to severe corrosion.

433. Mansfeld, F., and Gilman, S. 117, 1521, (1970)

**The Effect of Potential and Time on Deposition Characteristics of Zinc on a Zinc Single Crystal in KOH**

Details of early growth of the zinc electrodeposit are accessible through the use of the scanning electron microscope (SEM). Although SEM studies have been made of zinc electrodeposits, they were not made under conditions of potentiostatic control and are therefore not exactly comparable to the results of Powers or to the results obtained by the present authors in their studies of the effect of additives on the morphology of the electrodeposit.

434. Wales, C. P. 118, 7, (1971)

**The Microstructure of Sintered Silver Electrodes III. $Ag_2O$ Formation During Charges**

Ag electrodes were charged at the 20-hr rate of constant current and discharged at the 1-hr rate in 35% KOH solution at 25°C. Cross sections of samples cut from the electrodes during charges at cycles 1 to 30 were examined. Almost all Ag particles had a visible coating of $Ag_2O$ when an electrode was charged for half the capacity accepted at the $Ag/Ag_2O$ potential plateau. The electrode surface had the same structure as the interior. In a cycled electrode, approximately 60% of the Ag had been oxidized to $Ag_2O$ when the potential peak separating the $Ag/Ag_2O$ and $Ag_2O/AgO$ plateaus was reached.

435. Drazic, D. M., and Nagy, Z. 118, 255, (1971)

**Investigation of the Direct Reduction of Zinc Oxide in Alkaline Electrolytes**

In a Zn/ZnO alkaline battery electrode, the reaction, in principle, can proceed by two considerably different mechanisms: through a soluble intermediate by a dissolution-precipitation mechanism, or through a direct, solid-state reaction. The solution route has been generally favored, but no direct proof has appeared in the literature for excluding the solid-state process. On the contrary, recent solid-state reactions were proposed as the predominant mechanism. The direct electrochemical reduction of zinc oxide, in aqueous electrolytes, to zinc and water has been reported.

436. Vander Lugt, L. A., and Dirkse, T. P. 118, 265, (1971)

**The Exchange of $Zn^{65}$ Between ZnO(s) and Potassium Zincate**

Studies of the system Zn/Zn(II), KOH, particularly in concentrations ordinarily used in battery systems, have revealed certain anomalies, including the ease of production and stability of supersaturated zincate solutions and the appearance of maximums and minimums in correlations of certain kinetic constants with KOH concentration (exchange currents, conductance, and passivation time constants). These anomadies appear to be connected with the electrolyte phase. A fuller understanding of the chemical characteristics of the electrolyte is needed to more fully understand the electrochemical behavior of the system.

437. Agruss, B. 118, 375, (1971)

**Testing Batteries for Vehicular Applications**
**III. Selection and Characterization of a Power Battery**

The objective was to find an acceptable "power" battery (i.e., a high power density battery to deliver short-term acceleration pulses) for an electric commuter-vehicle concept powered by a dual-battery system. A number of batteries were tested, both Pb-acid and Ni-Cd. The best battery was an Ni-Cd aircraft starting battery.

Several of the design batteries were built. Each consisted of seven cells containing 11 plates per cell. One of the batteries was tested. It delivered 15 consecutive 2500 W acceleration power pulses to 10.5 V. It weighed 32 pounds; hence, the entire power pack would weigh 256 pounds. Because the 11-plate cell performed so well, it was hoped that a 9-plate cell would deliver adequate power so that a 27-pound weight reduction could be realized. However, it could not deliver adequate power when tested. Nothing could be obtained at 2500 W. The voltage fell immediately below 10.5 V. In fact, only 1.8 minutes were obtained at 1900 W.

438. Rubin, E. J., and Baboian, R. 118, 428, (1971)

**A Correlation of the Solution Properties and the Electrochemical Behavior of the Nickel Hydroxide Electrode in Binary Aqueous Alkali Hydroxides**

The electrochemical behavior of the nickel-hydroxide electrode in binary aqueous alkali hydroxide solutions was investigated in the temperature range -40 to 60°C. Maxima were observed in the electrode capacity vs. temperature curve for each electrolyte. The nature of the interaction of the alkali metal ion had a marked effect on the charge acceptance of the electrode. At the higher temperatures, the charge acceptance was greatest with the $LiOH\text{-}H_2O$ electrolyte. At the lower temperatures, the charge acceptance was greatest with the $RbOH\text{-}H_2O$ and $CsOH\text{-}H_2O$ electrolytes. The results correlate with the variation in solution properties at these temperatures.

439. Kang, H. Y. 118, 462, (1971)

**The Low-Temperature Passivation of Cadmium in 8M KOH**

It has been reported that cadmium anodes have desirable properties for their use in primary alkaline cells at low temperatures. The discharge of cadmium electrodes is normally terminated by the onset of passivation. Although the passivation of cadmium in alkaline solutions has been studied by a number of authors, little data have been reported for the low-temperature range. In the present work, measurements of cadmium passivation at low temperatures were carried out to provide the data necessary for an analysis of the intrinsic rate capabilities of cadmium at low temperatures. The behavior of flat cadmium electrodes was studied in order to avoid the uncertainties associated with the interpretation of passivation data on porous electrodes. Eight-molar KOH solution was used as the electrolyte to cover a wider range of temperatures. The position of the cadmium (bottom) and the range of current densities (low) were chosen to minimize the effect of convection. The results fitted a kinetic expression proposed in the literature based on a dissolution-precipitation mechanism.

440. Gagnon, E. G., and Austin, L. G. 118, 447, (1971)

**Low-Temperature Cathode Performance of Porous $Ag/Ag_2O$ Electrodes**

The performance of porous, silver-silver oxide electrodes decreases rapidly below 0°C, and galvanostatic discharge curves show several different regions. Most of the work reported here was done on thin $Ag/Ag_2O$ electrodes prepared by electrodeposition or by powder-pressing. An attempt is made to explain the regions in the discharge curves and the apparent Tafel parameters from a plausible kinetic mechanism. The application of theories of porous electrode behavior is demonstrated by results from thick electrodes made by stacking thin electrodes together. Future work and the use of the information in designing electrodes are discussed.

441. Bro, P., and Kang, H. Y. 118, 519, (1971)

**Discharge Profiles in a Porous Cadmium Electrode**

Porous cadmium electrodes were discharged galvanostatically at current densities between 2 $mA/cm^2$ and 200 $mA/cm^2$ in 30% KOH at 25°C, and the discharge profiles were determined by chemical analyses of thin sections sliced from the electrode. The discharge

profiles were given by $q/q_0 = A \cosh B(1 - X)/\cosh B$, where A is the state of discharge at the front of the electrode and B is an electrochemical Thiele parameter. The retention of the discharge product in the electrode noticeably affected the discharge. The discharge efficiency was limited by both faradaic processes and mass transfer.

442. **Powers, R. W.** 118, 685, (1971)

**Film Formation and Hydrogen Evolution on the Alkaline Zinc Electrode**

The duplex structure of anodic films formed in concentrated KOH solutions with convection nearly absent—a hydrodynamic condition present near a battery plate in proximity to a separator—has been confirmed on high-purity polycrystalline zinc and, to a more limited degree, on some polycrystalline zinc alloys. Previously, the use of a very slow potential scan with simultaneous microscopic observation of single-crystal zinc electrodes showed that a precipitated coating of ZnO particles (type-I film) overlies a more coherent film also of ZnO (type II). The experimental conditions required for following stages in the formation of the precipitated film (the one most difficult to observe) are defined more explicitly in this paper. Evidence is presented that the type-II film serves as a catalyst for hydrogen evolution at potentials anodic to the zinc/zinc oxide equilibrium value. Hydrogen bubbles, whose formation is so catalyzed, can mechanically dislodge overlying passivating film to cause reactivation of the electrode. The presence of complex tin or lead anions at concentrations of about $10^{-3}$M (molar) in KOH solutions gives rise to very smooth, almost imperceptible, films of metallic tin or lead over the zinc electrode surface. However, such films are made visible during zinc dissolution as they rumple and eventually gather into a wad after being undercut. These foreign-metal films inhibit the dissolution of zinc to an extent that depends on the particular complex anion, its concentration, and the exposure time to the zinc surface. Lead films can be made sufficiently inhibitive that zinc dissolution is reduced to a rate at which very little precipitation of ZnO occurs.

443. **Wales, C. P.** 118, 1021, (1971)

**The Microstructure of Sintered Silver Electrodes**
**IV. Formation of AgO During Charges**

Silver electrodes were cycled in 35% KOH solution and examined at various times during constant current charges. The initial formation of AgO took place on the surface of $Ag_2O$ after the charge potential rose to the $Ag_2O$/AgO plateau. Preferred locations for

initial oxidation of $Ag_2O$ were in the interior of the electrode, around the grid, and near large Ag particles where the $Ag_2O$ coating which formed earlier in the charge was comparatively thin. After initial AgO formation in an electrode, oxidation of nearby Ag and $Ag_2O$ took place as the charge continued. Little or no additional Ag was oxidized in other areas of the electrode until AgO had also formed there.

444. **Sato, Y., Niki, H., and Takamura, T.** 118, 1269, (1971)

**Effects of Carbonate on the Anodic Dissolution and the Passivation of Zinc Electrode in Concentrated Solution of Potassium Hydroxide**

The effect or carbonate ions on the anodic behavior of a horizontal zinc anode in concentrated KOH solutions has been investigated by measuring the passivation time at constant current. Anodic dissolution of zinc was found to be associated with the diffusion-controlled zincate ion saturation near the electrode, and the passivation time of the electrode (which is defined to be a period until the passivation occurs) was reduced with increasing concentration of carbonate ions at constant concentration of KOH. The phenomenon was explained from the linear relationship between $t_p$ and $1/\eta$ as a result of the increase in viscosity $\eta$ of the solution.

445. **Boden, D. P., Wylie, R. B., and Spera, V. J.** 118, 1298, (1971)

**The Electrode Potential of Zinc Amalgam in Alkaline Zincate Solutions**

The electrode potential of zinc amalgams has been measured in potassium hydroxide solutions containing dissolved zincate. Curvature in the Nernst plots was observed at high zincate concentrations in agreement with the results of other workers. The curvature is explained as being attributable to the dependence of the hydroxyl and zincate ion activity on concentration in strong potassium hydroxide solutions. The data yield a value of -1.205 V (vs. Standard Hydrogen Electrode) for the standard potential of the zinc, zincate ion electrode (International Union of Pure and Applied Chemistry–Stockholm convention), and -205.86 kcal for the free energy of formation of the zincate ion at 25°C.

446. Mahefkey, E. T., and Kreitman, M. M. 118, 1382, (1971)

### An Intercell Planar Heat Pipe for the Removal of Heat During the Cycling of a High Rate Nickel Cadmium Battery

Two 22 Ah nickel-cadmium cells were continuously cycled at a 1c charge rate and at a 2c discharge rate, with cooling provided by an intercell planar (rectangular cross section) heat pipe. For purposes of comparison, thermocouple measurements were also taken with an aluminum conduction fin substituting for the heat pipe. The aluminum fin and heat pipe were cooled by forced air of room temperature. Thermally insulated cells were also cycled at the same rates. Cell-case temperatures were measured during cycling, and a maximum of 29°C with a 5°-C thermal excursion was noted with the heat pipe under conditions of thermal equilibrium which were observed after three complete cycles. For the aluminum fin configuration, a maximum of 42°C with a 7°-C thermal excursion was obtained near thermal equilibrium after five complete cycles. The insulated configuration yielded a battery-case temperature of 83°C after five cycles, and thermal equilibrium was never reached. Coulombic efficiency values for the heat-pipe-cooled battery were found to be several percent greater than ~95%, which was recorded for the aluminum fin configuration. The specific heat of the cells was measured to be 0.27 cal/g°C. From this and the measured values of the total heat generated per cycle, the effectiveness of the heat pipe in removing battery heat was calculated to be approximately 26% greater than the aluminum fin at or near equilibrium. It is surmised that the significantly lower operating temperatures produced by the heat pipe should lead to an important lengthening of battery-cycle life and an associated reduction of capacity degradation.

447. Justice, D. D., and Hurd, R. M. 118, 1417, (1971)

### Electrochemical Dissolution of ZnO Single Crystals

Dissolution rates for the zinc face of ZnO single crystals were measured as a function of potential in KOH solutions. In the absence of light, no potential dependency existed between -1.2 and +3.0 V vs. Standard Calomel Electrode. Upon irradiation with light of sufficient energy to produce electron-hole pairs, a potential-dependent dissolution process was superimposed on the continuing potential-independent process. The results are interpreted on the basis of a combination of both electrochemical and chemical dissolution processes.

448. Bro, P., and Kang, H. Y. 118, 1430, (1971)

**The Low-Temperature Activity of Water in Concentrated KOH Solutions**

The vapor pressures of $H_2O$-KOH solutions were measured manometrically between -40° and 25°C for concentrations between 2*M* KOH and 15*M* KOH. The effect of the temperature on the vapor pressure agreed with that predicted from the Clapeyron equation. An increase in the KOH concentration decreased the vapor pressure. The logarithm of the relative activity of KOH increased almost linearly with the KOH concentration, but it changed little with temperature. The data suggest that KOH hydrates occur as solid phases in the low-concentration portion of the phase diagram. Furthermore, the existence of a eutectic point in the system was reflected in the properties of the solutions at temperatures far above the eutectic point.

449. Brooman, E. W., and McCallum, J. 118, 1518, (1971)

**Thermal Conductivity Measurements of Nickel-Cadmium Aerospace Cells I: Cell Conductivities**

Thermal conductivities of four types of sealed, 20 Ah nickel-cadmium cells have been measured perpendicular to ($x$-direction), and parallel with ($y$-direction), the plane of the electrodes. The average conductivities for the discharged cells described are about 0.0030 and 0.0065 (cal/cm$^2$/sec)/(C/cm) for these $x$- and $y$-directions, respectively. Thermal resistance network models give reasonable quantitative agreement with the $k_x$ measurements using conductivity values of 0.0019, 0.0016, and 0.0011 (cal/cm$^2$/sec)/(C/cm), determined in some preliminary experiments, for the wetted negative and positive electrodes and the separator, respectively. The thermal conductivity of the cells is found to change very little with state of charge.

450. Dirkse, T. P., Vander Lugt, L. A., and Hampson, N. A. 118, 1606, (1971)

**Exchange in the Zn, Zincate, ZnO System**

The results of a radiochemical study of the system Zn/Zn(II), $OH^-$/ZnO are presented. It is shown that the exchange of tagged Zn(II) between solid ZnO and zincate ion is slow and appears to be negligible in zincate solutions based on 30% KOH. Commercial implications are discussed. Attempts to study the charge-transfer reaction as a solid-zinc electrode were unsuccessful because of the high parasitic corrosion rate.

451. Gilman, S., and Sangermano, L. D. 118, 1953, (1971)

**Adsorption of Cadmium Ions from KOH Solution at a Platinum Electrode**

Wagner noted the degradation of the platinum-catalyzed oxygen electrode in an experimental cadmium-air battery cell and suggested that the effect might be caused by the adsorption of cadmium ions. In this study, the degradation effect was verified, and the nature and extent of the adsorption process responsible for the degradation was evaluated.

452. Bockris, J. O'M., Nagy, Z., and Damjanovic, A. 119, 285, (1972)

**On the Deposition and Dissolution of Zinc in Alkaline Solutions**

The zinc/KOH-zincate electrode reaction was investigated under high-purity conditions with galvanostatic and potentiostatic transient techniques in the 0.1 to 3.0M KOH and 0.0001 to 0.5M zincate concentration range. The exchange current density was found to be between 8 and 370 mA/cm$^2$, with 40 mV/decade anodic and 120 mV/decade cathodic nominal Tafel slopes; an overpotential range of ±100 mV was covered. The cathodic reaction orders were 1 for zincate and -1 for hydroxyl ions. A four-step mechanism, consistent with the kinetic data, is suggested. It consists of four consecutive dissociation reactions of the zincate complex, two of which incorporate a single electron charge transfer. The rate-determining step is

$$Zn(OH)_3^- + e = Zn(OH)_2^- + OH^-$$

The mechanism of the anodic and cathodic reactions is the same. The transients indicate only double-layer charging and charge-transfer processes. No surface diffusion effects or intermediate buildup was observed (no pseudocapacitance). A rationalization is given for the mechanism. The effect of zinc surface preparation is discussed.

453. Gross, S. 119, 347, (1972)

**Transient Pressure Considerations in Charge Control of Sealed Batteries**

When sealed batteries with imperfect charge efficiency approach full charge, gas often evolves and increases pressure. In addition to the problems caused by increased heat and pressure, gassing causes mechanical forces within pores that contribute to structural

breakdown; mechanical breakage causes loss in capacity and promotes shorting, and thus should be minimized. In this Technical Article, it is shown that when it occurs, cell structural damage can be greatest at the start of gassing because of transient pressure effects. An analysis is developed to compare the relative severity of this effect by the use of cell transient-pressure data.

454. McHenry, E. J., and Hubbauer, P. 119, 564, (1972)

**Hermetic Compression Seals for Alkaline Batteries**

An accelerated thermal cycle test is described which has been used to evaluate the long-term reliability of seals for nickel-cadmium batteries in Bell System use. Results of this test correlate well with life-test results on long-term overcharge. Two new types of seals have been developed for use in nickel-cadmium or other alkaline batteries. The first is a simple modification of the seal developed by A. W. Ziegler for submarine cable use. It entails substitution of an injection molded-nylon bushing for the machined Kel-F bushing used by Ziegler, thus eliminating a costly machining operation and greatly simplifying fabrication of the seal. The second is a design employing the same principles as the Ziegler seal, but is simpler and can be made in smaller sizes than the Ziegler seal. Both designs have been subjected to accelerated thermal cycle tests and found to be superior to the seals used on commercial alkaline cells.

455. Gagnon, E. G., and Austin, L. G. 119, 807, (1972)

**A Description of the Discharge Mode of Porous $Ag/Ag_2O$ Electrodes at Low Temperatures in KOH**

Further results are presented on the anodic discharge of electroformed and pressed-powder electrodes of $Ag/Ag_2O$ in eutectic KOH (aq) solution at low temperatures. It is concluded that the results are consistent with a mechanism $Ag_2O(s) + H_2O \rightarrow [Ag_2O(aq)] \rightarrow 2Ag^+ + 2\,OH^-$, $Ag(s) + Ag^+ + e^-$ slow $\rightarrow 2Ag(s)$. Loss of capacity at low porosity, high current density, and low temperature may be attributable to deposition of solid phases in the electrolyte.

456. Nagy, Z., and Bockris, J. O'M. 119, 1129, (1972)

**On The Electrochemistry of Porous Zinc Electrodes in Alkaline Solutions**

Porous zinc electrodes were discharged galvanostatically in aqueous potassium-hydroxide solutions. The morphology of the zinc-oxide film that formed was investigated with a scanning electron microscope. The current distribution in the porous electrode, and its dependence on current density, was determined by microslicing the electrode after discharge and chemical analysis. The oxide film had a porous, "carpet-like" structure, consisting of long needle crystals with occasional sidearms. The formation of this type of film can be explained by a dissolution-precipitation mechanism. The current distribution in the porous electrode and its dependence on current density could also be explained, based on a model of oxide film consisting of a thin, high-resistance compact film beneath the porous oxide.

457. Gregory, D. P., Jones, P. C., and Redfearn, D. P. 119, 1288, (1972)

**The Corrosion of Zinc Anodes in Aqueous Alkaline Electrolytes**

Rates of self-discharge of porous zinc electrodes in alkaline electrolytes have been measured under a variety of conditions by monitoring the rate of hydrogen evolution. The rate was found to decrease with the addition of lead or mercury to the zinc, the presence of zincate in the electrolyte, and increasing electrolyte concentration up to 5M KOH. Above 5M KOH, the rate increased with increasing KOH concentration.

458. Scarr, R. F., and Meszaros, F. W. 119, 1443, (1972)

**A Computer-Operated Facility for Research Testing of Secondary Batteries**

A working computer-operated system for the cyclic testing of up to 192 secondary batteries is described. The computer, operating on-line in a time-sharing mode, may conduct as many as 12 independent tests simultaneously. This approach has several advantages over other automated methods, including greater flexibility in test formating, real-time updating of characteristic quantities for each battery, real-time data reduction, systematic information filing, and a logical capability which facilitates the handling of contingencies. System technique, configuration, and capabilities are discussed as an approach to battery testing.

459. McBreen, J. 119, 1620, (1972)

**Zinc Electrode Shape Change in Secondary Cells**

Shape change, the reduction in zinc-electrode area with cycling, is a limiting factor in the life of most secondary zinc batteries. This investigation was an attempt to elucidate the mechanism of shape change by monitoring the pattern of current and potential distribution over the surface of a zinc electrode during cycling. This was done while keeping all electrode and cell parameters similar to those found in conventional cells. Differences in the secondary current distribution during charge and discharge result in exhaustion of the reducible zinc species at the plate periphery in the early stages of cycling. This generates a concentration cell which corrodes zinc off the plate edge and deposits it in the plate center. Shape change is a result of these concentration cell effects and the transfer of zincate from the plate periphery to the plate center in the early stages of discharge. Many other hitherto unexplained phenomena related to shape change were rationalized on the basis of these findings and mechanisms.

460. Will, F. G., and Hess, H. J. 120, 1, (1973)

**Morphology and Capacity of a Cadmium Electrode Studies on a Simulated Pore**

Conditions in a single pore of a battery plate were simulated by using a cadmium chip of millimeter dimensions covered with an electrolyte film of micron thickness. *In situ* microscopy was applied to study changes in the electrode morphology during charge and discharge. Passivation and increases in particle sizes because of precipitation and electrodeposition of dissolved cadmium species were found to cause profound loss in electrode capacity on repeated charge and discharge.

461. Hopper, M. A., and Ord, J. L. 120, 183, (1973)

**An Optical Study of the Growth and Oxidation of Nickel Hydroxide Films**

The formation and oxidation of nickel-hydroxide films under a variety of experimental conditions are studied using *in situ* ellipsometric measurements. Two forms of the hydroxide, which are assumed to be the $\alpha$- and $\beta$-hydroxide layers, are both transparent with real refractive indices of 1.52 and 1.46, respectively, at 6328A. Upon oxidation, the two

forms of hydroxide convert to different oxides, both of which absorb light. The process involved in the conversion of the β-hydroxide appears to be similar to the process postulated for the charging of the nickel-battery electrode.

462. Dunning, J. S., Bennion, D. N., and Newman, J. 120, 906, (1973)

**Analysis of Porous Electrodes with Sparingly Soluble Reactants II. Variable Solution Properties, Convection, and Complexing**

The galvanostatic operation of flooded porous electrodes employing metal/metal salt couples is analyzed. A model is developed for a single, circular pore configuration which accounts for the effects of differing equivalent volumes of the solid reactants. The model also includes effects of variation in solution properties and effects of complexing of the sparingly soluble salt with the bulk electrolyte anion. The $Cd/Cd(OH)_2$ couple in concentrated aqueous potassium hydroxide and the Ag/AgCl couple in concentrated potassium-chloride solutions are considered. Overpotential is computed as a function of time for solid-film and solution-diffusion versions of the model. The solid-film model shows a linear overpotential-time relationship and nearly uniform current distribution. The solution-diffusion model shows a variety of overpotential-time curves, based on different physical parameters. In general, anodic failure is caused by blockage of pores or by complete coverage of the metal surface by product crystallites. Cathodic failure is caused by low mass transport which leads to limiting currents in the electrode. The solution-diffusion model may generate extremely nonuniform current distributions, often with maxima inside the pore. These persistent nonuniform current distributions are important in terms of the analysis of cycling behavior.

463. Gordy, D. J., Luksha, E., and Menard, C. J. 120, 1447, (1973)

**Controlled Porosity and Pore Size Substrates for Nickel-Cadmium Cells**

A novel process for the preparation of improved cadmium-electrode plaques with precisely controlled pore size and porosity is described. The requirements for these plaques include far better uniformity, reproducibility, and life than is currently available with conventional materials. The key features of the work were preparation of plaques by a powder metallurgical technique which consisted of isostatically compacting a blend of a nickel powder with a fugitive pore-former and subsequently sintering the "green" compact. Cadmium electrodes were prepared from these materials and cycle-tested in negative-limited cells using

an accelerated, fortuous test regime. Results were obtained which showed the new structures yielded electrodes that were superior to the conventional structures in mechanical properties and performance. BET surface areas, scanning electron microscope photomicrographs, and mechanical strengths using a three-point bend test were used to help in the thorough characterization of the electrodes and the components prepared.

464. Gagnon, E. G. 121, 512, (1974)

**The Triangular Voltage Sweep Method for Determining Double-Layer Capacity of Porous Electrodes III. Porous Nickel in Potassium Hydroxide**

The effects of faradaic current and distributed capacity on the measurement of double-layer capacity of porous nickel were analyzed as a function of electrode thickness and temperature. Faradaic current observed with electrodes at -46°C was negligible compared to results obtained at 22°C. Distributed capacity effects increased with electrode thickness and with decreasing temperature; the results agreed well with values predicted from a previously developed model. In the potential range of 0 to -0.40 V vs. Hg/HgO, the capacity based on the BET area of the electrode was about 30 $\mu F/cm^2$.

465. Wales, C. P. 121, 727, (1974)

**Reduction of the Silver Oxide Electrode in CsOH Solutions**

The electrical characteristics and changes in structure when sintered Ag electrodes were cycled in 8.4M- or 3.6M-CsOH solutions were compared with results for similar electrodes cycled in KOH solutions. The products of reduction were the same in the two electrolytes. Solutions of CsOH gave a better capacity when the Ag electrodes were cycled repeatedly, using slow discharges, because the Ag which formed during reduction had a smaller average particle size in CsOH than in KOH because of lower ionic mobility in the CsOH. Because polarization was higher in CsOH, KOH was preferable to CsOH at moderate and high rates of discharge.

466. Vorkapic, L. Z., Drazic, D. M., and Despic, A. R. 121, 1385, (1974)

**Corrosion of Pure and Amalgamated Zinc in Concentrated Alkali Hydroxide Solutions**

Corrosion of pure and amalgamated zinc in pure, concentrated KOH solutions was investigated using two methods: (a) galvanostatic measurements of the kinetics of hydrogen evolution with electrodic assessment of corrosion properties of the system, and (b) volumetric measurement of the hydrogen evolution reflecting directly the rate of corrosion. The latter was followed as a function of time during 150 hours. It was found that the corrosion rate varies considerably with time, and it was suggested that different factors control the initial and the steady-state corrosion. The initial corrosion rate increases with increasing KOH concentration which is indicative of the chemical mechanism of hydrogen evolution. The change of the corrosion rate with time and the steady-state corrosion rate can be explained in terms of formation of an impermeable ZnO film at the surface. In such a case, the concentration dependence of the corrosion rate is inverse with time, which explains some results reported in literature. The amalgamated zinc surface gives complex galvanostatic transients which indicate a new phase formation in the process of initiation of hydrogen evolution, which could pertain to some solid potassium-zinc-mercury alloy.

500. Santhanakrishnan, S., Vijayavalli, R., Rao, P. V., and Udupa, V. K. 18, 112, (1969)

**Performance Characteristics of Sintered Plate Nickel-Cadmium Cells III. Chargeability at Subzero Temperatures**

The chargeability and performance of 1.2 V, 35 Ah starter-type cells at 28, 0, -10, -20, -30, and -40°C were studied. With decrease in charging temperature, the cell voltage increases, which may be attributable to an increase in the ohmic drop at low temperatures. The discharge at low temperature also affects the charging voltage in the subsequent cycle. The previous history of the cell has no marked influence on the subsequent charging voltage even though the cells have been brought to room temperature before charging at lower temperatures for the next cycle. This increase in overvoltage for charging is probably related to the property of the active materials themselves–the passivation and grain size, etc. At room temperatures, the charging curve shows a steady value between 1.38 and 1.42 V until current equal to the rated capacity has been passed through the cell, whereas, at 0° and -10°, the voltage rises after current of ∿80% of the rated capacity has been passed. At -30° and -40°, the cell voltage increases even in the initial states of charging, and, for charging the current of ∿80% of the rated capacity, the voltage remains steady until the end of charging, which may represent more gas evolution than charging. The discharge curves at different temperatures after charging at different temperatures do not show much change up to -20°, and, below this temperature, the performance is very much affected. Charging below -20° yielded capacity to an extent of only 80% of the rated capacity. At -40°, after charging at the same temperature, the discharge voltage fell steeply. As the temperature of charging decreases, the output capacity also decreases.

501. Rao, P. V., Vijayavalli, R., Santhanakrishnan, S., and Udupa, V. K. 18, 122, (1969)

**Performance Characteristics of Sintered Plate Nickel-Cadmium Cells IV. Capacity Tests on Button-Type Cells**

The discharge characteristics of completely sealed button-type Ni-Cd cells made at this institute (CECRI) were studied at subzero (0° to -40°) and room temperatures, and the results were compared with those of imported cells. A higher ohmic drop was indicated in the imported cells. At -40°, the difference between these cells was marked; the CECRI cells gave 46% of their capacity, and the imported cells gave only 15%.

502. **Krishnan, R., Gunaseelam, S., Sabapathi, L., and Rao, P. V.** — 19, 42, (1970)

**Characteristics of Sintered Plate Nickel-Cadmium Cells**
**I. Performance Tests**

Cells were subjected to various discharge rates at room temperature and down to -40°. The capacity at -40° was ~60% of that at 30° and was approximately linear with temperature. Most of the voltage drop during discharge was ohmic in nature.

503. **Sabapathy, R., Santhanakrishnan, S., Chidambaram, Vr., and Rao, P. V.** — 19, 47, (1970)

**Performance Characteristics of Sintered Plate Nickel**

The title cells were subjected to environmental tests based on military specifications. For normal temperature operation, positive-plate capacity was important; however, for low-temperature operation, the negative-plate capacity determines the discharge characteristics. The rate of discharge did not markedly influence the total capacity of the cells.

504. **Prema, R., Rao, P. V., and Udupa, V. K.** — 22, 303, (1973)

**Composite Nickel Powder for Preparing Plaques for Nickel Cadmium Batteries**

For producing sintered matrixes for Ni-Cd battery plates and for fuel-cell electrodes, a process for production of composite Ni powder with inert core materials like $TiO_2$ was developed. The core materials are coated at a high temperature to prepare the oxide-coated core. This is reduced in an H or cracked $NH_3$ atmosphere to obtain the composite powder. Samples prepared from such powder alone have a high electrical resistance; therefore, pure Ni powder must be added to improve the electrical condition so that the sintered plaque can be used as a battery plate. The chemical attack resistance and the polarization characteristics of the composite powder with 50% Ni powder are as good as those of one prepared from pure Ni powder.

## ELECTROCHIMICA ACTA

600. Conway, B. E., Sattar, M. A., and Gilroy, D. 14, 677, (1969)

### Electrochemistry of the Nickel-Oxide Electrode V. Self-Passivation Effects in Oxygen-Evolution Kinetics

Potentiostatic studies on the oxygen-evolution reaction at nickel and oxidized-nickel surfaces reveal inhibition effects (self-passivation) analogous to those found in anodic organic oxidations at the noble metals. Here, however, the inhibiting species (surface oxides) are directly involved in the overall reaction. Similar effects are shown to arise at platinum in alkaline solutions, and comparative experiments are also reported for silver, in which easily distinguishable states of surface oxidation can be related to the oxygen-evolution kinetics at oxidized-silver surfaces.

A kinetic theory of the self-inhibition effects is presented in general terms for various supposed oxidation states of the surface region of the electrode interphase.

601. Sattar, M. A., and Conway, B. E. 14, 695, (1969)

### Electrochemistry of the Nickel-Oxide Electrode VI. Surface Oxidation of Nickel Anodes in Alkaline Solution

Applications of a potentiostatic anodic-step charging method (described in the following paper) have been made to the study of the involvement of surface oxide species in the oxygen-evolution reaction at nickel electrodes in alkaline solution. The potential range covered included a region where faradaic oxygen evolution can occur. Under these conditions, a method based on principles described in the following paper must be adopted, because currents of both a faradaic (for the overall reaction) and a pseudofaradaic (for the surface-charging process) origin pass in a common range of potentials. The potential sweep method under these conditions yields results that are difficult to interpret. Comparison of the results obtained with those from the latter method and from the galvanostatic reduction method is made over appropriate ranges of potential. The formation of various oxide species at the electrode surface is indicated by studies on the stoichiometry of the oxide, as determined by chemical methods. The surface oxide formation or reduction charges are found to be logarithmic with potential up to, and well beyond, apparent monolayer coverage.

602. Conway, B. E., Sattar, M. A., and Gilroy, D. 14, 711, (1969)

**Electrochemistry of the Nickel-Oxide Electrode**
**VII. Potentiostatic Step Method for Study of Adsorbed Intermediates**

A method for calculating the charge associated with deposition of adsorbed intermediates at an electrode surface is derived kinetically for the case of current/time transients arising from a potential step when the steady-state rate of the overall process is changed, as well as the coverage by species involved in that process. As an example, two previously proposed mechanisms for oxygen evolution at an anode surface are considered. The method has been applied experimentally in the preceding paper in this series to the determination of charge and, hence, pseudocapacitance associated with surface species arising in the oxygen-evolution reaction at nickel electrodes under various conditions. The method is also applicable to determinations of charge associated with adsorbed H in the hydrogen-evolution reaction at cathodes.

Limitations of the method are discussed, and applications to the more complex case of oxide growth are briefly considered.

603. Casey, E. J., and Vergette, J. B. 14, 897, (1969)

**On Porous Cadmium Electrodes:**
**I. Characterization,**
**II. Carbonate Removal by Thermal Decomposition**

By means of a new labor-saving instrument for automatic measurement of the charge delivered by porous nickel electrodes impregnated with cadmium as a function of geometric current density, it has been shown that:

(a) The performance is quantitatively dependent upon the free (pore) volume accessible to the solution. A new concept, the "choking index," has been defined and evaluated from the results.

(b) Porous cadmium electrodes contaminated with carbonate can be simply and successfully rejuvenated by thermal cracking of the carbonates, provided that rather critical process boundaries, which have been delineated, are not exceeded.

Possible application to the study of other electrodes and the required theoretical development are indicated.

604. Cowling, R. D., and Riddiford, A. C. 14, 981, (1969)

### The Anodic Behaviour of Cobalt in Alkaline Solutions

The anodic polarization of cobalt in sodium-hydroxide solutions has been studied under potentiostatic and galvanostatic conditions. Only two stages in the oxidation were found. It is suggested that these correspond to the transitions $Co/Co(OH)_2$ and $Co(OH)_2/Co(OH)_3$. The nucleation and growth of the passivating layer of cobaltous hydroxide is discussed by analysis of the current/time curves at various constant potentials.

605. Feuillade, G., and Jacoud, R. 14, 1297, (1969)

### Ionic Transfer During the Anodic Oxidation of Nickel Hydroxide

The aim is to determine the nature and the intensity of the anion transfer that is the basis of the oxidation of bivalent nickel hydroxide obtained in thin layers by cathodic electrodeposition. Isotopic exchange $^{16}O$-$^{18}O$, associated with the estimation of oxygen by means of a nuclear reaction, has been used. Other more blassical physicochemical or isotopic ($^1H$-$^3H$) techniques have also been used. The results show the importance of $OH^-$ ion exchange and permit the calculation of the exchange current and anion self-diffusion coefficient. It is shown that these phenomena are closely related to the irreversibility of ionic transport so that a precise and fixed stoichiometry cannot be found.

606. Euler, K. J. 15, 33, (1970)

### Indirect Factors and Source Occurrences in Porous Separators

By the application of new measuring equipment, separator resistances have been measured much more accurately than previously. Current and voltage were measured, but with movable voltage electrodes. A purely sinusoidal current was used by exactly matching generators and electrode arrangement and by the application of a tuned electronic voltmeter. The possible error of the separator resistance is, for instance, $\Delta R = 0.25\ \Omega\ cm^2 \pm 2.5\%$. The phase angle can be measured within ±1.5 deg.

The separator pores must be filled very carefully with the acid. Shrinkage effects of the separator material may be observed at rising acid density, and some of the pores do not take part in conduction processes until they are "opened" in a sufficiently concentrated acid environment. Between acid and separator material, interactions must be accepted;

however, there is no indication of membrane potentials, the separator resistance being purely ohmic without measurable phase angle.

Changes in separator resistance between -15 and +30°C have been measured. Also, the aging of the resistance has been followed up to 20 months.

607. **Ewe, H. H., and Kalberlah, A.** 15, 1185, (1970)

**Surface Diffusion of Proton During the Oxidation of Nickel**

A porous disk of sintered-nickel powder was placed as a separating diaphragm between two electrolyte-solution spaces, and both its flow resistance for the solution and the electrical diaphragm resistance were measured. By successive anodic oxidations, nickel oxides were produced on the surface, causing a decrease of porosity indicated by an increase of flow resistance; simultaneously, the electrical diaphragm resistance diminished. Thus, the electric current is now carried not only by the ions of the electrolyte in the pores of the nickel disk, but the additional charge transport is assumed to be proton diffusion on the oxidized nickel surface.

608. **Breiter, M. W.** 15, 1297, (1970)

**Dissolution and Passivation of Vertical Porous Zinc Electrodes in Alkaline Solution**

The anodic dissolution and passivation of vertical porous zinc electrodes that were prepared by pressing zinc powder or amalgamated zinc powder into small disks were studied in 6 M KOH + 0.25 M ZnO by measuring potentiostatic current/potential curves at a rate of 1 mV/s and by taking photomicrographs of the electrodes at the beginning of the runs and after repeated cycling. Comparison of the current/potential curves of porous and smooth electrodes demonstrates that only a small fraction of the interior of the different porous electrodes participates in the electrochemical processes. The lower part (about 10%) of vertical electrodes of smooth zinc or pressed zinc powder are much less reactive than the rest of the electrodes. Repeated cycling leads to a finer porosity of electrodes made of zinc powder. Amalgamation (5% to 10%) appears to reduce the latter two effects.

609. **Brook, M. J., and Hampson, N. A.** 15, 1749, (1970)

**The Anodic Behaviour of Zinc in KOH Solution**
**IV. Anodic Experiments in Flowing Electrolyte**

The passivation of zinc electrodes in alkaline solution has been studied at various rates of solution flow. At constant current density, the passivation time is increased by an increase in solution velocity. Passivation-time/current-density data can be correlated in the form

$$(i - i_1)\, t^{1/2} = k,$$

where $i_1$ and $k$ are constants for given systems. In this work, $k$ was slightly dependent on [Zn(II)], but was independent of the solution velocity; $i_1$ was strongly dependent on the solution velocity.

A qualitative model is proposed.

610. **Dennstedt, W., and Loeser, W.** 16, 429, (1971)

**Nickel Hydroxide Electrode**
**III. Thermogravimetric Investigations on Nickel(II) Hydroxides**

Water contained in Ni hydroxide influences its electrochemical reactivity. The water content of $\alpha$- and $\beta$-Ni hydroxides is different with respect to the amount and bond strength. Thermogravimetric experiments show that the water of the $\beta$-Ni hydroxide exceeding the stoichiometric composition is completely removed at 160°. The water contained in the interlayers of the $\alpha$-hydroxide, however, is removed only at higher temperatures, together with the water originating from the decomposition of the hydroxide. These differences are attributed to the formation of H bonds within the interlayers and between interlayers and adjacent main layers. An attempt is made to explain the relations between water content and the oxidizability of the Ni hydroxides.

611. **Hampson, N. A., Lee, J. B., and Morley, J. R.** 16, 637, (1971)

**Electrochemistry of Oxides of Silver. Short Review.**

The electrochemistry of the several Ag oxides that can take part in electrode reactions is reviewed.

612. Takehara, Z., Kato, M., and Yoshizawa, S. 16, 833, (1971)

**Electrode Kinetics of Nickel Hydroxide in Alkaline Solution**

The electrode kinetics of a nickel-hydroxide electrode and the effects of $Li^+$ ions and rare-Earth compounds were studied by the means of observation of decay and growth of polarization and measurement of electrode impedance. From the experimental results, the rate-determining step of the charge and discharge reaction is considered to be the diffusion process of protons and/or defects in the hydroxide layer. The values of $\sqrt{D}/\phi$ or $\sqrt{D}\cdot L$ in the hydroxide layer can be obtained from theoretical treatment of the observed data. These values may be used as the measure of activity of the nickel-hydroxide electrode. By the addition of $Li^+$ ions to the electrolyte, the values of $\sqrt{D}\cdot L$ were increased for charge, but were slightly decreased for the discharge. Such phenomena may be explained as the effect of the $Li^+$ ion, which has lower valency than the nickel ion in nickel hydroxide, an n-type semiconductor during charge and p-type semiconductor during discharge. Then, by addition of rare-Earth compounds to the electrolyte solution, the values of $\sqrt{D}\cdot L$ were slightly increased for charge and discharge, probably because of the increase of active centers on the electrode surface.

613. Vijayavalli, R., Rao, P. V., and Udupa, V. K. 16, 1197, (1971)

**Effect of AC Superimposition on DC in the Cathodic Polarization of Anodized Cadmium in Alkaline Solution**

The polarization behaviour of the cadmium electrode in alkaline solution is of interest in elucidating the mechanism of the negative electrode in the nickel-cadmium battery system. During charging of the negative electrode in service, an a.c. ripple is usually associated with the d.c. The effects of the magnitude of the a.c., and of the ratio of a.c. to d.c., have been studied.

614. Dirkse, T. P., and Hampson, N. A. 16, 2049, (1971)

**The Anodic Behaviour of Zinc in Aqueous KOH Solution**
**I. Passivation Experiments at Very High Current Densities**

The anodic behaviour of zinc in aqueous potassium hydroxide has been investigated at very high current densities (1 to 10 $A/cm^2$). Galvanostatic experiments have been made in aqueous KOH (1 to 12.8 M) for reaction times 0.1 $s^{-0.2}$ ms.

The relationship between the current density and the passivation time follows a $\sqrt{t}$ relationship. The forms of the overpotential/time curves indicate changes in the ohmic component of the total polarization.

Within the time range investigated, no evidence was found for a change in the mode of passivation.

The effect of an increase of temperature was to increase the passivation time: the magnitude of the increase was greater than expected from the increase in the diffusion coefficient alone.

615. **Dirkse, T. P., and Hampson, N. A.** 17, 135, (1972)

**The Zn(II)/An Exchange Reaction in KOH Solution**
**I. Exchange Current Density Measurements Using the Galvanostatic Method**

Exchange current-density determinations have been made using a fast rise-time single-pulse galvanostatic circuit. Measurements are limited to overpotentials of less than ±30 mV, because of the appearance of a peak on the overpotential/time response curve at high current densities. The results indicate that a maximum in the $i_0$/[KOH] correlation occurred at about 8 mol/l. The exchange current density is independent of the zincate concentration.

616. **Dirkse, T. P., and Hampson, N. A.** 17, 387, (1972)

**The Anodic Behaviour of Zinc in Aqueous KOH Solution**
**II. Passivation Experiments Using Linear Sweep Voltammetry**

Potentiodynamic experiments in the range 60-6.0 mV/s, designed to elucidate the processes by which the zinc electrode in alkali becomes passive, are described. At low overpotentials the dissolution process is a complex solution mechanism in which soluble zincate species leave the electrode by the processes of mass transport in solution. At overpotentials in the region 0.4-1.5 V, the dissolution process is slow and involves the formation of a layer of ZnO on the electrode. The lattice dissolves through this layer at a low rate. The electrode is not covered by a mechanically sound film of ZnO until the overpotential has risen to *ca* 1.5 V. It is not possible to decide whether the initially formed film of ZnO comes from the electrolyte or is formed *in situ* on the lattice by direct oxidation.

617. Azim, A. A., and El-Sobki, K. M. 17, 601, (1970)

**On the Mechanism of Passivation of the Cadmium Electrode in Alkaline Solutions**

The electrochemical behaviour of the Cd electrode in 0.1-6 N NaOH has been investigated. Both the potentiostatic and galvanostatic techniques were employed. It has been shown that the electrode surface is primarily covered with a porous layer of $Cd(OH)_2$ which is precipitated from the solution. Above the Flade potential, CdO starts to form at the exposed metal parts. The results are discussed in the light of the dissolution-precipitation and solid-phase transport mechanisms.

618. Bode, H., and Dennstedt, W. 17, 609, (1972)

**Note on the Nickel-Hydroxide Electrode V. Analysis and Electrochemical Behaviour of Cadmium-Nickel Hydroxide**

Cadmium hydroxide dissolves homogeneously in α-nickel hydroxide to 28 mol-% and in β-nickel hydroxide to 10 mol-%. When treated in potassium hydroxide solution, α-cadmium-nickel hydroxide changes to β-cadmium-nickel hydroxide, as in the case of pure α-nickel hydroxide. If the amount of cadmium ions in α-cadmium-nickel hydroxide is higher than the solubility of cadmium ions in β-nickel hydroxide, in the course of the conversion process, the excess of cadmium ions is set free as β-cadmium hydroxide separate from the β-nickel hydroxide.

Electrochemical experiments on sintered plates with bulk electrodes show that β-nickel hydroxide contains an electrochemically inactive amount of cadmium hydroxide, about 10 mol-% dissolved homogeneously in β-nickel hydroxide.

619. Dirkse, T. P., and Hampson, N. A. 17, 813, (1972)

**The Anodic Behaviour of Zinc in Aqueous Solution III. Passivation in Mixed KF-KOH Solutions**

Results on active dissolution of zinc in KOH solutions are presented. The effect of the ionic concentration on the transition time was studied. At constant ionic concentration, increase in [KOH] increases the transition time; at constant [KOH], increase in ionic

concentration decreases the transition time. These two effects satisfactorily account for the maximum observed in transition-time/[KOH] correlations.

620. **Dirkse, T. P., and Hampson, N. A.** 17, 1113, (1972)

**The Zn(II)/Zn Exchange Reaction in KOH Solution**
**III. Exchange Current Measurements Using the Potentiostatic Method**

The results of short-time (50 $\mu$s) and long-time (1000 $\mu$s) potentiostatic experiments are presented. At higher overpotentials (>|10| mV), results are complicated by metallurgical effects. At low overpotentials, the apparent exchange current densities are dependent upon the elapsed time of the experiment. This dependency is discussed in relation to these and previously reported experimental data.

The exchange current densities of systems Zn/Zn(II), $OH^-$ are independent of the zincate-ion concentration in the bulk electrolyte.

The mechanism of the Zn/Zn(II) exchange in alkali is discussed in the light of data presented in this and earlier papers of this series. It is shown that the charge-transfer reaction involves the participation of molecules both of water and hydroxide. The possible reason for this is discussed in the light of the present state of knowledge.

621. **Bagotzky, V. S., Shumilova, N. A., Samoilov, G. P., and Khrushcheva, E. I.** 17, 1625, (1972)

**Electrochemical Oxygen Reduction on Nickel Electrodes in Alkaline Solutions–II**

Electrochemical reduction of oxygen on a nickel electrode in alkaline solutions has been studied using the rotating ring-disk-electrode method. Oxidation of the nickel-electrode surface leads to considerable inhibition of oxygen reduction, accompanied by increased hydrogen-peroxide yields. In LiOH solution, the contribution of the reaction with intermediate hydrogen-peroxide formation is less than that of the KOH solution. The constants of individual reaction steps of the oxygen-reduction reaction have been calculated.

A study has been made of the hydrogen-peroxide reduction, oxidation, and catalytic decomposition of the nickel electrode. Hydrogen peroxide does not undergo decomposition. Increase in the oxidation state of the electrode surface inhibits hydrogen-peroxide reduction, but scarcely affects its electrochemical oxidation.

622. LeBihan, S., and Figlarz, M. 18, 123, (1973)

**A Note to the Article:**
**Nickel-Hydroxide Electrode**
**III. Thermogravimetric Investigations of Nickel(II) Hydroxide**

A critique of a paper by W. Dennstedt and W. Loser (*ibid.* 1971, 16, 429) is given.

623. Ewe, H. H. 18, 127, (1973)

**Surface Diffusion of Oxidized Nickel**

A porous electrode of sintered nickel powder was used as a separating diaphragm between two electrolyte-solution spaces, and its flow resistance for the solution and the electrical diaphragm resistance was measured. The electrode was oxidized on the surface of $Ni(OH)_2$ and NiOOH by galvanostatic or potentiostatic oxidation, causing a decrease of pore volume indicated by an increase of flow resistance. In contrast, under certain conditions, the electrical diaphragm resistance simultaneously diminished. Therefore, the electrical current was carried not only by the ions of the electrolyte in the pores of the electrode, but also by an additonal charge transport, which was assumed to be proton diffusion on the oxidized nickel surface. The thickness of the diffusion layer, the diffusion coefficient, and the temperature dependence of proton diffusion were measured.

624. Merkulova, N. D., Zhutaeva, G. V., Shumilova, N. A., and Bagotzky, V. S. 18, 169, (1973)

**Reactions of Hydrogen Peroxide on a Silver Electrode in Alkaline Solution**

Reactions with hydrogen peroxide on silver in alkaline solutions with $H_2O_2$ concentrations $5 \times 10^{-7}$ mol/ml have been studied with the ring-disk electrode. The amount of oxygen formed on the disk as the result of catalytic decomposition of hydrogen peroxide and its oxidation was established on the ring-electrode made from pyrographite. The rate constants of $H_2O_2$ electrochemical reduction ($k_3$), its oxidation ($k_2'$) and catalytic decomposition ($k_4$), and their dependence on potential have been evaluated. The constant $k_4$ scarcely depends on potential; it is *ca* $10^{-2}$ cm/s.

625. Ratzer-Scheibe, H. J., and Feller, H. G. 18, 175, (1973)

**Dynamic Current Density and Capacity Measurements Using Electrochemical Adsorption Reaction on the Nickel Electrode**

The experimental relations between potentiodynamically measured current-density/ and capacitance/potential curves of the Ni electrode are explained by theoretical derivations of a simple charge-transfer reaction.

In the transpassive potential region, the specific influence of $SO_4^{2-}$ and $HSO_4^-$ ions of the sulphuric-acid electrolyte has been demonstrated by capacitance measurements. Even small additions of $F^-$ ions to the solution greatly influence the electrochemical processes at higher potentials.

The fast potential-sweep method has been used to study the current density in relation to the redox reaction between $Ni(OH)_2$ and NiOOH that occurs in alkaline solution.

626. Euler, K. J. 18, 385, (1973)

**Spatial Current Distribution in Non-Isotropic Conductors (with Implication for Porous Electrodes)**

The geometric situation in practical battery electrodes can be characterized as parallel or antiparallel geometry and cross-current geometry. In the positive pocket plates of alkaline storage batteries, electrons and positive ions penetrate the active mass during its discharge in a parallel direction; e.g., from the perforated steel sheet to the interior of the plate. During charge, or in negative pocket plates, the direction remains parallel, but the direction changes its sign. In layer-built dry-cell stacks, the positive electrodes consist of the usual black-mix made from manganese dioxide and carbon black. The connector is a thin sheet of electronically conducting plastics. During discharge, the electrons and positive ions have nearly opposite directions.

The use of cross-geometry electrodes is much more common than the use of parallel-geometry electrodes. The most important example is the grid plate of automotive or industrial lead-acid secondary cells. Electrons are fed to the active mass coming from the individual grid rods, along the grid plane. Obviously, the ions must migrate perpendicularly to the direction of the electrons. In dry-cell cores and in the tubes of iron-clad plates, a certain amount of the electron current is transported not by the carbon pencil or the lead spine, but by the active mass. The magnitude of the "active mass carried" electronic current depends on the formula and state of discharge of the electrode.

627. Sato, N., and Shimizu, Y. 18, 567, (1973)

### Anodic Oxide on Silver in Alkaline Solution

$Ag_2O$ and AgO formed by potentiostatic oxidation of silver in 0.1N KOH have been chemically analyzed for the mean valency of silver ion. The anodic-oxide formation proceeds in two stages, and the silver ion in the oxide changes from $Ag^+$ to $Ag^{2+}$ at a transition potential. The reduction of AgO at constant cathodic current results from two potential arrests. However, the transition from the first to the second potential arrest does not correspond to the complete reduction of AgO to $Ag_2O$.

628. Justinijanovic, I. N., and Despic, A. R. 18, 709, (1973)

### Some Observations on the Properties of Zinc Electrodeposited from Alkaline Zincate Solutions

Zinc was electrodeposited from alkaline zincate solutions onto steel substrate, and its properties were investigated as a function of overpotential of deposition. The ratio of disperse to compact deposit could be estimated from the results of anodic stripping coulometry. Electron microscopy, stereoscanning electron microscopy, and X-ray diffraction were used to study the morphology, crystal orientation, and lattice parameters, and the BET method was used to obtain information about the specific surface area of the disperse part of the deposit. The yield and degree of dispersion of the disperse (dendritic) deposit increased with overpotential. The lattice parameters indicated residual stress in the compact part of the deposit. In one deposit, the orientation of the compact part was found to be ⟨0001⟩ and that of the dendrites was ⟨1010⟩ or ⟨1120⟩. This selectivity of the two types of growth for particular types of crystal nuclei is explained in terms of a much faster growth on the (1010) or (1120) plane than on the (0001) plane, favored by the structure of the plane at which continuous formation of new layers is possible by the mechanism of unidimensional nucleation.

629. Ambrose, J., and Barradas, R. G. 19, 781, (1974)

### The Electrochemical Formation of $Ag_2O$ in KOH Electrolyte

In recent years, there has been some conflicting information in the literature regarding the initial stages of the formation of a multilayer of $Ag_2O$ by anodic oxidation of Ag in aqueous alkaline solutions. The formation of $Ag_2O$ and the pre-$Ag_2O$ oxidation stages

were reexamined by cyclic voltammetry, rotating disk, and rotating ring-disk electrode techniques to help resolve the controversy. The results support the conclusion that the initial oxidation of Ag is a 1-electron dissolution step controlled by diffusion of a soluble species, $Ag(OH)_2^-$, away from the electrode surface. In addition, the electrochemical findings help to explain the formation of surface phases on the electrode during the process of $Ag_2O$ growth.

## ENERGY CONVERSION

700. Gross, S. 11, 39, (1971)

### Causes of Failure in Sealed Nickel-Cadmium Batteries

Power system reliability for many long-life satellites is determined primarily by the battery. Failures are identified by low discharge voltage, loss of capacity, high self-discharge rate, internal shorts, generation of H (sometimes exploding) loss of electrolyte, or high charge voltage. Some fundamental causes of battery failure are not well understood, because the failure process is slow and hard to diagnose. However, many causes of failure have been identified, including faulty seals, contaminants and foreign objects in the cells, poor manufacturing process control, dendrite formation, sinter corrosion, separator deterioration, migration and redistribution of active material, and shedding of active materials.

701. Ewe, H. H., Justi, E. W., and Kalberlah, A. W. 11, 149, (1971)

### Electrochemical Storage of Energy by Three-Electrode Storage Cells

In outlining the development of a three-electrode storage cell, a detailed assessment is given of an inexpensive electrocatalyst for $O_2$ evolution at minimum overvoltage with the necessary porosity and mechanical strength; the anodic performance of porous Ni in 6*N* KOH was unsatisfactory at 20° and low current density. Carbonyl Ni and Raney Al-Ni powders were also assessed in the activated state after hot-pressing, as well as "preserved" Raney Ni (i.e., activated and preoxidized before hot-pressing); both powders were superior in performance to pure carbonyl Ni. $\gamma$-NiOOH was chiefly catalytically active for $O_2$ evolution. Preserved Raney Ni electrodes were assessed under bilateral loading both with and without electrolyte flushing; without flushing, a limiting-current behavior occurred at relatively low current densities (>60-70 mA/cm$^2$ at 22°). Flushing also aids in the corrosion resistance of $O_2$ anodes with asbestos coatings under positive potential conditions attained under limiting-current condition.

702. Bauer, M., Ewe, H. H., and Justi, E. W. 12, 149, (1972)

**Passivating Oxide Layers on Porous Nickel Electrodes**

The surfaces of Ni battery electrodes in alkaline electrolytes are passivated by formation of a thin layer of NiO by heating for 10 hr at 200°. The resulting electrodes are only very slightly oxidized and are expected to have a long life at higher temperatures. Care must be taken at these temperatures that H is not liberated; otherwise the passivity is lost.

800. Hull, M. N., and Toni, J. E. 67, 1128, (1971)

### Formation and Reduction of Films on Amalgamated and Non-Amalgamated Zinc Electrodes in Alkaline Solutions

The formation of surface films on amalgamated and nonamalgamated zinc electrodes in KOH electrolyte has been investigated by linear sweep voltammetry and by using a rotating-disk electrode and a ring-disk electrode. The results indicate that such films are formed by an adsorption as opposed to a "dissolution-precipitation model." In addition, the cathodic behaviour of both amalgamated and nonamalgamated zinc electrodes subsequent to an anodic oxidation has been studied. For nonamalgamated zinc electrodes in quiescent solutions and for cathodic sweeps commenced in the potential region of zinc passivity, two distinct reduction processes may be distinguished in addition to that which results from reduction of zincate species dissolved in the solution. The former reduction processes result from the reduction of two different types of surface films present on nonamalgamated electrodes following reactivation from the passive state. This behaviour is compared to that of similarly treated amalgamated electrodes where only one reduction process is observed under similar experimental conditions.

801. Briggs, G. W. D., and Fleischmann, M. 67, 2397, (1971)

### Oxidation and Reduction of Nickel Hydroxide at Constant Potential

The electrochemical oxidation of $\alpha$-$Ni(OH)_2$ to $\gamma$-NiOOh follows a composite pattern. A small portion of the charge is taken up by a process controlled by diffusion through the hydroxide layer and the major part by the nucleation and two-dimensional growth of centers of oxidized material. The expanding interface, however, does not necessarily correspond to a phase boundary. The discharge of fully formed layers of NiOOH, as well as the recharging process, is normally controlled by diffusion of species through or within the layer.

## INTERNATIONAL POWER SOURCES SYMPOSIUM

**The 1968 Symposium Proceedings Published in Power Sources 2, 1968, Edited by D. H. Collins, Oriel Press (1970).**

**900. Will, F. G.** 6, 149, (1968)

### Current Distribution and pH Gradients in a Model of a Battery Plate

Measurements have been performed on a scaled-up model of a cadmium battery plate which cannot be performed on an actual battery plate. The model consists of a flat, horizontal cadmium plate arranged so that a highly nonuniform current distribution similar to that in the pores of a battery plate is produced. The distribution of current density, potential, and charge along the model electrode was measured. The occurrence of pH gradients in the thin electrolyte film covering the plate was established. The pH gradients produced local concentration cells that induce the flow of currents between different areas of the plate. The implications of these results for actual battery plates are discussed. Certain capacity loss and recovery phenomena can be readily explained on the basis of the "pH mechanism" that was found in the model.

**901. Sheinhartz, I., and Dickinson, C. D.** 6, 167, (1968)

### Coated Nickel Electrodes

A new high-energy-density, reversible nickle-battery electrode is described. The electrode is made by the direct anodization of an extremely active form of nickel. It has the same potential as the conventional sintered electrode, but it differs in composition and structure. The procedures used to make these electrodes and the results of tests made to characterize them are described.

902. Carson, W. N., Jr., and Hadley, R. L. 6, 181, (1968)

### Rapid Recharging of Nickel-Cadmium Batteries

Rapid recharging capability materially increases the utility of secondary batteries by making it possible to reduce the size of the battery required in many applications, and by making it possible to use secondary batteries in applications heretofore blocked by the need for long recharging times. Rapid recharging of vented nickel-cadmium cells is well established; the cell design provides an end-of-charge signal suitable for reliable control of charging to minimize water losses by electrolysis and overheating caused by excessive rates of overcharging. Rapid recharging of sealed cells requires special control inputs to prevent excessive overcharging of the cell with concomitant unsafe rise in internal gas pressure. Useful inputs are differential voltage input from the cell or battery, auxiliary electrode signals, and coulometer signals. The use of these inputs for charge control and the related circuitry is given; the effect on cell life and behavior is described. Experimentally, tests on very high charging rates appear to show that there is no upper limit on the charging rate that a cell will accept at high efficiency without damage, provided that the cell is not subjected to overcharging at the high rates. Tests were carried out up to the 4000°C rate, which will charge a cell in 1 second. Useful charging rates are determined more by the economic factors involved than by the technical factors.

903. Newton, D. O. 6, 213, (1968)

### Computer Use in Automatic Data Acquisition Systems for Battery Testing

Automated data acquisition systems are desirable for large-volume, routine testing. Hard-wired control of such systems is simple, reliable, and inflexible. Programmed digital computer control is flexible, and can provide feedback control of the experiment. The U.S. Navy has a hard-wired portable battery-testing system that provides cycle control and simple data printout and a computerized submarine battery data-acquisition system.

The ideal computerized system would include the simplest high-speed computer that would handle the input-data and experiment-control assignments and access to a large computer for program preparation, computation, record keeping, and report preparation purposes.

904. Howard, P. L., and Huff, J. R. 6, 401, (1968)

### A Kinetic Study of the Zinc Electrode by Modified Techniques

In order to further the knowledge of the kinetics of the zinc electrode, studies were carried out to determine what takes place at the surface of the zinc electrode in both the anodic and cathodic conditions in 15- to 45-percent potassium-hydroxide solutions over a current range of 5 $\mu$A to 80 mA. This was investigated by: (1) studying the surface concentration gradients at the top and bottom of the electrode with reference electrodes, (2) polarographic studies of the differences between chemical and electrochemically produced reaction products, and (3) analysis of the various solutions by differential thermal analysis.

The results to date indicate that a $Zn(H_2O)_x(OH)_y$ -type complex forms at the surface which may be converted in the bulk electrolyte to $Zn(OH)_4^=$ and Zn(OH) complexes. There is a concentration gradient from top to bottom of the electrode, and the bottom is the most concentrated. This takes place in the surface layer even with the separator present because the surface layer is not penetrated by the separator. This may account for the well-known shape change of the zinc electrode.

905. Dirkse, T. P. 6, 411, (1968)

### A Comparison of Amalgamated and Non-Amalgamated Zinc Electrodes

Amalgamated and nonamalgamated zinc electrodes were compared by measuring the polarization at these electrodes in KOH solutions, by measuring the double-layer capacity of these electrodes, and by the use of cyclic voltammetry. In all cases, the amalgamated electrodes had a larger discharge capacity and a lower double-layer capacitance. The latter suggests that $OH^-$ ion adsorption plays a much larger role in the anodic oxidation of a non-amalgamated electrode than of an amalgamated electrode. However, both types of electrodes seem to be subject to diffusion control in the measurements reported here. There is no unequivocal evidence to determine whether it is the $OH^-$ or zincate ion that is limiting the diffusion process.

**The 1970 Symposium Proceedings Published in Power Sources, 3, Edited by D. H. Collins, Oriel Press, (1971).**

**906. MacArthur, D. M. 7, 91, (1970)**

**Electrochemical Properties of Nickel Hydroxide Electrodes**

Recent work using sintered and film-type electrodes in an effort to understand the reaction mechanism and mode of failure of the hydrated nickel-hydroxide electrode is presented. An experiment to compare the electrochemical precipitation method of positive electrode impregnation with the chemical precipitation method is described; the effect of degree of overcharge and of rate on life-cycle performance was also investigated. No significant difference in the characteristics of the two types of electrodes was found, but overcharge, particularly at high rates, was detrimental.

The preparation of film-type electrodes by nitrate reduction is described and the mechanism of the nitrate reaction is considered using data from rotated ring-disk experiments. The electrochemical characteristics of film-type electrodes and the mode of failure are discussed. It is shown that the addition of chloride ion to the nitrate solution used to prepare the film electrodes leads to electrodes with increased life. Evidence is presented showing that the nickel reaction is primarily a solid-state reaction during which the proton diffuses through the solid. Values for the proton-diffusion coefficient obtained from potential-step experiments are included.

The mechanism of the oxygen reaction on the nickel electrode is considered with particular attention to the potential region where the oxidation state of the nickel changes. A computer-aided method of using this information to predict the charging efficiency curves for a nickel electrode is described.

**907. Barney, D. L., Catotti, A. J., and Pensabene, S. F. 7, 119, (1970)**

**Effect of Carbonate on the Performance of Sealed Nickel-Cadmium Cells**

A study was made of the effect of carbonate on the performance of sealed nickel-cadmium cells. It was shown that the presence of carbonate in sealed cells lowered discharge voltage levels, raised charging voltages, lowered cycle life, decreased charge acceptance, and increased cell pressures on overcharge. Electrode-carbonate interactions responsible for such behavior are proposed. Effects of carbonate on cell performance were studied at charge rates from C/10 to 4 C and discharge rates from 1 C to 10 C. Carbonate levels in cells investigated ranged from 0 to 100 percent.

908. Lerner, S., Lennon, H., and Seiger, H. N. 7, 135, (1970)

**Development of an Alkaline Battery State of Charge Indicator**

Three methods of state-of-charge indication were investigated. These were: (1) use of a specific ion ($K^+$) electrode, (2) the phase-shift method, and (3) the current-sharing in parallel operation of batteries.

Batteries in various states of charge were tested using all three methods. The only method which produced consistent results and allowed state-of-charge determination was the current-sharing method.

A full-size prototype module has been designed, built, and delivered to the Naval Ammunition Depot, Crane, Indiana, for further testing and evaluation.

909. Williams, N. J., Ashcroft, T. B., and Turner, T. S. 7, 149, (1970)

**Porous-Nickel Alkaline-Battery Electrodes Made from Woven Cotton Cloth**

The paper describes the production and testing of nickel battery plates with a novel porous structure derived from woven cotton cloth. The plates are markedly superior in terms of physical properties when compared to loose sintered plates of similar porosity made from carbonyl-nickel powder. The choice of a suitable starting cloth yields electrodes with electrochemical capacities that are superior to those achieved with powder plates of similar porosity.

910. Beccu, K. D., and Stohr, H. 7, 169, (1970)

**Investigation of the Thermal Decomposition of Nickel Ammine Complexes for Producing the Positive, Active Mass in Sintered Electrodes**

The thermal decomposition of suitable nickel complexes has been studied in order to overcome the well-known drawbacks of the nickel-nitrate impregnation process for introducing the positive, active mass into porous sintered plates. Nickel-ammine formate has been found to be one of the most suitable compounds with respect to molar-nickel concentration, solubility in water, decomposition kinetics, and electrochemical activity of the formed product. This product has been analyzed by chemical and X-ray diffraction techniques and found to be highly active nickel which is readily converted during cycling to $Ni(OH)_2$. The thermal

decomposition process achieves impregnation of the porous plates with active mass within a much shorter time than by the chemical nitrate impregnation, avoids corrosive attack of the sintered plate, and leaves no detrimental $NO_3^-$ ions in the active mass.

911. **Hodge, B. J. R., and Lecouffe, Y.** 7, 191, (1970)

**Military Sealed Nickel-Cadmium Batteries**

Sealed, thin sintered-plate, nickel-cadmium rechargeable batteries are compared to other systems and are shown to be the best for a broad spectrum of military applications. Details are given of typical uses by the British and French Armies: for regular deep-cycling (Clansman Radio and Olifant Radar); for occasional use (Entac Missile, Blood Cabinet); and in a last-ditch emergency (Chieftain Tank). Clansman is covered in depth, because it provides a good example of the interdependence of battery and charging system. Finally, there is a report on improving battery performance in high ambients.

912. **Kober, F. P., and Charkey, A.** 7, 309, (1970)

**Nickel-Zinc: A Practical High Energy Secondary Batter**

Nickel-zinc cells having capacities up to 25 Ah have surpassed 350 charge-discharge cycles at energy densities for most of this cycle life in excess of 20 Wh/lb and 1.5 Wh/in.$^3$. Power densities exceeding 100 W/lb have been achieved in cells varying in capacity from 5 to 25 Ah.

The cycle life and capacity maintenance are closely related to charging mode, rate and depth of discharge, and cell construction. The interdependence of these factors has been studied with particular emphasis upon cell construction and charging method. The cycling data will encompass discharge rates varying between C/5 and 4 C and depths of 20 percent to 100 percent of measured capacity.

Cells utilizing a new class of inorganic membranes will be described, and data will be presented. It will be shown how this class of separators promises a significant increase in cycle-life capabilities, thus making Ni-Zn a serious contender for practical high-rate applications.

913. Fydelor, P. J., Messenger, A., Partridge, G., Bant, J. A., and Johnson, D. 7, 327, (1970)

**Development of Graft Copolymers as Separators in Silver Alkaline Cells**

For many years, separators for primary and secondary silver alkaline cells have been produced from cellulosic materials. Separating materials may also be prepared by introducing chemically bonded ionizable groups into inert polymer films. This process is commonly termed graft copolymerization; examples of such a system are polyolefins copolymerized with vinyl-carboxylic acids. Separators based on such graft copolymers have been shown to exhibit greater stability in electrolyte solutions at elevated temperatures and have a much reduced tendency to accumulate metallic silver.

This paper describes the preparation of graft copolymer separators and includes a study of many inert polymer films reacted with ionizable comonomer. Simple electrical and chemical screening tests have been employed to reject unsuitable separators, and a number of selected separators have been subjected to rigorous testing for electrical resistance, stability in electrolyte, and, finally, performance in long-stand primary cells and multiple cycled secondary cells.

914. Dirkse, T. P. 7, 485, (1970)

**Passivation Studies on the Zinc Electrode**

Information relating to the passivation of the zinc electrode in KOH solutions has been obtained. The weight change and the electrode potential of zinc were measured during the anodization process. Diffusion coefficients of the zincate ion have been measured over a temperature range of -30 to 50°C and in a wide range of KOH concentrations. The electrolyte has been analyzed for zincate content at the time the zinc became passive. The results obtained suggest that the dissolving of the passivating film is an important parameter in the kinetics of the anodic zinc processes.

**The 1972 Symposium Proceedings Published in Power Sources, 4, Edited by D. H. Collins, Oriel Press (1973).**

**915. Charkey, A.** **8, 93, (1972)**

### Sealed, Rechargeable Nickel-Zinc Cells

Recent work has shown that vented nickel-zinc cells are capable of 150 to 200 cycles depending on construction and cycling regimen (Charkey, 1969; Sulkes, 1969). Failure modes for cells with conventional electrodes and cellulosic separators have been separator degradation and loss of capacity through zinc penetration and zinc shape change (Kober and Charkey, 1970). Inherent in the operation of a vented system are loss of water during overcharge, carbonation of the electrolyte, and electrode charge imbalance. These conditions require frequent water additions and deep discharge of the cell to 0.0 V to restore the original surplus of zinc oxide. A large excess of ZnO must also be incorporated in the cell as designed to ensure a positive limiting situation during charge which prevents premature shorting through formation of dendritic zinc. These deficiencies have precluded the use of nickel-zinc cells for military and commercial applications presently fulfilled by silver-zinc and nickel-cadmium batteries.

At Energy Research Corporation, work has been in progress to develop a new generation of nickel-zinc cell consistent with long-life operation and economic construction. The developments discussed in this paper are for sealed cells constructed with nonsintered-type active nickel electrodes and inorganic separator systems.

**916. Boden, D. P., and Pearlman, E.** **8, 103, (1972)**

### Nickel-Zinc Cells with Non-Sintered Electrodes

Nickel-zinc cells have been fabricated from positive electrodes prepared by a unique, low-cost milling technique. These cells are capable of being discharged at the 4C rate with little capacity loss. At reduced temperatures, no capacity loss is observed down to -18°C, but, at -30°C, approximately one-half of the room temperature capacity is obtained.

One hundred and sixty full-depth cycles have been obtained when a simple conditioning procedure was applied periodically.

917. Adams, L. B., Fydelor, P. J., Partridge, G., and West, R. H. 8, 141, (1972)

**Functional Aspects of Separators for Silver-Zinc Alkaline Storage Batteries**

Graft copolymer separators, prepared by radiation-initiated grafting of carboxylic acids onto polymer films, have been developed as substitutes for Cellophane in an attempt to improve the shelf life and cycling performance of silver-zinc batteries.

Comparison of the properties of films prepared by various grafting techniques and of their performance as battery separators are given. The results obtained from the structural analysis of the materials before and after use are outlined.

Various methods of preparing graft copolymer materials as an integral part of the electrode structure are discussed, and their performance is compared to that of wrapped film separators.

918. Wales, C. P. 8, 163, (1972)

**Effects of KOH Concentration on Morphology and Electrical Characteristics of Sintered Silver Electrodes**

The electrodes were cycled in 25 to 45 percent KOH, and structural changes were noted. Capacity at the 20-hr discharge rate was best in 45 percent KOH. Discharges at the 1-hr rate produced smaller silver particles and better capacity. These smaller particles (mainly 0.5 to 5 $\mu$m instead of 5 to 20 $\mu$m) could be oxidized more completely during charge. Conductivity became a problem when electrodes were discharged at the 1-hr rate in 45% KOH because the small silver particles oxidized almost completely to AgO near the current-carrying grid unless sufficient large silver particles were present. Conductivity was not a problem when slow discharges formed large particles.

919. Schwartz, H. J., and Soltis, D. G. 8, 185, (1972)

**A Versatile Silver Oxide-Zinc Battery for Synchronous Orbit and Planetary Missions**

A new kind of silver-zinc cell has been developed and tested under NASA support which can withstand severe heat sterilization requirements and does not display the traditional life-limiting aspect of zinc electrodes (i.e., shape change). These cells could be used on a

planetary lander mission that requires wet-stand periods of over 1 year and a modest number of cycles (400 to 500), and may require dry-heat sterilization. The weight advantage of these cells over the traditional nickel-cadmium batteries also makes them an attractive alternative for synchronous orbit service where 400 to 500 cycles would be required over a 5-year period.

920. Kelson, P., Sperrin, A. D., and Tye, F. L. 8, 201, (1972)

**The Behaviour of Sintered Plate Nickel Hydroxide Electrodes in Lithiated Electrolyte Solutions**

The importance of measuring true charge acceptance when studying the charge/discharge behaviour of nickel-hydroxide electrodes is discussed, and two techniques developed for this purpose are described. The quantitative effects of additional lithium hydroxide to the electrolyte on charge acceptance at charge rates between 0.05C and 0.65C in the range 10°C to 70°C have been investigated. Lithium is shown to improve charge acceptance significantly only at temperatures above 35°C, except at very low charge rates when some improvement is obtained at lower temperatures. Discharge efficiency is unaffected. The mechanism by which lithium affects electrode behaviour has been examined by considering the charge/discharge potentials observed in pure potassium hydroxide and lithiated electrolyte.

921. Bring, B., and Landstedt, S. 8, 243, (1972)

**Studies on Current Distribution at Nickel and Cadmium Electrodes by Laser Interferometry**

An optical method has been used for measuring local current densities in the electrolyte close to the electrodes. The basic components and principles of operation of a laser interferometer are described. The paper discusses variations in the density of hydroxyl ions and explains the origin of the heat observed. On the basis of these discussions, it is shown that the local current density can be measured from interferograms. As a result, it is shown that the current-density distribution is not critical for either sintered or pocket-type electrodes at the current densities used.

922. Gross, S., and Malcolm, J. 8, 257, (1972)

**Thermal Considerations of Sealed Nickel-Cadmium Batteries**

Nickel-cadmium cells were tested and analyzed to predict thermal behaviour for battery designs that provide improved thermal performance. Correlations have been developed to accurately predict cell-heat generation and thermal-joint resistance. A thermal model was derived, experimentally verified, and then used to conduct a parametric study of the variables that determine the effectiveness of the packaging design. Cooling arrangement, materials, and heat-generation uniformity were variables.

923. Ford, F. E. 8, 277, (1972)

**Characterization of the 20-Ah Nickel-Cadmium Cell Used for Energy Storage on the Orbiting Astronomical Observatory**

Tests were conducted on 20-Ah sealed nickel-cadmium cells to evaluate initial and long-term performance at various charge rates, temperatures, and voltage-control levels. An average ampere-hour recharge of 103 percent per orbit at 13°C was sufficient for maintaining cell capacity; required watt-hour recharge on an orbital basis was 8 to 10% greater than required ampere-hour recharge. Cells exhibited an early life "burn-in" characteristic. A discharge after periods of repetitive cycling yielded two voltage plateaus that were temporarily eliminated by the discharge. There was a degradation in the amount of watt-hours a battery will store with life, but the amount of watt-hours attainable on discharge to 1.0 V/cell at any specific point in the life is essentially constant, the difference being the voltage at which the watt-hours can be attained.

924. Przybyla, F., and Ramsay, G. R. 8, 401, (1972)

**Passivation of a Porous Cadmium Electrode in Potassium Hydroxide Solution**

Passivation time of a porous cadmium anode in 31 percent KOH solution was determined as a function of porosity and current density for the temperature range -40°C to +23°C. Curves depicting passivation time versus initial porosity show a maximum near 66 percent. A relationship between passivation time, apparent current density, and temperature is derived.

## INTERSOCIETY ENERGY CONVERSION ENGINEERING CONFERENCE PROCEEDINGS*

**1000.** **Briggs, D. C., and Preusse, K. E.** 3, 13, (1968)

### Hermetically Sealed Nickel-Cadmium Batteries for the Initial Defense Communication Satellite Program/Augmentation (IDCSP/A)

This paper describes the IDCSP/A satellite battery design, testing, and integration concepts that are generally applicable to nickel-cadmium battery designs for synchronous satellites. The selected battery design employs two parallel batteries consisting of sixteen series-connected, 6-Ah hermetically sealed nickel-cadmium cells. The results of the development test program, which substantiate the design concepts, are presented.

**1001.** **Dunlop, J. D., and Bounds, R. W.** 3, 19, (1968)

### Adhydrode Control of Ni-Cd Battery Charging to Evaluate Charging Methods

In addition to its normal application, controlling overcharge, the "adhydrode" was used to compare pulse charging with constant current charging methods. A charge control circuit utilizing a differential comparator integrated circuit was developed. The results showed that pulse charging offers no significant advantages. However, the adhydrode charge control provides a reliable means for minimizing overcharge, extending cycle life at deep depths of discharge. For satellite application, the potential advantage is to increase usable energy density.

**1002.** **Lutwack, R.** 3, 25, (1968)

### Progress in Development of Heat-Sterilizable Ag-Zn Battery

The NASA-JPL heat-sterilizable battery program is comprised of efforts to develop: (1) the Ag-Zn, the Ag-Cd, and the Ni-Cd systems, and (2) the separator materials for the Ag-Zn system. The most extensive work has been done on the separator and the Ag-Zn

*Published by the American Society of Mechanical Engineers, 345 East 47th Street, New York, N.Y. 10017.

cell developments. The first phase of the Ag-Zn work, which is almost completed, is composed of studies in electrochemistry, cell fabrication, cell sealing, and designs for an impact-resistant cell. A second phase, which is now underway, is for the design, fabrication, and testing of primary and secondary batteries of various sizes, some of which have a high-impact requirement. The Ag-Zn program is being supplemented by Ni-Cd and remotely activated battery developments.

1003. **Meredith, R. E., and Uchiyama, A. A.** 3, 32, (1968)

**Theoretical Evaluation of Hot Spot Temperature of Silver-Zinc Batteries**

The hot-spot temperature (the maximum temperature increase at the center of a battery) has been theoretically examined for silver-zinc batteries. Such temperatures have been tabulated for various types of rectangular battery dimensions as a function of the current drawn from the battery, the number of battery electrodes, and the thermal conductivity parallel to the electrode surfaces. All computations were for isothermal wall conditions of 77°F (25°C) without heat sinking between cells.

1004. **Gross, S.** 3, 38, (1968)

**Heat Generation in Sealed Batteries**

Accurate prediction of heat generation is important in many applications for spacecraft. This paper provides analytical methods for heat-generation prediction. Heat-generation measurements are described, and correlation between predicted heat generation and test results is discussed. Experimental data are presented for nickel-cadmium, silver-cadmium, and silver-zinc cells. For example, overcharge ratio was found to be a critical parameter affecting heat generation in nickel-cadmium cells. Heat generation in silver-cadmium cells could be accurately predicted, using an enthalpy-voltage ranging from 1.3 volts to 1.43 volts. Limited tests on silver-zinc primary cells showed that the heat-generation rate during discharge was about 15 percent of the delivered power.

1005. **Hamlen, R. P., Siwek, E. G., Rampel, G., Wechsler, L. D., and Zampini, J.** — **4, 339, (1969)**

**Studies of Implantable Nickel Cadmium Cells for Heart Assist Devices**

The purpose of this work is the development of an implantable, rechargeable nickel-cadmium battery system with high efficiency and rapid-recharge capability. Auxiliary electrodes, along with appropriate charge-control circuitry, are employed to sense internal cell pressure and to control the charging current. Several cell types, designed for high temperature charge acceptance, are being evaluated. These cells are being tested at the 1- and 2-hour charge rates and the 0.75-hour discharge rate at body temperature. Three-cell batteries of two-terminal 4-Ah cells have also been cycled at body temperature at the 8-hour charge rate and the 1-hour discharge rate to observe changes in capacity and in charging efficiency.

1006. **Preusse, K. E., Shair, R. C., Betz, F. E., and Sylvia, J.** — **4, 705, (1969)**

**Parametric Charge Studies for Aerospace Nickel-Cadmium Batteries**

A common method of charge control in satellite vehicles is a two-step constant-current mode. This paper offers parametrically, as a function of capacity removed, the interrelationship of depth of discharge, limiting voltage, charge rate, and environmental temperature. Conclusions are based on the results of experiments conducted on conventional Gulton aerospace nickel-cadmium cells and Gulton adhydrode (third electrode) cells.

1007. **Seiger, H. N., Charlip, S., and Lerner, S.** — **4, 710, (1969)**

**Electrical Characteristics of a Sealed Nickel-Cadmium Battery Having a Bipolar Construction**

The bipolar construction eliminates intercell connectors and reduces internal resistance, giving the battery high rate capacilities and high specific power. Its ability to deliver high-power bursts is not dependent on capacity alone. It is a function of electrode area affecting current densities. Discharge characteristics, as a function of rate and temperature, as well as advantages and economics, are discussed.

**1008.** **Von Hartmann, W.** **4, 715, (1969)**

### The Application of Bench Tests in the Development of Heat-Sterilizable Battery Separators

The requirement that a spacecraft battery be heat-sterilizable places some strain on present technology. Among the affected components, the separator has been known to suffer considerably during sterilization. In order to reduce, if not eliminate, separator-related problems, the Jet Propulsion Laboratory (JPL) elected several years ago to contract with various firms throughout the United States to conduct research and development programs leading to a heat-sterilizable battery separator. At the same time, a limited in-house program was initiated with the aim of setting up test procedures for separator materials. This paper deals with this test program and its role in the continuing development of better separator materials.

**1009.** **Teresa, M. J., and Corbett, R. E.** **4, 721, (1969)**

### Two Year Flight Performance of the Lockheed Type XI Nickel-Cadmium Battery

A total of twelve Type-XI, 20-Ah nickel-cadmium (Ni-Cd) batteries have been flown on space vehicles. More than 40,000 vehicle operating hours were achieved without a power system failure. A total of 48,000 accumulated charge/discharge cycles were experienced by eight of these batteries over a variety of environmental and operational conditions. During these flights, the Type-XI battery has exhibited a high level of reliable, consistent, and predictable behavior.

The extensive ground and flight-test experience gained with this and similar Ni-Cd batteries has enabled Lockheed design and reliability personnel to assign a failure rate of one failure per million hours of operation to this device.

**1010.** **Charkey, A., and Klein, M.** **5, 1–5, (1970)**

### High Energy Density Nickel-Cadmium Cells

Based on recent developments in electrode technology, nickel-cadmium cells with improved energy density over conventional sintered-plate-type cells have been fabricated and

tested. These cells yield over 200 Wh/lb at rates of discharge from C/5 to C/2. Neither the positive nor negative electrodes employ any elemental nickel, which is the major weight savings of this new design. Test cells of 4-10 Ah capacities have demonstrated cycle lives of more than 200 cycles at 70% depth of discharge. Novel electrode-fabrication methods have been devised which promise to greatly reduce the cost of the nickel-cadmium system.

**1011. Charlip, S., and Lerner, S.** 5, 5–6, (1970)

**Electrical Characteristics of Nickel-Zinc Secondary Cells**

The nickel-zinc electrochemical system possesses unique performance characteristics that make it a desirable source of stored energy. It has a high rate capability with an energy density of about 25 Wh/lb. It has a flat voltage curve on discharge and good wet shelf life with moderate cycle life capabilities.

This paper discusses several design parameters of the zinc electrode and gives discharge characteristics of several nickel-zinc cells as a function of discharge rate and temperature. Capacities versus cycle life are given for 112 cycles. Advantages and economics are discussed.

**1012. Wilson, J. K., Standlee, D., Kinsey, R. H., and Self, S. R.** 5, 5–9, (1970)

**High Energy Density Long Life Secondary Silver-Zinc Batteries**

This paper presents the design, development, and usage history of a long-life, 7500-Wh secondary silver oxide-zinc battery.

Design and development data include plate separation design, charge-control technique, optimization of positive-plate state-of-charge for minimum on-charge voltage, as well as the results of environmental and thermal characterization testing.

1013. Kirsch, W. W., and Shikoh, A. 5, 5–21, (1970)

### Nickel-Cadmium Battery Evaluation for Apollo Telescope Mount Application

This report summarizes the operational testing and evaluation program conducted by Marshall Space Flight Center on nickel-cadmium (Ni-Cd) batteries for use on the Apollo Telescope Mount (ATM). The test program was initiated in 1967 to determine if the batteries could meet ATM mission requirements and to determine operating characteristics and methods. The ATM system power and battery-charging power for the Ni-Cd secondary batteries is provided by a solar array during the 58-minute daylight portion of the orbit; during the 36-minute night portion of the orbit, the Ni-Cd secondary batteries will supply ATM system power.

The test results herein reflect battery operating characteristics and parameters relative to simulated ATM orbital test conditions. Maximum voltage, charge requirements, capacity, temperature, and cyclic (charge/discharge) characteristics are presented.

1014. Coggi, J. V. 5, 7–20, (1970)

### Heat Pipe Thermal Control of Spacecraft Batteries

The lifetime and performance of spacecraft nickel-cadmium (Ni-Cd) battery subsystems can be improved by maintaining the battery at constant temperature by using a variable conductive heat-pipe cooling system. This paper describes an experimental program to: (1) define battery thermal losses, (2) reduce battery centerline temperatures by optimizing the resistance path to the heat sink, and (3) develop reliable, constant-temperature battery thermal-control systems.

The battery efficiency and thermal losses for 20-Ah Ni-Cd cells were measured as a function of operating temperature, charge and discharge rate, and overcharge ratio. A Ni-Cd battery was then combined with a heat-pipe temperature-control system and operated under simulated Earth-orbital space-station power-load profiles. The heat-pipe system was able to control the battery temperature within a range of ±4°F under severe thermal and electrical loads.

1015. Shinbrot, C. H., and Tonelli, A. D. 6, 152, (1971)

**Advance Deployment Solar Cell Battery Power System Development**

The results of design studies and hardware tests that are in progress under an in-house McDonnell Douglas development program are presented. Development efforts have been centered in three areas: (1) acquisition and development of accurate test equipment and flight-type components for *in-situ* power-system tests, (2) sealed Ni-Cd battery and third-electrode baseline performance tests, and (3) environmental tests of isogrid and flexible solar-cell arrays. The unique test facility includes an electronic solar-cell simulator that duplicates solar-cell array current-voltage characteristics within a wide range, including open-circuit voltage of 0 to 125 V, short-circuit current of 0 to 32 A, and peak power point to a maximum of 2600 W.

1016. Breeskin, S. D., and Taylor, A. D. 6, 181, (1971)

**Battery and Third Electrode Performance Characteristics for Varying Charge and Discharge Rates**

This paper presents the results of an in-house McDonnell Douglas development program to investigate battery system performance for long-duration manned and unmanned spacecraft. The objectives of the program were to determine baseline performance characteristics for nickel-cadmium batteries and to develop battery and end-of-charge control-system designs specifically optimized for use on future satellites and manned spacecraft.

Baseline performance characteristics were obtained for seven different constant-current charge and discharge rates for a 20-Ah, 24-cell, sealed, nickel-cadmium battery at ambient temperature.

1017. Gaz, R. A. 6, 188, (1971)

**Battery Cell with Third Electrode Performance Test Results**

The objective of this study was to determine the thermal and electrical performance characteristics of a sealed, 20-Ah nickel-cadmium cell. Electrical measurements were obtained to determine: (1) the cell and the third-electrode voltage characteristics for temperatures between 30 and 80°F, and (2) cell and third-electrode performance as a function of charge and discharge rate for a controlled temperature of 50°F for monitoring resistance values of

250 and 600 ohms. In addition, the cell heat-generation rate was determined as a function of the discharge rate. The tests were conducted to obtain the characteristics of one battery cell prior to performing overall battery and system integration tests.

1018. **Stockel, J. F., Van Ommering, G., Swette, L., and Gaines, L.** 7, 87, (1972)

**A Nickel-Hydrogen Secondary Cell for Synchronous Orbit Application**

Nickel-hydrogen cells were constructed and cycle tested. Both single electrode and multielectrode cells were employed in the test program. A study of the multielectrode configuration was made to determine if this cell was capable of achieving a useful energy density.

The multielectrode cells consist of modules containing a nickel/nickel-hydroxide electrode sandwiched between two separator disks and two gas-diffusion electrodes with high activity as hydrogen electrodes. The modules, separated by gas-diffusion screens, are electrically connected in parallel and are enclosed in a cylindrical pressure vessel.

The cells were cycle tested in modes applicable to synchronous-orbit operation. Different types of nickel electrodes were tested in single-electrode cells. Stable cycle performance was observed. The cells demonstrated good overcharge and reversal protection qualities.

1019. **Menard, C. J.** 7, 95, (1972)

**High Energy Density Nickel-Cadmium Batteries**

Data are presented for high energy density, sealed cylindrical-type cells that yield between 22 to 27 Wh/lb at the 5-hr rate discharge, depending on electrode configurations and cell size. The cathode and anode in these cells consist of porous sintered-nickel substrates loaded with their respective active materials. The cell construction is that of the conventional coiled-electrode design. The increase in energy density over commerical cells is accomplished through improvements in the internal cell components.

The performance characteristics of these high energy density systems are discussed. Projections are made for future high energy density nickel-cadmium batteries based on the cylindircal cell data and experience on other nickel-cadmium designs.

1020. Fono, P. 7, 98, (1972)

### Spacecraft Nickel-Cadmium Battery Cycle-Life Assessment

Spacecraft battery design requires information on battery cycle life. Most of the battery cycle-life test data published to date were taken under simulated low-altitude Earth-orbit conditions. Cycle-life tests that were conducted by various testing laboratories are compared with tests conducted at the Navy's Quality Evaluation Laboratory, Crane, Indiana.

The analysis of the battery-life information indicates a relationship between cycle-life and cycle duration. Cycle-life curves for cycles of different time durations are constructed and presented.

1021. Kerr, R. L., and Stager, D. N. 7, 103, (1972)

### Kilowatt Battery Systems

High energy density, kilowatt-level battery systems are being developed to meet new spacecraft needs. The goals of systems supplying 1 and 2 kW of power, respectively, to a spacecraft in synchronous orbit are 7 and 8 Wh/lb with 7 years of life at 0.95 reliability. The systems are radiation-hardened and are compatible with typical spacecraft internal temperatures and bus voltage. A high depth-of-discharge allows maximum use of energy. Electronics for both forward and reverse cell-current bypass provide maximum cell protection and recharge capability. Added cells in series provide for individual cell degradation or failure. Oxygen-sensing electrode signals control charging through reliable electronics. The battery average temperature of 40°F is maintained by variable conductance heat pipes connecting the battery system to an external spacecraft radiator. One complete 1-kW prototype system has been assembled and is on life test.

1022. Charkey, A. 7, 110, (1972)

### Nickel-Zinc Cells for Sustained High Rate Discharge Applications

Although the nickel-zinc couple has been studied since the late 1920's and early 1930's, its development into a viable battery system has been extremely limited and subject to many technological questions. A flurry of activity again erupted in the late 1960's when the nickel-zinc system was "redeveloped" using components "borrowed" from sintered-plate

nickel-cadmium and high-rate silver-zinc cells. The performance obtained from these cells were scattered with cycle life ranging from 100 to 250 cycles on moderately low-rate discharge regimens.

Cycle-life capabilities of these cells were usually limited by capacity loss through zinc shorting, zinc-shape charge, and separator degradation. From the total performance and manufacturing standpoint, even good performance was subject to the weight limitations of the sintered positive electrode and the high cost of battery production. The resultant battery was therefore only moderately superior to nickel-cadmium on an energy-density and cost basis.

At Energy Research Corporation, work is in progress to develop a new generation of nickel-zinc cells consistent with long-life operation and economic construction. The developments discussed here will be confined to a particular cell that was designed for high-rate discharge applications (i.e., 8C rate) for application as the propulsion system for a torpedo-target drone.

**1023. Snider, W. E., and Nagle, W. J.** **7, 125, (1972)**

**Non-Leaking Battery Terminals**

The potassium-hydroxide (KOH) electrolyte used in conventional alkaline batteries is contained in a metal case and cover, with ceramic insulators around the terminals. The silver-zinc or silver-cadmium batteries using a potassium-hydroxide (KOH) electrolyte require a plastic battery case and cover to prevent internal shorting of the battery. Covering of the interior of a metal case and cover with plastic has not been satisfactory. The previous terminal seals on silver-zinc battery cases and covers have not been successful for extended periods of time. The use of silver-zinc or silver-cadmium batteries for space vehicles or satellites require an extended life up to 5 years with a 100-percent reliability. Previous designs have failed at as low as 9 months.

Three different terminals were designed for use in a 40-Ah silver-zinc battery that has a 45-percent KOH by weight electrolyte in a plastic battery case.

**1024. Kirsch, W. W.** **8, 78, (1973)**

**Nickel-Cadmium Battery Performance Prediction Models**
**Apollo Telescope Mount Application**

This paper describes the experimental design, testing and results, and subsequent Ni-Cd battery-performance prediction-model development.

Two deterministic performance models were developed. A capacity-degradation model describes the expected usable battery capacity as a function of time, temperature, and depth of discharge. Both transient and steady-state parameter variations are considered.

A cyclic charge/discharge model was developed which describes charge and discharge voltages as a function of state of charge over a range of temperatures, charge and discharge rates, and electrical loads. Average cyclic characteristics such as heat, efficiency, and recharge fraction are also included.

**1025. Haas, R. J., and Briggs, D. C.** 8, 116, (1973)

**High Energy Density Silver-Hydrogen Cells for Space and Terrestrial Applications**

This paper describes the performance and design characteristics of silver-hydrogen cells developed by Philco-Ford Corporation. The first phase of this program encompassed design and electrical cycling of single and multiple-plate cells. Based on the high-rate (2C), long cycle-life performance demonstrated by these cells, a series of production-type 4.0- and 20.0-Ah cells were designed, constructed, and electrically characterized. The basic cell design consists of rectangular silver and catalized fuel-cell plates alternately stacked in a hermetically sealed prismatic container. Electrical connection is provided by ceramic-metal seals. Heat is dissipated from the cell core through the flat container surfaces to intercostal thermal shunts, minimizing temperature gradients within the cell. Production-type silver-hydrogen cells have been electrically characterized and life-tested. In general, the performance indicates that this design is capable of producing energy densities in excess of 60 Wh/lb. Life tests presented in this paper show that these cells can deliver at least 600 deep-discharge cycles (i.e., 80 to 90 percent of name-plate capacity) at 20°C. Cell voltage-polarization data for high-rate pulse loads demonstrate that the silver-hydrogen cell has an excellent power-density capability.

**1026. Klein, M., and Baker, B. S.** 9, 118, (1974)

**Nickel-Hydrogen Battery System**

The nickel-hydrogen secondary battery system offers the advantages of long cycle life, insensitivity to overcharge, and reversal and high energy density.

By using single cylindrical self-contained cells as a building block, the system constraints are reviewed. Consideration is given to heat generation and transfer, charge/overcharge

control, multicell grouping, and individual cell bypass. By using existing cells, it is estimated that a 28-volt 50-Ah battery run at 80% depth will deliver 18 Wh/lb, and near-term improvements will raise this to 20 Wh/lb.

1027. Gandel, M. G., Chang, R., and Harsch, W. C. 9, 123, (1974)

**Nickel-Hydrogen Battery Development for Synchronous Satellites**

In order to meet critical weight limitations in long-life synchronous satellites, Lockheed Missile and Space Company has been pursuing the development of nickel-hydrogen batteries. Weight, power, reliability, and mission capability are critical tradeoffs; in communications satellites, the number of channels is linear with power. Ni-$H_2$ now offers a viable alternative to Ni-Cd batteries for energy storage in solar-powered satellites, with a potential 50-percent weight savings.

*The Lockheed program includes cell development contracted to Eagle-Picher. The* effort is directed to development of a Ni-$H_2$ cell design and battery configuration that can be integrated into a satellite and offer significant advantages over nickel-cadmium. The cell's thin-wall, hydrogen-pressure-vessel design imposes a number of mechanical, thermal, and reliability constraints that are being tested. Results to date are presented.

1028. Fono, P. 9, 128, (1974)

**Battery and Cell Redundancy Considerations for Long Duration Space Missions**

The redundancy requirements in spacecraft nickel-cadmium battery systems are analyzed. Failure modes of both the batteries and control circuits are considered. Designs with multiple batteries are compared to those with single batteries that incorporate cell-failure protection and series-redundant cells to meet reliability goals. Battery control and load-sharing circuit efficiencies are evaluated for battery sizing. Sample designs are made for both 50- and 100-Ah batteries. Battery-system weights are determined as a function of bus voltage with either boost- or buck-discharge regulators. Both low Earth-orbit and synchronous-orbit missions are considered. The functional and weight analyses indicate that multiple batteries seem to be an acceptable compromise between the minimum weight and minimum cost systems. For voltages above 100 volts, a single battery should be seriously considered.

1029. Corbett, R. E., Glass, M. C., and Matsui, R. G. 9, 137, (1974)

**Development of a Power Module Using Third-Electrode Battery-Charge Control**

The module contains the power controls and telemetry instrumentation and commands required for all power-system functions. These include undervoltage load-switching provisions; battery overtemperature protection circuits; trickle-charge circuits; system current, voltage, and temperature instrumentation; and ground-equipment interfaces. The unit is designed to work with an unregulated solar-array input.

In the final assembly, two battery units attach to the structural member on which are mounted all electronic boards and large components (power controls) not integral to the batteries. This permits equipment-level acceptance testing of the batteries and the power-control assembly prior to final assembly. The unit was qualified at the module level under sine, random, shock, and thermal-vacuum cycling environments.

1030. Levy, E., Jr., and Rogers, H. H. 9, 846, (1974)

**Spacecraft Integration and Problem Area Studies on Nickel Hydrogen Cells**

Nickel-hydrogen cell electrochemistry and performance previously described in the literature have led to predictions of long-life lightweight cells that would offer considerable advantages over current nickel-cadmium cells. The studies described in this paper consider the problems of assembling cells into batteries and mounting the cells/batteries on spacecraft, with proper consideration of important interface factors. Also presented are two problem areas observed during cell development and test which provide additional insight into nickel-hydrogen-cell operation.

1031. Seiger, H. N., Puglisi, V. J., Ritterman, P. F., and Pickett, D. F. 9, 868, (1974)

**High Energy Density Sintered Plate Type Sealed Nickel Cadmium Battery Cells I. The Positive Electrode/Plaque Relationships**

This paper, the first of a series, describes the work done in these laboratories to accomplish the goals. This paper deals with the physical and chemical interaction of the

sintered-plaque material and the behavior of highly loaded positive electrodes. The work has: (1) produced experimental evidence that the use of active materials depends rather strongly on sinter porosity, (2) indicated that there appears to be an upper limit to the loading of active material ($Ni(OH)_2$) into the voids present in the plaque, and (3) produced a hypothesis that reasonably explains the blistering that is often observed in positive electrodes and the thickening of positive electrodes that usually occurs even after cell manufacture. These topics are important in designing and processing plaques into positive electrodes for the higher energy densities desired.

1032. **Puglisi, V. J., Seiger, H. N., and Pickett, D. F.** 9, 873, (1974)

**High Energy Density Sintered Plate Type Nickel-Cadmium Battery Cells II. Electrochemical Impregnation Methods to Produce Nickel Oxide Electrodes**

A resurgence of interest in the feasibility of electrochemical methods of impregnating plaque with active material to produce $Ni(OH)_2/\beta$-NiOOH electrodes has surfaced in recent years. The advantages have always been apparent and include fast process times, a one-step impregnation, minimal plate handling, and the use of less concentrated solutions. The primary stimulus, however, has been an attempt to obtain an increase in cell energy-density from the present state-of-the-art 15 to 17 Wh/lb to 20 Wh/lb. The disadvantages include the need for a more technologically sophisticated facility and the need for undertaking a development program to establish the conditions which would result in a process competitive both economically and product quality wise, with those presently being used.

The nickel-oxide electrode impregnation processes differ with respect to both bath makeup and temperature. This paper reports the effort to produce high specific-capacity nickel-oxide electrodes by using electrochemical impregnation techniques as presently being carried out by Heliotek-WPAF Aeropropulsion Laboratories.

1033. **Juvinall, G. L., Luksha, E., and Menard, C. J.** 9, 881, (1974)

**A Novel Negative-Limited Sealed Nickel-Cadmium Cell**

The development of the negative-limited, sealed, nickel-cadmium cells described in this paper stems from a need for a reliable cell that is essentially free of gassing during operation. Elimination of the gassing problem results in a long-lived cell that is immune to catastrophic failure and does not require the complex charge-control systems used by conventional cells.

The new cell is designed to be negative-limited on charge and uses a negative electrode that incorporates a substrate possessing high-hydrogen overvoltage characteristics. The negative-limited feature of the cell precludes the formation of appreciable amounts of oxygen because the positive electrode is never overcharged. The effect of the high hydrogen overvoltage substrate is to provide a rapid rise in voltage at the end-of-charge, which is used to terminate charge and prevent the formation of hydrogen. Thus, the performance of the cell under controlled conditions is essentially gas-free.

1034. Easter, R. W. 9, 888, (1974)

**Predicted Energy Densities for Nickel-Hydrogen and Silver-Hydrogen Cells Embodying Metallic Hydrides for Hydrogen Storage**

Considerable interest in metal-hydrogen secondary batteries exists, especially in nickel-hydrogen and, to a lesser extent, silver-hydrogen batteries. Metal-hydrogen batteries offer higher gravimetric energy densities (Wh/kilogram) than do the nickel-cadmium cells presently used in space applications, and the cycle life (of the nickel-hydrogen at least) is potentially comparable. Silver-hydrogen offers a substantial increase in gravimetric energy density relative to nickel-hydrogen but with considerably lower cycle lifetimes. Other attractive features of metal-hydrogen systems are deep discharge capability, insensitivity to overcharge and overdischarge, and the availability of the hydrogen pressure as a state-of-charge indicator.

1100. Newman, B. 23, 56, (1969)

**Demand-Pulse Charging for Nickel-Cadmium Batteries**

This paper presents the design and block diagram of the demand-pulse charger—a new system for battery charging in preference to constant voltage or current charging suitable for Ni-Cd cells. The device could provide rapid charging and has self-feedback tendencies that can automatically adjust for cell and battery variations. This allows battery charging until the upper trip voltage is reached, at which point the charge current is interrupted and stays off until the battery voltage decays to the lower trip voltage, when the current is reapplied and the cycle continues. The battery first receives a long pulse when 80 to 90% of the charge is restored. The system tends to equalize because of the continuance of the cyclic action of shorter and shorter pulses spaced farther and farther apart until 100% of the charge is restored. The mismatched cells tend to equalize, low-temperature battery performance improves, and rapid deterioration and failures are avoided.

1101. Ford, F. E., and Henningan, T. J. 24, 1, (1970)

**Nickel-Cadmium Batteries for the Orbiting Astronomical Observatory Spacecraft—II (OAO)**

The batteries for the OAO-2 spacecraft consist of three groups of 21 series-connected 20-Ah Ni-Cd cells. One cell in each of the three batteries contains a third electrode for overcharge control. The three batteries are charged and discharged in parallel. Charging of the batteries is controlled by a temperature-compensated voltage limit with eight discrete levels, any one of which can be selected by command. Through the use of the third-electrode voltage, battery voltage levels have been selected for optimum battery operation during preorbital operations, orbital stabilization, and orbital flight for extended periods.

1102. Kroger, H. H., and Catotti, A. J. 24, 4, (1970)

**Chemical Analysis of Nickel-Cadmium Electrodes**

In the evaluation of cell performance, it is sometimes desirable to corroborate the findings of conventional electrochemical methods by means of other independent procedures.

*Published by PSC Publications Committee, P.O. Box 891, Red Bank, New Jersey, 07701.

In the past few years, therefore, either new analytical methods have been developed or existing wet chemical analyses have been adapted for the investigation of electrode materials. Although the electrode materials used here are porous nickel sinter structures impregnated with nickel or cadmium hydroxide, respectively, the application of the method is not restricted to these examples.

1103. Krause, S. J. 24, 7, (1970)

**Design, Testing, and Flight Performance of the Mariner Mars 1969 Spacecraft Batteries**

The Mariner Mars 1969 spacecraft battery comprises 18 hermetically sealed AgO-Zn cells contained within a magnesium chassis and wired for connection to the spacecraft power system. Total battery weight is 76.1 kg with a volume of 9.17 $cm^3$.

The Mariner 69 battery design satisfies the need for a hermetically sealed, low cycle-life, secondary AgO-Zn battery having an energy density of over 17 Wh/kg in addition to a nominal 1-year lifetime at 25°C. The battery also has the capability to withstand the launch environment of the Atlas-Centaur vehicle which was used to send Mariners-VI and -VII to Mars.

1104. Settembre, E. J. 24, 10, (1970)

**High Energy Density, Long Life Zn-AgO Secondary Battery BB-534( )/U**

The high energy density of the vented zinc-silver-oxide electrochemical system has always been an attraction to military hardware users. However, until fairly recently, its use was limited because of short cycle life and limited activated shelf-stand.

A program sponsored by U.S. Army Electronics Command to develop a family of standard, vented Zn-AgO cells has clearly demonstrated the capability of long-life, high energy density batteries with high power outputs capable of meeting the constant demand for high power, lightweight power sources for use with military equipment.

The overall objectives of the program have been achieved. Lightweight, injection-molded plastic cases, employing a minimum of metallic parts, have been designed and evaluated, and have successfully demonstrated the capability of meeting the requirement for use in military batteries.

1105. Dirkse, T. P. 24, 14, (1970)

### Zinc as a Secondary Battery Electrode

For the past decade or so, the zinc anode has been the subject of study in a variety of research and development contracts. A partial listing of some of this work is given at the end of the paper. The zinc anode is of special interest because of its availability and because its use with an alkaline electrolyte offers much promise in terms of desirable energy-density factors. The work on the zinc electrode has been motivated by the fact that, as a secondary or rechargeable anode, zinc has some severe limitations. The electrode tends to lose capacity with continued cycling. Cycling brings about a redistribution of zinc on the electrode (shape change) and throughout the cell.

In the past, various research activities have sought to: (1) determine the mechanisms of the zinc electrode processes; (2) establish the reasons for the loss of capacity by zinc on cycling; and (3) investigate methods for improving the cycle-life behavior of zinc.

1106. Von Hartmann, W. 24, 104, (1970)

### Heat-Sterilizable Remotely Activated Battery

Experiments are described which show that a properly designed, remotely activated Zn-AgO battery can be heat-sterilized, activated, and discharged. However, sterilization is responsible for a 40% loss in capacity (based upon actual capacity) which is caused by AgO reduction at this elevated temperature (135°). A major problem is the pressure buildup in the battery. Because gassing during the high-rate discharge may be unavoidable, a vent or a pressure vessel may have to be incorporated in the design. A study of the gassing phenomenon is recommended.

1107. Dunlop, J. D., and Earl, M. 25, 40, (1972)

### Evaluation of Intelsat-IV Nickel-Cadmium Cells

Beginning in December 1969, Intelsat-IV 15-Ah nickel-cadmium cells were tested to simulate the Intelsat-IV synchronous orbit mission in real time. Two different storage methods were used: continuous trickle charge and open-circuit charged stand with recharge every 30 days. On each eclipse season, one cell was removed from each group for electrochemical and chemical analyses. Data from these anlyses were used to evaluate the expected cell performance for the Intelsat-IV mission.

1108. Ford, F. E. 25, 43, (1972)

### Performance of 3rd Electrode Cells in OAO

On December 7, 1968, the Orbiting Astronomical Observatory-2 (OAO-2) was placed in a near-Earth orbit. This satellite was the first to use nickel-cadmium batteries with auxiliary (signal) electrodes for overcharge control. During the early life of the satellite, these third-electrode signals provided the ground control center with an orbit-by-orbit indication of the overcharge that the batteries were receiving. By ground command, the battery charger was adjusted on a "need basis" to provide optimum recharge conditions as indicated by the third-electrode signals during all phases of spacecraft operations and orientations. After more than 2 years (over 10,000 orbits), an unusual degradation in third-electrode signals was observed and provided the first indication of battery degradation. The analysis of the battery system and type of battery degradation observed in the OAO-2 spacecraft is the subject of this paper.

1109. Levy, E. Jr., and Kerr, R. L. 25, 47, (1972)

### Nickel-Cadmium Cells for Low Earth Orbit Applications

A battery system for use in low Earth-orbiting satellites has been designed, developed, and fabricated, and has successfully completed 6 months of cycling in a vacuum chamber. The test demonstrated that the new system can provide power to a 0- to 500-watt load during a 35-minute time period and fully recharge during the succeeding 75 minutes.

The battery system interfaces with a 24- to 32-volt solar panel. Charge control is automatic; the battery charges when the solar panel has available charge power until sufficient charge has been returned to the battery to ensure a full state of charge. Battery discharge is also implemented automatically, with the satellite bus maintained above 24.0 volts at all times. The charge/discharge cycling can be either continuous at the 35/75 minute times or varying, depending on length of satellite exposure to sunlight during an orbit.

To achieve its maximum capacity of 500 watts, the battery system uses sixteen 50-Ah nickel-cadmium cells. The electronics package underneath the two 8-cell packs provides all charge and discharge control functions needed to connect the battery system to the solar panel.

1110. Chua, D., and Diefendorf, R. J. 25, 52, (1972)

### Effect of Electrode Structures on Capacity of Sealed Cells During Cycling

Many studies on the electrochemical and chemical properties in the nickel-cadmium system have been published. The results of these studies indicate that $\beta$-NiOOH and Cd are the final products formed during charging, and that $Ni(OH)_2$ and $Cd(OH)_2$ are formed during discharging. Information on the changes in the physical structure of the electrodes has often been overlooked. Hence, the investigation of the microstructural changes in the positive and the negative electrodes is the basis of this work. In this paper, the variables studied are cycling and temperatures. Particular emphasis has been placed on the effect of cycling on the structure of the electrodes, because a long cycle life is important in the nickel-cadmium system. The discussion is limited to the cadmium electrode.

1111. Tanis, C., and Lander, J. J. 25, 55, (1972)

### Long-Life, High Energy Ni-Cd Aerospace Cells

For many years, nickel-cadmium aircraft battery-cell designs have used two or three layers of separator materials (total dry thickness $\cong$ 4 to 7 mils), one of which is cellophane; the others may be macroporous dynel and/or woven or felted nylon. The cellophane provides a semipermeable barrier; however, it is chemically unstable in the cell environment. One of the failure modes of thin-plate, close-packed nickel-cadmium cells has been observed to be short-circuiting because of a slow growth of cadmium away from the surface of the negative plate toward the positive plate. This process is abetted by swelling of the positive plate in thickness and loss of the semipermeable barrier through chemical degradation. The total process accelerates sharply with temperature increase.

This paper presents the results of testing an aircraft cell design in which the cellophane layer of the separation is replaced with a single layer of P-2291, as well as plans for large-scale testing in aircraft batteries.

1112. Carr, E. S. 25, 57, (1972)

### Lightweight Sponge Negative Plates for Nickel-Cadmium Batteries

A primary aim in battery technology is to maximize the energy density of each battery system. For this reason, battery manufacturers direct a major part of their internal

research and development programs toward the improvement in the energy density of their batteries. This effort is particularly important because the users frequently increase the performance requirements for batteries.

This paper presents the results of USAECOM Contract Number DAAB07-70-C-0/46 for the development and production of the BB-460( )/U battery. The success of this program was a direct result of the application of the Eagle-Picher lightweight sponge-cadmium plate in the BB-460( )/U battery. Cycle test results are also presented of sealed spacecraft nickel-cadmium cells incorporating similar sponge-cadmium plates. These programs have resulted in nickel-cadmium cells of 19 to 25 Wh/lb with a standard energy-density range of about 12 to 16 Wh/lb.

Sponge negative-cell designs can replace standard sintered-plate designs in many applications utilizing nickel-cadmium batteries. This replacement provides a battery user with nickel-cadmium batteries that have energy densities of 19 to 25 Wh/lb. This range is substantially higher than that of current state-of-the-art batteries.

1113. **Henningan, T. J., and Palandati, C. F.** 25, 60, (1972)

**Sealed Silver Oxide Zinc Cells for Orbiting and Planetary Missions**

Several test programs were carried out to determine the performance of sealed silver-zinc cells for: (1) synchronous-orbit mission, (2) applications requiring a maximum of six cycles per day, or (3) missions to other planets requiring maintenance of maximum capacity for probe operations during planet encounter. This report summarizes the results with respect to capacity maintenance during cycling, cycle life, charged-stand effects, and internal-pressure characteristics. The charge-control system developed for these programs maintained internal pressures at less than two atmospheres absolute by minimizing overcharge and preventing cell-voltage unbalance, especially during long-float periods. The sealed operation of silver-zinc cells has been shown to be feasible for orbiting and planetary missions. However, the life of zinc-silver-oxide cells is limited to 1 to 2 years over the temperature range of 0°C to 24°C.

The test program performed on the sealed silver-zinc cells showed that, under various conditions of cycling during synchronous orbits and orbit conditions requiring a maximum of six cycles per day, the life of the cells is between 1 and 2 years.

1114. **Charkey, A.** 25, 64, (1972)

**Sealed Nickel-Zinc Cells**

Recent work has shown that vented nickel-zinc cells are capable of 150 to 200 cycles, depending on construction and cycling regimen. Failure modes for cells with conventional electrodes and cellulosic separators are separator degradation and loss of capacity because of zinc penetration and zinc shape change. Inherent in the operation of the vented cells are: loss of water during overcharge, carbonation of the electrolyte and electrode charge imbalance. These conditions call for frequent water additions to the cells and deep discharge of the cells to 0.0 volt to restore the original surplus of zinc oxide. A large excess of ZnO must be incorporated in the cell to ensure a positive-limiting situation during charge. This prevents premature shorting by dendritic zinc. These deficiencies have precluded the use of vented nickel-zinc cells for military and commercial applications which are presently *fulfilled* by silver-zinc and nickel-cadmium batteries.

1115. **Feldman, K., Haines, R. L., and LePage, W. A.** 26, 80, (1974)

**Nickel/Cadmium Batteries in Aircraft Engine Starting**

Problems with nickel-cadmium batteries used for aircraft engine starts led the Defence Research Establishment (Ottawa) to investigate battery behavior in this area. The items reported in this paper form part of this investigation. They deal with battery resistance and battery temperatures during high-rate discharges. The findings have implications in battery design, collection, and use.

1116. **Miller, G. H.** 26, 83, (1974)

**Accelerated Life Tests for Nickel Cadmium Cells**

The United States Air Force is interested in reliable, lightweight, long-life nickel-cadmium power supplies for space missions. Insisting on reliable devices necessitates using only proven designs. Weight requirements often necessitate giving up some of the expected life. Therefore, an "accelerated life test" is desirable as a tool for maximizing the combinations of life, weight requirements, and reliability.

The practical service life of nickel-cadmium batteries for spacecraft applications depends on the battery's ability to deliver a minimum ampere-hour capacity at a minimum end-of-discharge voltage.

1117. Charkey, A. 26, 87, (1974)

### Long Life Zinc Silver-Oxide Cells

The performance of zinc-silver-oxide cells is severely limited by degradation of the zinc-electrode capacity. Loss of capacity results from redistribution of active material attributable to electrochemical and mechanical phenomena. This redistribution of zinc has been variously termed "slumping, washing, shape change, etc."

At present, there is no adequate explanation for the migration of material from the edges of the plate to the center, but unequal current distribution throughout the collector may be a contributing factor. This transfer or redistribution of material may also result from concentration gradients of varying zincate quantity from the top to bottom of the cell and partitioning effects between the separator and the bulk electrolyte. The transfer of material from the top to the bottom of the electrode is a result of the greater zincate ion concentration at the bottom of a cell. Current flows as a result of the concentration cell setup between KOH and KOH saturated with ZnO.

1118. Dougherty, M. P. 26, 90, (1974)

### Charged Wet Storage Test of Zinc Silver-Oxide Cells

A total of 505 specially fabricated zinc-silver-oxide cells was purchased during the period July 1971 through October 1971 from Eagle-Picher Industries, Inc. (AF Contract F33615-71-C-1243). The cells were a standard commercial-package size with a nominal capacity of 20 ampere-hours, and contained a vent valve with opening pressure in the range of 2 to 20 psig. The positive plates were pure silver on an expanded silver grid. The negative plates were teflonated zinc oxide with 3% by weight mercuric oxide also on an expanded silver grid. The negative plates in all cells were unwrapped, and all positive plates were wrapped with one layer of Webril (E 1408). The electrolyte was 45% by weight potassium hydroxide.

In addition to the one layer of Webril, 135 cells had positive plates wrapped with two layers of RAI P-2291 (40/60), 135 with three layers of RAI P-2291 (40/60), 135 with four layers of RAI P-2291 (40/60), and 100 with four layers of fibrous sausage casing (FSC). The RAI materials are radiation-grafted polyethylenes. Cells with less than the control thickness of separation (four layers of FSC) were shimmed to maintain the same cell-tightness factor.

1119. Katan, T., Szpak, S., and Bennion, D. N. 26, 93, (1974)

**Practical Aspects of Electrode Modeling**

Modeling of battery electrodes is based upon analysis of a set of elementary processes that occur during battery operation and, usually, within the confines of a porous structure.

Theoretical aspects of electrode modeling have advanced to a high degree of sophistication: From a simple picture developed by Daniel'-Bek in 1948, models that apply to complex situations have evolved. Today's models contain elements such as the effects of surface morphology and the change in reaction kinetics, as well as the change in transport properties or pore geometry with time evolution of reaction profiles.

No such progress has been reported with regard to the practical aspects of electrode modeling, however. The purpose of this report is to outline methods and techniques used for studying the development of reaction profiles during the course of electrode operation. The Ag/AgCl system was selected as representative of the essential features of the sparingly soluble, conductive-matrix system.

1120. Wagner, O. C., and Williams, D. D. 26, 196, (1974)

**Investigation of Charging Methods for Nickel-Cadmium Batteries**

This paper presents data on the effects of pulse and direct-current charging on the electrical performance of nickel-cadmium batteries.

Reflex charging with an average charge rate of 2C, a frequency range of 30 to 2000 Hz, and a minimum negative-pulse energy of 2.5 milliwatt-seconds increased the charge acceptance of vented and sealed nickel-cadmium batteries by 10 to 15 percent in the temperature range of -40°F to about 100°F.

Reflex charging and positive-pulse charging provide an excellent means for restoring the capacity lost by vented and sealed nickel-cadmium batteries.

Life cycling of a vented nickel-cadmium battery using the reflex mode of charge showed that the battery maintained its capacity at about 100% of theoretical up to the 500 cycles tested.

## SOVIET ELECTROCHEMISTRY*

1200. Budevski, E., Vitanov, T., Sevast'yanov, E. S., and Popov, A. 5, 79, (1969)

### Zero-Charge Potentials of Individual Faces of Silver Single Crystals

It is known that, in dilute solutions, the minimum on the differential capacity potential curves is less pronounced. It is much less pronounced on solid polycrystalline electrodes than it is on mercury. According to Frumkin, the explanation of this effect must be sought in the difference of the zero-charge potentials for the individual crystallographic faces of polycrystalline electrodes. The development of a method of obtaining electrodes that exhibit particular crystallographic planes opened up the possibility to study the effect of crystallographic surface structure on the structure of the electric double layer.

1201. Dunaeva, T. I., and Skalozubov, M. F. 5, 234, (1969)

### Changing the Electrical Characteristics of the Silver Electrode in Chemical Current Sources

As new techniques have been developed, interest has grown in the silver-alkaline electrode system, which has the highest specific characteristics among chemical current sources. This system has some disadvantages, however. Among these are the two-stage discharge curve of the silver electrode and the sharp drop in electrical capacitance after discharge at small currents. In this paper, a method is proposed for eliminating these disadvantages and for studying the processes that occur at this electrode.

1202. Ivanov, E. A., Popova, T. I., and Kabanov, B. N. 5, 321, (1969)

### Passivation of Zinc in KOH Solutions Supersaturated with Zincate Impedance Determination

From the dependence of the impedance components on a.c. frequency, and allowing for the other electrochemical characteristics of the electrode, the parameters of a selected electrical equivalent circuit can be determined which quantitatively characterize the kinetics

*Translations from the Russian Journal, "Elektrokhimiya."

of the electrode reactions occurring during anodic metal dissolution. This method has been used in studying the anodic behavior of zinc in alkaline solutions.

It has been shown that, during anodic polarization of zinc in alkaline solutions at potentials between 0.2 and 1.0 V (nhe) (which correspond to a state of deep passivity of the electrode), the rate of anodic dissolution is found to be potential-independent and that, for solutions supersaturated with respect to zincate, it is also independent of solution composition. It is hypothesized that, under these conditions, the greater part of the anodic current corresponds to direct electrochemical dissolution, which does not go through a stage of zinc-oxide formation and which occurs without participation of hydroxyl ions:

$$Zn \rightarrow Zn^{2+} + 2e^-$$

1203. **L'vova, L. A., and Fortunatov, A. V.** 5, 366, (1969)

### The Effect of Additives on the Anodic Oxidation of Cadmium in Alkaline Solution

The effect of a large number of inorganic and organic substances on the anodic oxidation of cadmium in concentrated alkali solutions has been investigated. Although the point of zero charge on the cadmium lies in the active potential region, only a small number of compounds exercise any appreciable effect on the anodic oxidation of cadmium. Substances which form stable complexes with cadmium cations accelerate the process under consideration. Sulfide ions and thio-compounds that are adsorbed on the surface of the cadmium electrode have a retarding effect on the anodic oxidation of this in alkali solutions.

1204. **Past, V. E., Tamm, Yu. K., and Tokhver, L. V.** 5, 487, (1969)

### The State of a Silver Surface During the Cathodic Liberation of Hydrogen in Alkaline Solutions

The behavior of a silver electrode in 0.05 to 0.5 N solutions of LiOH, NaOH, and KOH and 0.05 to 0.3 N $Ba(OH)_2$ in the cathodic liberation of hydrogen was studied. To determine the pseduocapacitance of the electrode C, a new variation of current-switching curves was proposed to permit a determination of C within a broad region of cathodic potentials $\varphi$. The experimentally determined coverage of the surface by electrochemically active hydrogen has an average value of $0.22 \pm 0.03$ at $\varphi$ from -0.2 to -0.5 V (hydrogen electrode in the test solution) in all the investigated solutions. It was found that the potential of the maximum $\varphi_M$ of the ionization of the alkali metal depends on the pH of the

solution and $\varphi_M$ of the ionization of electrochemically active hydrogen at -0.03 to -0.09 V does not depend on the pH. Deposition of the alkali metal in amounts up to 0.2 of a monolayer does not influence the adsorption of electrochemically active hydrogen.

1205. L'vova, L. A., Grachev, D. K., and Panin, V. A. 5, 583, (1969)

**Impedance of a Cadmium Electrode in Concentrated KOH Solution**

The test electrode consisted of a cadmium wire 0.4 mm in diameter and 3 to 5 mm long, glued with epoxy resin into a glass capillary. Preliminary treatment of the electrode surface consisted of anodic oxidation in alkali, chemical polishing in $HNO_3$, and washing with a large amount of double-distilled water. Special experiments revealed that the use of a cadmium-planted platinum wire sealed into glass and treatment of the electrode surface by the method described previously do not appreciably affect either the value or the frequency dependence of the electrode impedance.

A solution of 2.5, 5.0, and 10 N KOH was prepared by dissolving in double-distilled water. Before each experiment, the solutions were subjected to prolonged cathodic-anodic purification. The cell had separate cathode and anode spaces and was thermostated to within 0.1°C. The experiments were performed in an atmosphere of hydrogen.

1206. Ivanov, E. A., Popova, T. I., and Kabanov, B. N. 5, 643, (1969)

**Passivation and Activation of Zinc Electrodes in Alkaline Solutions Supersaturated with Zincates**
**I. Measurements at Constant Current Density**

During investigations on rapid anodic passivation of zinc in alkaline solutions, the following relationship between current i and passivation time $t_p$ has been determined:

$$(i - i_0)\, t_p^{1/2} = K, \qquad (1)$$

where $i_0$ and $K$ are constants independent of the speed of stirring. Equation (1) was explained by a nonstationary diffusion of reacting particles towards the electrode. At high $i$, the relationship changes into a linear correlation between $i$ and $1/t_p$.

The aim of the present work was to investigate the kinetics of the passivation and activation of zinc under conditions that would prevent the film forming on the surface of electrode from dissolving chemically (i. e., in alkaline solutions supersaturated with zincates).

1207. **Kabanov, B. N., Popova, T. I., Oshe, A. I., and Kulyavik, Ya. Ya.** 5, 915, (1969)

### Determination of the Composition of the Complex of Zinc in Zincate Solutions in KOH

There are diverse opinions concerning the participation of water in the anodic dissolution of zinc in alkali, which can be written in general as:

$$Zn + 4OH^- + xH_2O = [Zn(OH)_4 xH_2O]^{2-} + 2e^-$$

Although water is the reaction product and x = -2, water is the reagent and three to four molecules of it are contained in the complex. It should be kept in mind that the composition of the complex may depend on the concentration of alkali.

A determination of the composition of the complex in concentrated solutions (up to 14 M), chiefly at determination of the coefficient x, was the purpose of this investigation.

1208. **Muller, L., Yaniets, P., and Landsberg, R.** 5, 943, (1969)

### Change in Electrochemical Properties of a Silver Electrode when Coated with a Thin Layer of $Ag_2O$

In the investigations on the reduction of $S_2O_8^{2-}$ on a bright silver electrode (electrode free from oxides) and on an electrode covered with a thin layer of the oxide $Ag_2O$, the half-wave potential ($\varphi_{i/2}$) on the latter was displaced in a positive direction. In addition, it appeared that the strong retardation of the process, which takes place on a bright silver electrode in the potential region $\varphi$ = 0.5 to 0.25 V, did not occur on the electrode coated with $Ag_2O$.

The objective of the investigation was to determine the reasons for the different behavior of the bright electrode and the electrode covered with the $Ag_2O$ oxide.

1209. Yatskovskii, A. M., and Fedotov, N. A. 5, 991, (1969)

## Solubility and Diffusion of Oxygen in Solutions of Potassium Hydroxide and Phosphoric Acid

The literature data on the solubility of oxygen in solutions of potassium hydroxide and phosphoric acid are comparatively scanty and differ appreciably in the region of high KOH concentrations. Data on the solubility of oxygen at 25°C in solutions of phosphoric acid were published. No information could be found in the literature on the solubility of oxygen in solutions of KOH and $H_3PO_4$ at increased pressures. The data published on the diffusion coefficients of oxygen in solutions of potassium hydroxide are extremely scanty, and there are 10 to 20% discrepancies among them. No literature or data could be found on the diffusion coefficients of oxygen in solutions of phosphoric acid.

1210. Ivanov, E. A., Popova, T. I., and Kabanov, B. N. 6, 90, (1970)

## Potentiostatic Passivation and Galvanostatic Activation of Zinc in Supersaturated Zincate Solutions of KOH

The passivation of zinc occurs as a result of the formation of an adsorption layer of the oxide $ZnO_{1+m}$ (where $m<1$), containing excess oxygen (over the stoichiometric amount in ZnO). Only after this process can the formation of a phase-passivating layer begin, after the rate of dissolution of zinc has already been reduced by approximately two orders of magnitude. The anodic oxidation of zinc, coated with a phase-oxide layer, occurs when there is an increase in the potential that is necessary for ensuring migration of ions in the oxide layer, which, in turn, is necessary for increasing the thickness of the solid-oxide layer. At potentials above 0.5 V, the content of excess oxygen in the film is increased because of the discharging of hydroxyl ions, but its thickness remains practically constant.

The purpose of this study was to determine the influence of the composition of the solution on the mechanism and kinetics of the passivation process and on the content of excess oxygen in the oxide film formed in the anodic polarization of a zinc electrode in alkaline solutions saturated with zincate, in which the oxide film is not chemically soluble.

1211. **Kilimnik, A. B., and Rotinyan, A. L.** 6, 322, (1970)

### Hydrogen Overpotential on Silver

The hydrogen overpotential on silver in sulfuric and hydrochloric-acid solutions (0.5 to 2.0 N) has been investigated many times. In all cases, a Tafel relationship with a slope of 0.11 to 0.12 was obtained for significant current densities. However, the values for the constant, $a$, obtained by the various authors differed greatly.

Note that, because of the large number of differing opinions on the value of the zero-charge potential for the silver surface, it is not clear which sign of surface charge one or the other value for the constant $a$ corresponds. If, however, the zero-charge potential is taken as 0.05 V, the values of the $a$ constants will already correspond to a negative charge on the electrode surface.

1212. **Kazakevich, G. Z., Kirkinskii, V. A., and Yablokova, I. E.** 6, 355, (1970)

### Behavior of Silver in Alkali During Anodic Polarization by Asymmetrical Current

In a previous article, differences were described that arise when anodic polarization with direct current is replaced by anodic polarization with asymmetrical current on a silver electrode in alkali, and a preliminary explanation for the observed phenomena was given. The main differences comprise increased oxidation capacity and the appearance of additional potential arrests on the cathodic reduction curves of the electrode. The present report gives the results from further investigations in this field.

1213. **Burshtein, R. Kh., Vakhonin, V. A., Tarasevich, M. R., Khrushcheva, E. I., Chizmadzhev, Yu. A., and Chirkov, Yu. G.** 6, 911, (1970)

### Reduction of Oxygen on a Porous Silver Electrode

On the basis of a comparison of structural and electrochemical data, the contribution to the total current of different possible mechanisms of operation of electrodes was examined. It was shown that there is good agreement between theoretical and experimental results only if it is considered that generation of current by different mechanisms is possible, the ratio between which is determined by electrochemical and structural parameters.

1214. Bartenev, V. Ya., Sevast'yanov, E. S., and Leikis, D. I. 6, 1166, (1970)

**Differential Capacitance of a Zinc Electrode in Dilute Solutions**

The high overvoltage of hydrogen on zinc and the good reproducibility of the surface achievable by polishing has provided the basis for hoping that data on the structure and properties of the electrical double layer can be obtained on a zinc electrode, as on certain other metals.

The electrode was zinc wire. The measurement procedure was described. Before performing the measurements, the zinc was subjected to chemical etching in a solution of nitric acid until the appearance of a luster, after which it was rinsed several times and subjected to anodic polishing. Polishing was conducted in a solution of orthophosphoric acid at $i = 0.04 - 0.05$ A/cm$^2$. After this, the electrode was washed thoroughly with double-distilled water and transferred to a measuring cell. The stationary state, permitting the capacitance to be measured, was reached after 2 hours of cathodic polarization at $\varphi = -1.44$ (saturated calomel electrode).

1215. Uflyand, N. Yu., Mendeleva, S. V., and Rozentsveig, S. A. 6, 1268, (1970)

**Study of the Properties of the Nickel Oxide Electrode**
**III. Behavior of the Higher Nickel Oxides in LiOH Solution**

Study showed that the lithium nickelate formed by nickel-oxide electrode charging in 4 to 5 N LiO was electrochemically active and that the activity increased with a rise in the discharge temperature. Comparison of electrochemical and X-ray data made it possible to establish the reactions that occur during polarization of the nickel-oxide electrode in lithium-hydroxide solution.

1216. Ereiskaya, G. P., Dunaeva, T. I., Korolenko, V. A., and Skalozubov, M. F. 6, 1386, (1970)

**Structural and Operating Characteristics of a Silver-Silver-Oxide Electrode of Chemical Current Sources Under Various Discharge Conditions**

A number of papers on a silver-silver-oxide electrode of chemical-current sources noted that the electrical characteristics of the electrode depend on its structure. However, the literature contains no complete quantitative data on the change in the micro- and macrostructure as a function of the conditions used in the reduction process and the interrelationship

between the process condtions, the structure formed, the electrical capacitance, and the loss in active mass. The objective of this investigation was to study the effect of the cathodic reduction conditions of a porous silver-silver-oxide electrode on the parameters listed above, as well as to determine the relationship between them.

1217. **Lokshtanov, V. Z., and Rotinyan, A. L.** **6, 1569, (1970)**

**Hydrogen Overpotential on Nickel Cathodes During Electrolysis of Concentrated Alkali Solutions**

Hydrogen overpotential on nickel electrodes with flat and developed surfaces in LiOH, NaOH, KOH, RbOH, and CsOH solutions of different concentrations was investigated. With increasing alkali concentration, the coefficient b in Tafel's equation changes slightly, and the exchange decreases. At equal concentrations, the nature of the cation has no influence on the exchange current. Possible causes of these effects are discussed.

1218. **Uflyand, N. Yu., Mendeleva, S. V., and Rozentsveig, S. A.** **6, 1717, (1970)**

**Study of Properties of the Nickel Oxide Electrode and Behavior of the Nickel-Oxide Electrode in Hot, Concentrated NaOH Solutions**

Electrochemical and X-ray studies have shown that increasing the temperature to a point in the interval from +120 to +180°C will alter both the products of cathodic and anodic polarization of the nickel-oxide electrode in 75% NaOH solution and the mechanism of electrochemical reactions on this electrode. It is suggested that the discharge product is free sodium nickelate ($NaNiO_2 xH_2O$). This suggestion has been confirmed by chemical analysis. Under the working conditions adopted here, the solubility of this compound was of the order of $10^{-3}$ -M/1000 solution, a value high enough to support electrochemical and chemical reactions with the formation of nickel intermediates that are soluble in alkali.

1219. Oshe, E. K., and Rozenfel'd, I. L. 7, 1366, (1971)

**Study of Anodic Oxidation and Passivation of Silver in Alkali Hydroxide Solutions by the Photoelectric Polarization Method**

The photoelectric-polarization and polarization-curves methods were used to study the mechanism of the anodic oxidation and passivation of silver in alkali-hydroxide solutions.

In the anodic polarization of silver in an alkali-hydroxide solution, two oxidation steps are observed, each of which leads to the formation of silver oxides of different stoichiometric composition; $Ag_2O$ is formed in the first step, and AgO is formed in the second step. At certain values of the anodic potential, the oxidation stops in both steps as a result of the passivation of silver. A large number of papers have been devoted to the study of these processes. Until now, however, the internal, "intimate" mechanism of the oxidation and passivation of silver (as well as that of most other metals) remains unexplained. This paper presents an attempt to clarify this mechanism using the photoelectric-polarization method in combination with the method of polarization curves.

1220. Korovin, N. V., Savel'eva, V. N., and Shishkov, Yu. I. 7, 1439, (1971)

**Anodic Dissolution of Nickel in Ammoniacal Alkaline Solution**

Nickel has a high corrosion resistance in alkaline solutions. The rate of dissolution of nickel increases considerably, however, in the presence of activators and complex-forming reagents.

Because ammonia is used as a fuel in cells with an alkali electrolyte, it is appropriate to study the influence of ammonia on the anodic dissolution of nickel in alkali solution.

The studies were made by a potentiostatic method with a TsLA 5611 potentiostat in a cell with three sections, separated by taps. The potentiostatic curve was recorded in the range of potentials 0.0 to 1.4 V at 25-mV intervals. The electrode was kept at each potential until a stationary current value was established. The studies were made in 0.1- to 10-M KOH solution with the addition of ammonia at concentrations from $10^{-3}$ M to saturation. For comparison, the volt-ampere curves were recorded without the addition of ammonia. The potentials were measured by means of a mercuric oxide reference electrode with an alkali solution of the concentration studied. The potentials on the scale of a hydrogen electrode in the same alkali solution as the solution being studied are denoted $\varphi_1$, and those on the scale of the standard electrode are denoted $\varphi$.

1221. Zytner, Ya. D., Maksimyuk, E. A., Nikol'skii, V. A. Alekseeva, N. I., and Berkman, E. A. 7, 1531, (1971)

**Kinetics of Cadmium Passivation in a KOH Solution**

This paper gives a kinetic analysis of the potentiostatic and galvanostatic curves obtained for electrolytic cadmium in KOH solutions of different concentrations. It is assumed that the small Tafel slopes during active solution of the metal, and the appearance of maxima on the potentiostatic curves are attributable to adsorption of hydroxyl ions and surface oxide on the electrode.

One of the most important but least studied aspects of the theory of metal passivity during anodic polarization in alkalis is the transition of active solution of the metal to passive solution. The aim of this paper is to determine the passivity mechanism of cadmium in a KOH solution.

1222. Kaminskaya, E. A., Uflyand, N. Yu., and Rozentsveig, S. A. 7, 1776, (1971)

**Behavior of Higher Nickel Oxides in Lithium-Containing KOH Solutions**

It is well known that lithium activates the nickel-oxide electrode of an alkaline accumulator, being readily absorbed by higher oxides of nickel. Penetration of lithium into the crystal lattice of nickel oxides leads to its rearrangement and to formation of a new crystal structure – lithium nickelate ($LiNiO_2$). A previous communication showed that the compound formed during the operation of a nickel-oxide electrode in an LiOH solution and having the structure of $LiNiO_2$ is electrochemically active. The behavior of this compound, which is apparently lithium hydroxonickelate, differs from that of $\beta$- and $\gamma$-NiOOH that is formed during discharge of a nickel-oxide electrode in NaOH and KOH solutions.

1223. Popova, T. I. 8, 469, (1972)

**Passivation of Zinc in Alkaline Solution**

The properties of passivating oxide layers formed on zinc during anodic polarization in concentrated solutions of alkali are discussed. The influence of the potential of formation of the film, time, and composition of the electrolyte on the properties of oxide films was demonstrated. As a result of the consideration of various studies, it was concluded that thin oxide films containing a small excess of oxygen with respect to the oxide ZnO are responsible for passivation.

1224. Troshin, V. P., and Zvyagina, E. V. 8, 487, (1972)

### Electrical Transfer in Solutions of Potassium Hydroxide at High Concentrations

A measurement scheme based on the moving-boundary method is presented, and the results from an investigation of the true ion-transport numbers and mass transfer as a function of the concentration of potassium hydroxide solution are given. It was shown that the transport number of the $OH^-$ ion is considerably greater than that of the $K^+$ ion and increases from 0.79 to 0.847 with increase in the concentration of the solution from 1 to 12 N. It was further shown that the $OH^-$ ion is not hydrated (does not convey water during its motion) and that it moves under the influence of the electric field as an individual ion.

1225. Ob"edkov, Yu. I., and L'vova, L. A. 9, 1547, (1973)

### The Cathodic Process in the $Cd/Cd(OH)_2/KOH$ System

The cathodic processes in the $Cd/Cd(OH)_2$ KOH system, which in many ways determine the operational characteristics of Ni-Cd accumulators, have still not been studied sufficiently. Thus, in the opinion of some authors, reduction of cadmium hydroxide in alkali proceeds by a solid-phase mechanism, whereas, according to others, it involves the participation of soluble intermediate products. One shortcoming of these investigations is the fact that, as a rule, the cathodic process is studied over a relatively narrow range of potentials without control of the preliminary anodic oxidation of the cadmium electrode. Apart from this, the literature contains practically no quantitative data on the equivalence of the anodic and cathodic processes in the system studied.

1226. Ob"edkov, Yu. I., and L'vova, L. A. 10, 341, (1974)

### The Cathodic Process in the System $Cd/Cd(OH)_2/KOH$. II

The cathodic reduction of an anodically oxidized cadmium electrode in 8.1-N KOH has been studied by the potentiostatic and potentiodynamic methods. The potentiodynamic measurements have shown, as did the galvanostatic experiments performed previously, that cathodic reduction of cadmium hydroxide proceeds by two different mechanisms in two regions which differ sharply in potential. It has been proposed that the rate of cathodic reduction of cadmium hydroxide with the participation of soluble intermediate products

is determined by the rate of its chemical solution. It has been established that the kinetic opportunities for reduction through a solution of cadmium hydroxide in the "active" form are ten times greater than those for the "inactive" form.

## ZINC-SILVER OXIDE BATTERIES SYMPOSIUM PAPERS*

**1300. Bode, H., Oliapuram, V., Berndt, D., and Ness, P. 7, (1971)**

### Thermodynamics of the Zinc-Silver Oxide Battery

Fundamental thermodynamic data of Ag-Ag-oxide and Zn-Zn-oxide electrodes were used to obtain the thermodynamic characteristics of Zn-Ag-oxide cell.

**1301. Ruetschi, P. 117, (1971)**

### Nature and Stability of Silver Oxides

The stability of $Ag_2O$ electrodes is limited by the thermal decomposition of $Ag_2O$ at low $O_2$ partial pressures, by the dissolution of the oxide by the electrolyte with subsequent precipitation of Ag by Zn electrodes and by cellulosic separator material, and by the reduction of H. The decomposition of AgO to $Ag_2O$ is governed by the anodic $O_2$ evolution reaction, and the rate varies with $\alpha_{OH^-}{}^{1-\alpha}$ and $\alpha_{H_2O}{}^{\alpha}$, where $\alpha$ is the transfer coefficient. Dissolution of AgO appears to be accompanied by decomposition to $Ag_2O$. Reduction of AgO, as well as of $Ag_2O$, by H is extremely fast for unwetted electrodes but is inhibited in the presence of electrolyte films. No conclusive evidence is available to date for the existence of higher oxide phase (e.g., $Ag_2O_3$, acting as intermediate in the formation of AgO or $O_2$).

**1302. Thirsk, H. R., and Lax, D. J. 153, (1971)**

### Correlated Structural and Kinetic Studies in the Silver/Argentous [Silver (I)] Oxide/Argentic [Silver (II)] Oxide System

In electrochemical reactions dealing with the Ag oxide system, work is being pursued on: (1) the anodic dissolution of the metal prior to complete $Ag_2O$ coverage; (2) the reduction of AgO to $Ag_2O$; and (3) the reduction of $Ag_2O$ to Ag. The present work is divided into three sections: (a) the texture, growth, and orientation of the oxides; (b) the phase change to $Ag_2O$; and (c) the phase change of $Ag_2O$ to AgO. Discrete $Ag_2O$ and AgO nuclei are formed and grow on anodized Ag electrodes in alkaline solutions. In the potential regions investigated, the initial phase change involved is always $Ag_2O \rightarrow AgO$, which takes

*Published in 1971 by Wiley and Sons; edited by J. Lander and A. Feischer.

place at the surface of the electrode in contact with the solution. Constant potential measurements have shown that a critical overpotential of 100 mV is necessary before the oxidation process will proceed in alkaline solution. Kinetic studies in the $Ag/Ag_2O$ system showed that $Ag_2O$ can be accepted $Ag_2O/AgO$ equilibrium potential. Rate formulas are developed mathematically from data obtained in this work.

**1303. Keralla, J. A.** 183, (1971)

**Zinc Electrode Manufacture**

Materials, processes, and control measures used in the manufacture of Zn electrodes by electrodeposition and pressed-powder methods are reviewed.

**1304. Falk, S. U., and Fleischer, A.** 199, (1971)

**Sintered Silver Electrodes**

Ag electrodes based on sintering techniques are reviewed. Their advantages are high energy density, very flat discharge curve, excellent rate performance, outstanding charge efficiency, low self-discharge, and considerable cycle life.

**1305. Wilburn, N. T.** 209, (1971)

**Chemically Prepared Silver Oxide Plates**

Laboratory scale preparation of bivalent Ag oxide electrodes eliminated the conventional electroforming, washing, and drying steps, and resulted in 20 to 30% greater coulombic efficiency at normal discharge rates. Ag grids were coated with 1% CM-cellulose and coated with 4.0 g AgO each to yield test electrodes of 21.0 $cm^2$ area. These were pressed at 224-1072 $kg/cm^2$, and tested for discharge characteristics at 167 $mA/cm^2$ to give efficiencies that ranged from ~74% for a 0.1-V drop to 88% for a 0.3-V drop. Later work indicated that the 1% CM-cellulose binder can be replaced by $H_2O$ applied by a vaporizer. Engineering studies to make the process commercially feasible are underway.

1306. Gregor, H. P. 219, (1971)

**Polymeric Membranes as Effective Silver-Zinc Battery Separators**

Current knowledge of the requirements of Ag-Zn battery separators was summarized, and known polymer systems that could be applicable were discussed. The electrolyte space was divided into four regions: the Ag spacer, the argentistatic spacer, the dendristatic spacer, and the Zn spacer.

1307. Shaw, M., and Remanick, A. H. 233, (1971)

**Mass Transfer Properties of Membranes and Their Effect on Alkaline Battery Performance**

Measurements of KOH diffusion and transference through some typical cell membranes, and of KOH absorption by the latter, indicated that changes in electrolyte concentration could occur, which might adversely affect the performance of alkaline batteries. The changes in KOH concentration were related to the mass-transfer characteristics of membrances as a function of time, current, and temperature. In the lower concentration ranges, the diffusion coefficient was controlled by solution properties, but at higher concentration, the membrane properties appeared to be the controlling factor.

1308. Post, R. E. 263, (1971)

**Nature of Cellulose as Related to its Application as a Zinc-Silver Oxide Battery Separator**

The properties of cellulose that relate to the requirements for Zn-Ag oxide battery separators are described. Modifications are suggested for improving the separator performance of commercial cellulose films. As a barrier film, regenerated cellulose could be improved by introduction of highest quality pulp, emphasizing a high degree of polymerization and crystallinity in manufacturing, crosslinking, and chemical pretreatment to reduce aldehyde content. High wet-modulus rayon appeared to be promising. The tendency for a compact cuticle to be formed on viscose cellophane could also be used.

1309. Moe, G., and Arranee, F. E. 295, (1971)

**Inorganic Separators**

Progress in the development of flexible and rigid inorganic interelectrode separators for Zn-AgO cells is reviewed. Characteristics of separator materials, including strength, porosity, structure, compatibility with KOH, resistance to oxidation, resistivity in KOH, ionic screening, Ag diffusion, zincate diffusion, and zinc penetration are reviewed, as well as applications and typical performance data.

1310. Chreitzberg, A. M. 313, (1971)

**Cell and Battery Case Materials, Cell Sealing Techniques for Sealed Silver-Zinc Batteries**

A review.

1311. Lander, J. J. 321, (1971)

**Theoretical Design of Primary and Secondary Cells**

The theoretical maximum energy yield for a Zn/AgO cells is 483 Wh/kg or 3.6 Wh/$cm^3$; but on a practical basis, yields of 80 to 90% AgO and 60 to 80% Zn can be obtained. At -20 to 60° and electrolyte concentrations of 7.7-10M KOH, the capacity of Zn electrodes is a linear function of the electrolyte concentration times its volume, except at high current densities where the capacity is diffusion-limited. At 440 g KOH/l and a 15-minute discharge time, the optimum volume is 35 $cm^3$ Zn/$dm^2$. Lowering the current density by increasing surface area substantially improves performance. An optimized cell for a rate of 0.035 Ah had plate dimensions of 2.54 $cm^2$, 1.46 ml 38% KOH, 50% porous AgO, and 80% porous Zn, and a cell resistance of 0.013 ohms. A secondary cell design for high energy yield is difficult if maximum cycle life is required; for 60 to 600 cycles, yields are in the range of 88 to 44 Wh/kg. High cycle rates require thick cellulose separators with a 25% depth of discharge: 50 cycles require 0.15 mm; 200 cycles, 0.30 mm; and 1700 cycles, 0.61 mm. The percentage of Zn use decreases with cycle life: 1000 to 1300 6.25-Ah cycles used 12.5% Zn; 30 to 50 18.8-Ah cycles used 47% Zn.

1312. Edelstein, F., Lehrfeld, D., and Doan, D. J. 343, (1971)

**Heat Generation on Discharge for Zinc-Silver Oxide Cells**

A multiple regression analysis model is described for predicting heat-generation rate and voltage as a function of the operating variables for descent- and ascent-type cells analogous to those used in the Grumman Lunar Module. A general regression expression of the form $Y = K + A_1 X_1 + A_2 X_2 \ldots A_n X_n$ was used, where Y is the response in appropriate units, K is the regression constant, X are the controlled variables, and A are the regression coefficients. The nominal capacity was 300 Ah for the ascent cell and 400 Ah for the descent cell. Typical curves of voltage and heat generation versus amount discharged are described.

1313. Bowers, F. M., and Gubner, E. 347, (1971)

**Shelf Life of Unactivated Dry-Charged Zinc-Silver Oxide Cells**

Unactivated dry-charged Zn-Ag-oxide batteries can be stored at 4°and 21°for at least 2 years without change in cathode chemical composition or in total capacity. Batteries stored at 43° for 2 years may lose ∿10% of the total capacity, but this can be minimized by keeping the internal cell components dry. Storage at 54° results in ∿15% loss of the total capacity during the first 3 months. After 20 months, the loss is ∿30%, and, during this time, ∿80% of the AgO decomposes to $Ag_2O$. At 71°, most of the AgO decomposes in the first 3 months; after this time, the capacity is relatively stable at 60 to 70% of the initial value. Polyamide electrolyte retainer mats suffered severe deterioration at the higher temperatures after only several months in storage. The α-cellulose separators showed no signs of deterioration. Ag carbonate was found to be dispersed throughout the cathode-active material. Calculating the capacity from the chemical composition is a useful and accurate method for predicting the total capacity available.

1314. Carson, W. N., Jr. 445, (1971)

**Auxiliary Electrodes for Sealed Silver Cells**

Problems involved in providing for the recombination of $H_2$ and $O_2$ formed during the operation of sealed secondary cells are reviewed. The use of auxiliary electrodes for recombination of $H_2$ is discussed in detail, including circuits for recombination and charge control.

**1400. Tarasov, E.**

### Mechanism of Processes on a Silver Oxide Electrode During Anodic Oxidation

*Dokl. Mezhvuz. Nauch.-Teor. Konf. Aspir., Rostov.-na-Donu Gos. Pedagog. Inst.* **1970**, 100-5. The mechanism of processes that occur during anodic oxidation of $Ag_2O$ electrode at current densities of 0.1, 1, 10, and 500 mA/cm$^2$ was explained. An $Ag_2O$ electrode was prepared from finely divided Ag powder of 1.3 to 1.5 g/cm$^2$ bulk density by compressing it at 350 kg/cm$^2$. Charging of the electrode was done in 10N KOH at 25° at the above current densities by using two Ag oxide counter electrodes. During the anodic polarization, the effect of anodic current was seen on the charging curves in the form of two steps. Porosity of the $Ag_2O$ electrode at the various oxidation steps was calculated. For the first step, anodic oxidation of Ag occurs by a liquid-phase mechanism because of complex ion formation and $Ag_2O$ deposition; further oxidation occurs because of a solid-phase mechanism. For the second step, anodic oxidation of $Ag_2O$ to AgO occurs mainly by liquid-phase mechanism.

**1401. Bayunov, V. V., and Dasoyan, M. A.**

### Effect of Asymmetric Alternating Current Charging on the Current-Density Distribution on Storage Battery Electrodes

*Elektrotekhnika* **1974**, (3), 61-2. During constant-current charging (CC) and asymmetric a.c. charging (AC) of Pb-acid and Ag-Zn alkaline, under similar charging current $i_p$ and a.c. charging, irregular distribution of charging was significantly higher for Pb-acid than for Ag-Zn batteries. Similarly, divergences of a.c. charging parameters from the optimum one, with an increase of the electrode length, was more for Pb-acid than for Ag-Zn batteries. Also, under identical charging conditions, irregular distribution of current density along the height of the electrode was less for CC than for AC.

1402. Kosholkin, V. N., and Ksenzhek, O. S.

**Current Distribution in Storage Batteries**
**I. Effect of Nonuniformity of the Current Distribution on Some Characteristics of Storage Batteries**

*Issled. Obl. Khim. Istochnikov Toka* **1971**, No. 2, 43-50. Current distribution along the electrode height in batteries with current outlets on one or both sides was analyzed, and an equation was derived for the battery-discharge duration, taking into account the nonuniform current distribution. Conditions are considered under which a uniform current distribution is possible; e.g., in nonlaminated Ni-Cd batteries.

1403. Kosholkin, V. N., and Ksenzhek, O. S.

**Current Distribution in Storage Batteries**
**II. Experimental Verification of Current Distribution Along the Electrode Height**

*Issled. Obl. Khim. Istochnikov Toka* **1971**, No. 2, 51-7. The polarographic and specific electrical conductivity, $k$, were studied for NiO cermet and Cd-coated electrodes of a Ni-Cd battery. The $k$ of the Cd electrode was almost linearly dependent on its charge. The $k$ of the NiO electrode was independent of its charge. The experimental validation of the equation for calculating the current distribution along the electrode height revealed good agreement between theoretical and experimental values of the voltage drop on the electrodes.

1404. Chikisheva, A. P.

**Preparation of a Nickel(II) Hydroxide Activating Additive**

*Issled. Obl. Khim. Istochnikov Toka* **1971**, No. 28, 135-7. The effect of the grain size of $Ni(OH)_2$, prepared by vibrogrinding and used as an additive in Cd alkaline batteries, was studied on the Cd-current efficiency. The maximum Cd-current efficiency (55 to 65%) was observed at 150 cycles during cycling of the segment prepared with the addition of 3 and 5% $Ni(OH)_2$, vibrogrinded for 10 to 15 minutes to obtain 85 to 90% of the particles with $<63\mu$ diameter.

1405. **Volkov, V. I., and Poroikova, V. S.**

**Effect of Binders on the Self-Discharge and Electrical Characteristics of Zinc Electrodes of Silver-Zinc Batteries**

*Izv. Vyssh. Ucheb. Zaved., Khim. Khim. Tekhnol.* **1969**, 12(3), 299-302. The performance of electrodes composed of 75% ZnO and 25% powdered Zn is improved by the addition to the composition of 0.3 to 1% of starch, CM-cellulose (I), styrene-maleic anhydride copolymer (II), or poly(vinyl chloride) (III), added as a 1% aqueous dispersion. The most effective additive consists of 1% III + 0.3% II, for which the capacity loss after three low-rate charge/discharge cycles was only 17.5% compared to 43.2% without the additive. A similar beneficial effect was observed in high-rate discharge cycles. These effects are associated with better preservation of the surface characteristics of the porous mass and with less increase in electrical conductivity.

1406. **Andryushchenko, F. K., Bairahnyi, B. I., Nekrasov, A. P., and Popova, M. G.**

**Use of Pulsed Systems During the Formation of Cadmium-Nickel Storage Cells**

*Izv. Vyssh. Ucheb. Zaved., Khim. Khim. Tekhnol.* **1974**, 17(3), 409-11. A hermetically sealed Cd-Ni storage cell of 0.9-Ah capacity was charged in 14 minutes by a pulsed charging current compared to the 3 hours required for charging to 1.6 V by a constant current of 0.3 A. The pulsed current was supplied in 20 to 30-$\mu$s pulses at a frequency of 71-100 GHz. Discharge characteristics at -30 to 20° of the storage cells charged by pulsed and steady currents were indistinguishable.

1407. **Andryushchenko, F. K., Bairahnyi, B. I., Popova, M. G., and Nekrasov, A. P.**

**Electrochemical Properties of a Cadmium Mass Applied by a Pyrolytic Method on a Laminafree Base**

*Izv. Vyssh. Ucheb. Zaved., Khim. Khim. Tekhnol.* **1974**, 17(5), 731-33. A method was developed for preparing nonlamellar cadmiated electrodes for storage batteries. Graphite fiber or a porous Ni base was impregnated with $Cd(NO_3)_2$ and pyrolyzed at 300 to 800°. The discharge curves of the resulting electrodes were determined. With the Ni base, the maximum utilization coefficient (45 to 50%) was obtained for samples pyrolyzed at 500 to 550°.

With the fibrous graphite base, 400° was the optimum pyrolysis temperature with respect to the utilization coefficient (75 to 80%), and the electrodes withstood repeated cycling.

1408. **Antonenko, P. A., Gulyamov, Yu. M., and Sagoyan, L. N.**

### Specific Electrical Conductivity of the Active Material of a Nickel Oxide Electrode

*Khim. Tekhnol. (Kharkov).* **1971**, No. 23, 44-51. The specific electrical conductivity of hydrated NiO (β-NiOOH) was determined as it depends on the temperature from -50 to +50° and the content of active O 30 to 70%. The samples were prepared electrochemically from $Ni(OH)_2$ by charge/discharge cycles in solutions of NaOH 20, KOH 20, and LiOH 7.5%. The equations showing the dependence of the specific electrical conductivity on the temperature for various contents of active O and on the content of active O for various temperatures are given. Because of the change of specific electrical conductivity with the change of contact pressure up to ~1050 kg/cm$^2$, the samples were measured at a contact pressure of 1200 kg/cm$^2$.

1409. **Khanin, E. P., and Zendrovskaya, I. V.**

### Thermal-Analysis of Powdered Nickel Hydoroxide and an Active Material for Alkaline Batteries

*Matemat. Nekot. Pril. Metod. Prepodav.* **1972**, 108-12. The thermal effects were determined during wetting of samples containing powdered $Ni(OH)_2$ and an active material for alkaline batteries. The thermogravimetric method was used under constant thermostatic conditions. The correlation between the specific active surface of the positive active material of alkaline batteries and the capacity was observed in a control cycle.

1410. **Tarasov, E. A.**

### Changes in the Porosity of Silver Oxide Electrodes at Various Points of the Charging Curve in Relation to Electrolyte Concentration

*Matemat. Nekot. Pril. Metod. Prepodav.* **1972**, 116-20. The title electrodes were made from a finely divided Ag powder (bulk density 1.3 to 1.5 g/cm$^3$) by pressing on a current-conducting frame at 350 kg/cm$^2$. An examination revealed some changes in the porosity

of electrodes during charging, which depended on the concentration of the electrolyte. The dependence of electrochemical properties of the electrodes on the charging conditions can be approximated by analytical expressions.

1411. **Pozin, Yu. M.**

**Expediency of the Drying Operation in the Production of Sintered Electrodes for Alkaline Batteries**

*Porosh. Met.* **1970**, 10(1), 98-101. The kinetics of the process of porous Ni-plate impregnation with solutions of Ni and Cd salts in the production of electrodes for storage batteries is considered. Data are obtained concerning the change in the sample porosity and the rate of the capillary rise of the solution during repeated impregnation. Because of the poor wetting of the plates by the solutions, it is not expedient to impregnate the dried plates. In this case, the penetration of the salt solution into the pores occurs by means of convection and diffusion, and the wetting conditions have no significant value.

1412. **Kloss, A. I., and Novoselova, V. D.**

**Sources of Carbonate in Sealed Nickel-Cadmium Foil Batteries**

*Sb. Rab. Khim. Istochnikam Toka.* **1969**, No. 4, 49-55. The sources of carbonates in sealed Ni-Cd battery electrolytes are not exhausted by the active materials. Solar oil, a stabilizing additive in Cd electrodes, oxidizes and carbonates the electrolyte. Potential possibilities of this source are as high as 100 to 200 g $K_2CO_3$/1. The Kapron fiber separator is not the source of carbonates. The increase in $K_2CO_3$ content in battery electrolyte from C-supports was insignificant.

1413. **Ten'kovtsev, V. V., Boldin, R. V., Akbulatova, A. D., and Slobodskaya, T. D.**

**Operating Conditions and Service Life of Sealed Average-Size Cadmium Nickel Storage Batteries**

*Sb. Rab. Khim. Istochnikam Toka.* **1969**, No. 4, 56-66. Test results of KNG- and KNGK-type Cd-Ni storage batteries indicated the main reasons for premature capacity loss: recharge, high cycling rate, high final discharge voltage. Operating conditions for preventing this loss are proposed: low cycling rate at a ~70%-charge level, cycling with periodic discharge to low levels, and several successive complete charge/discharge cycles.

1414. Mashevich, M. N., Arkhangel'skaya, Z. P., and Andreeva, G. P.

**Effect of Zincate Solution Aging Inhibitors on the Processes Taking Place During Anodic Polarization of Reticular Zinc Electrode**

*Sb. Rab. Khim. Istochnikam Toka. Nauch.-Issled. Akkumulyatorn. Inst.* **1969**, No. 4, 158-64. The effects of LiOH and $K_2SiO_3$ additives on processes taking place in alkaline zincate electrolytes and on reticular-type Zn electrodes were studied during anodic polarization at various current densities. The effect of the additives on the anodic dissolution kinetics of Zn appeared as a decrease in the secondary process rates. The phase composition and structure of Zn-oxide compounds that formed on the electrodes did not change in the presence of additives. The presence of additives at intense discharge conditions decreased the Zn-electrode capacity. In all cases, only ZnO was observed on the electrode surface during discharge.

1415. Arkhangel'skaya, Z. P., and Frolova, S. P.

**Processes Taking Place During Storage of Charged Silver-Zinc Batteries**

*Sb. Rab. Khim. Istochnikam Toka. Nauch.-Issled. Akkumulyatorn. Inst.* **1969**, No. 4, 165-76. Processes taking place on positive and negative electrodes were studied during storage of Ag-Zn batteries. Capacity loss by positive electrodes at 20.5° was 1 to 3% per month and was caused by gradual dissolution of Ag oxides from the electrode and by the decrease of the degree of oxidation of the active material because of predominant AgO dissolution. The self-discharge of the batteries, determined by gas generation, is 0.63% per month. Actual capacity loss during battery discharges under intense conditions exceeded the capacity loss during the self-discharge; this is explained by structural changes of the active material during storage.

1416. Zhivotinskii, P. B., Bessonova, T. M., Ivanova, N. I., and Lygovtsova, N. A.

**Capillary Properties of Separator Fabrics and Performance of the Fabrics in Sealed Storage Batteries**

*Sb. Rab. Khim. Istochnikam Toka.* **1970**, No. 5, 63-79. The rate of soaking with KOH of separator fabrics from Kapron (polycaprolactam fiber), Khlorin (vinal fiber), and polypropylene) for sealed alkaline storage batteries was investigated. The amount of

electrolyte absorbed by separators dependent on the treatment with surface active substances (KPK-2, (detergent mixture of sulfonaphthenic acids) OP-7, OP-10, and tanning agent no. 4) was determined. The effect of the fabric properites on the capacity and pressure in Cd-Ni sealed batteries was also examined. The necessity was revealed for treating fabrics intended for performance in KOH solutions with solutions of surfactants, of which KPK-2 (3-5 g/l.) was the most efficient. Analysis of the capacity and pressure of gases in sealed batteries indicated that most of the O liberated on charging at the positive electrode passed over to the negative electrode around the separator, so that only a small part penetrated the separator fabric.

**1417. Kloss, A. I., and Novoselova, V. D.**

**Selection of an Electrolyte for Nickel-Cadmium Storage Batteries Operating at Temperatures Below 0°**

*Sb. Rab. Khim. Istochnikam Toka.* **1970**, No. 5, 87-96. The selection was studied of an electrode for Ni-Cd storage batteries intended for operation at below-zero temperatures (e.g., -40°). The electrolytes used, with various densities and based on KOH, contained $K_2CO_3$ and LiOH additions in amounts of 10 g/l. Characteristics of the batteries were determined by using electrolytes with various densities (1.29, 1.37, and 1.45 g/cm$^3$) and various compositions (243-418 g KOH/l + 82-177 g $K_2CO_3$/l). Electrolytes for storage batteries operating at low temperatures should not be selected according to the soly. polytherm in the KOH-$H_2O$ system, but according to soly. isotherms in the system KOH-$H_2CO_3$-$H_2O$. The composition of the electrolyte of the charged battery should correspond to the region of nonsaturated solutions of the soly. isotherm in the given system. This principle should be considered when selecting electrolytes for all batteries using alkaline electrolytes.

**1418. Shapot, M. B., Levenfish, P. G., Levin, N. I., and Kochetova, T. I.**

**Causes of Short Circuits in a Silver-Zinc Storage Battery**

*Sb. Rab. Khim. Istochnikam Toka.* **1970**, No. 5, 124-31. The operations of Ag-Zn storage batteries were analyzed to explain the cause of interelectrode short circuits. The reason for their occurrence was Zn crystal intergrowth through the separator layer during charging on the negative plate. A decrease in zincate concentration near the plate favored this process. A prolonged stability for this type of storage battery can be attained by increasing the supply of ZnO in the negative electrode and by selecting appropriate conditions of charging, limiting the decrease in zincate ion concentration in the catholyte area, and

thereby diminishing the tendency toward intergrowth of Zn dendrites through the separator. Excess ZnO in the negative electrode reduced the rate of accumulation of passive Zn in the electrode, thus prolonging the life of the Ag-Zn storage battery to >120 charging cycles.

**1419. Andreeva, G. P., and Arkhangel'skaya, Z. P.**

**Increase and Stabilization of Silver Electrode Capacity**

*Sb. Rab. Khim. Istochnikam Toka.* **1970**, No. 5, 132-7. The electrochemical behavior was studied of positive electrodes of Ag-Cd and Ag-Zn storage batteries produced by rolling or pressing AgCl onto the shell supplying the current, compared to battery electrodes produced from Ag powder by using the metal-ceramic method. Tests were made on electrodes, 0.5 and 0.8 mm thick, installed in storage batteries of 2.5 Ah capacity at 20°, and at charge/discharge current densities ranging 0.18-1.0 A/cm$^2$. Under defined conditions, AgCl is a more effective starting material for the active material of positive plates of Ag-Cd and AgZn batteries than Ag powder. Compared to metal-ceramic electrodes, the AgCl electrodes are characterized by a longer life (>430 cycles), and, when charged to the 1st potential stage, they are able to maintain a sufficiently stable and high coefficient of utilization (20-5%).

**1420. Lipunova, N. B., and Molotkova, E. N.**

**Storage of Silver-Cadmium Storage Batteries in the Discharged State**

*Sb. Rab. Khim. Istochniham Toka.* **1970**, No. 5, 138-43. The behavior was studied on alkaline Ag-Cd storage batteries after long-term storage at 20, 35, and 50° in a partially discharged state and in a completely discharged state. The storage period lasted $\leqslant$ 4 years. Every 6 months, the electrical characteristics, state, strength properties, and Ag content of the separator-cellulose hydrate, as well as the composition of the electrolyte, were verified. Before storage, the completely discharged batteries remained entirely suitable for operation during storage for $\geqslant$ 4 years at 20°, $\geqslant$ 2 years at 35°, and $\geqslant$ 1.5 years at 50°. The electrical characteristics, state of the separators, and composition of the electrolyte changed only slightly during this period. Storage batteries that were not entirely discharged lost both charge and discharge capacitance during storage, and the state of the separators after storage was much worse; this result was conditioned by the irreversible reaction of dissolution (in the electrolyte) of Ag oxides still present in the storage plates that were only paritally discharged, leading to a decrease in the amount of active material, to deterioration of the separator, and to changes in the electrolyte and in its characteristics. It also reduced the stability of the storage batteries.

1421. **Rozentsveig, S. A., and Gorleva, L. K.**

**Effect of Carbonate on the Behavior of an Alkaline-Battery Cadmium Electrode**

*Sb. Rab. Khim. Istochnikam Toka. Nauch.-Issled. Akkumulyator. Inst.* **1971**, No. 6, 46-9. The behavior of a Cd electrode in an alkaline electrolyte containing carbonate was studied. The emergence of a supplementary lag of potential, 0.2 V more positive than the potential of the basic process during discharging, is caused by the occurrence of the electrochemical process, $Cd \rightarrow CdCO_3$, and is accompanied by a decrease in the useful capacity of the electrode.

1422. **Shuvalova, I. N., and Arkhangel'skaya, Z. P.**

**Silver(II) Oxide Electrode**

*Sb. Rab. Khim. Istochnikam Toka. Nauch.-Issled. Akkumulyator Inst.* **1971**, No. 6, 95-103. Characteristics of the cathodic behavior of dry-charged Ag oxide electrodes prepared directly from AgO were studied. The working capability of electrodes of this type depends essentially on the structural parameters of the source material.

1423. **Molotkova, E. N., and Lipunova, N. B.**

**Processes During Storage of Charged Silver-Cadmium Batteries**

*Sb. Rab. Khim. Istochnikam Toka. Nauch.-Issled. Akkumulyator. Inst.* **1971**, No. 6, 107-17. Data are presented on the change in electical characteristics of batteries and the phase composition of active materials of electrodes, and composition of electrolyte and condition of the hydrate-cellulose separator film in the process of prolonged storage of charged Ag-Cd batteries at 20-50°. Possible mechanisms of self-discharge are considered.

1424. **Leonov, L. I., Chernyshov, V. A., Klyazin, B. S., and Zakharova, E. N.**

**Self-Discharge of Silver-Zinc Batteries Flooded with Electrolyte**

*Sb. Rab. Khim. Istochnikam Toka. Nauch.-Issled. Akkumulyator. Inst.* **1971**, No. 6, 128-34. The self-discharge of Ag-Zn batteries at different temperatures of storage in a flooded

condition was studied, and causes of lowering of their capacitance characteristics were determined. A method of accelerated determination of the safety of batteries is presented.

1425. **Papazova, E. I., Nikol'skii, V. A., Andreeva, G. P., and Berkman, E. A.**

**Efficiency of a Cadmium Electrode in a Silver-Cadmium Battery with Different Degrees of Charge**

*Sb. Rab. Khim. Istochnikam Toka. Nauch.-Issled. Akkumulyator. Inst.* **1972**, No. 6, 134-41. The Cd electrode of Ag-Cd battery was studied at different degrees of charge, and the active material utilization factor was determined as a function of the discharge current. The phase composition of the active material was determined chemically at different stages of cycling, true electrode surface area was determined by low-temperature desorption, and the phase composition and size of the active material single crystals were determined by X-ray analysis.

1426. **Kaminskaya, E. A., Uflyand, N. Yu., and Rozentsveig, S. A.**

**Effect of Lithium on an Alkaline-Battery Nickel-Oxide Electrode**

*Sb. Rab. Khim. Istochnikam Toka. Nauch.-Issled. Akkumulyator. Inst.* **1972**, No. 6, 50-5. The electrochemical behavior, and chemical and phase compositions of Ni-oxide electrodes operating in 5.3*N* KOH without Li and with the addition of LiOH are examined. Properties of electrodes under these conditions are determined by the presence of $KiNiO_2$ in them. Ni-oxide electrodes containing $LiNiO_2$ possess better characteristics at 50°.

1427. **Pozin, Yu. M., Miroshnichenko, A. S., Golub, Yu. S., and Nikol'skii, V. A.**

**Electroless Oxidation of Nickel Oxide Foil Electrodes**

*Sb. Rab. Khim. Istochnikam Toka, Vses, Nauch.-Issled. Akkumulyator. Inst.* **1972**, No. 7, 125-9. Results are given on the oxidation of the NiO-foil electrodes in alkaline KBrO solutions and the effectiveness of oxidation of $Ni(OH)_2$ in the pores of the electrode depending on the amount of oxidizing agent in the solution, concentration of alkalies,

temperature and oxidation, and time. The recommendation was to oxidize the electrodes in a 2.6-3.6*N* KOH solution containing KBrO 20-1 g/l. at 10-25° within 1 hour. The reaction rate was limited by the diffusion of oxidizing agent into the pores of the electrode and sharply decreased with time. The chemical oxidation of the foil electrodes was also possible on an industrial scale.

1428. **Boldin, R. V., Sushentsova, S. N., and Milyutin, N. N.**

**Wettability of the Casing and Electrolyte Leakage in Airtight Nickel-Cadmium Batteries**

*Sb. Rab. Khim. Istochnikam. Toka, Vses. Nauch.-Issled. Akkumulyator. Inst.* **1972**, No. 7, 161-3. The wettability of steel 08KP, used for manufacturing alkaline battery casings, was studied by using alkaline solutions at different metal-surface potentials. Greatest wettability, which determines the increased tendency to the electrolyte flow along the battery casing, was observed during electrical contact of the casing with the negative electrode block, and the least wettability was observed with insulation of the casing from the working electrodes.

1429. **Shuvalova, I. N., Fedorova, T. V., and Arkhangel'skaya, Z. P.**

**Anodic Process on a Silver Oxide Electrode of a Silver-Cadmium Battery**

*Sb. Rab. Khim. Istochnikam Toka. Vses. Nauch.-Issled Akkumulyator. Inst.* **1972**, No. 7, 171-4. This report presents a study of the characteristics of an anodic process on AgO electrodes that were produced by using different grain-size active materials. Under more intensive oxidation of a finely divided active material on the first potential stage, the electrode charge on the second stage occurred at an increased potential and was accompanied by evolution of small amounts of O.

1430. **Shuvalova, I. N., Fedorova, T. V., and Arkhangel'skaya, Z. P.**

**Capacity Decrease of a Silver Oxide Electrode During Long Reversible Operation**

*Sb. Rab. Khim. Istochinikam Toka, Vses. Nauch.-Issled. Akkumulyator. Inst.* **1972**, No. 7, 175-81. This report presents a study of the impairment of the efficiency of AgO

electrodes produced from different active materials (industrial Ag powder, finely divided $Ag_2O$ and Ag powder with $ZrO_2$ additive) under long cycling in Ag-Cd batteries. The decrease of the utilization factor of active materials in proportion to increase of the life of electrodes is associated with impairment of chargeability of the material because of its aggregation. The electrodes made of $Ag_2O$ maintained higher characteristics under long operation of the battery.

1431. **Vorob'ev, G. A., Levina, G. A., and Molotkova, E. N.**

**Reactions on the Cathodes of Charged Silver-Cadmium Batteries During Long-Term Storage**

*Sb. Rab. Khim. Istochnikam Toka, Vses. Nauch.-Issled. Akkumulyator. Inst.* **1972**, No. 7, 181-4. The reactions were considered taking place in charged Ag-Cd batteries during storage up to complete loss of capacity. The self-charging of an Ag electrode took place not only as a result of the decomposition of AgO and dissolution of $Ag_2O$, but also as a result of the reduction of Ag oxides on the electrode under the influence of dissolved decomposition products from a cellulose hydrate layer. This factor caused a complete loss of capacity, even before the appearance of short circuits.

1432. **Ardabatskii, V. P., Ivanov, E. G., and Nikol'skii, V. A.**

**Calculating the Capacity Loss of a Charged Silver-Electrode Storage Battery During Storage and an Accelerated Test of its Storability**

*Sb. Rab. Khim. Istochnikam Toka, Vses. Nauchno-Issled. Akkumulyator Inst.* **1973**, No. 8, 151-60. Abstract not available.

1433. **Kicheev, A. G.**

**Reduction Kinetics of Oxygen on Porous Silver Electrodes in Potassium Hydroxide**

*Tr. Mosk. Energ. Inst.* **1972**, No. 112, 53-8. The behavior of porous O-Ag electrodes is described in 6*N* KOH at O pressure $P = 2$ barometric atmosphere, at 60°, and in the presence of 0-0.3*M* $N_2H_4$. Both the steady-state potential of the electrodes and the reduction currents

of O depended on the logarithm of $N_2H_4$ concentration at low polarization. Taking into account the simultaneity of the cathodic (O reduction) and anodic (oxidation of $N_2H_4$) processes at an electrode, a kinetic equation is proposed, which directly suggested the relations that were found.

**1434. Zorokhovich, A. E., Kozhevnikov, O. A., and Zilitinkevich. A. Ya.**

**Stabilization of Load Voltage During the Buffer Action of an Alkaline Storage Battery with a d.c. Source**

*Tr. Mosk. Inst. Inzh. Zheleznodorozh. Transp.* **1969**, No. 299, 41-6. An assembly for voltage stabilization, by the buffer action of alkaline storage batteries with other d.c. sources, is described. The system was tested with an Ag-Cd battery consisting of two parts with 14 cells in each. The discharge was constant to within 5%. The current efficiency was 0.8 to 0.94. The additional regulators and voltage stabilizers weighed $\leqslant$20% of the weight of the battery.

**1435. Chebakov, V. D., Karev, B. D., and Kukoz, F. I.**

**Preparation of Highly Porous Nickel Substrates for Sintered Electrodes of Storage Batteries**

*Tr. Novocherkassk. Politekh. Inst.* **1970**, 21-3. The substrates were prepared by initially spraying the powder. A powder layer (0.5-mm) was sputtered onto both sides of an Ni foil and sintered at a maximum temperature of 950°. For comparison, the characteristics of the substrates obtained by pressing were investigated. Powders obtained by the sputtering method had a higher porosity (82 versus 71%) but a smaller surface area (633 versus 754 $cm^2/cm^3$). A decrease in the specific capacitance and in the utilization of active material was also observed for the sputtered powders. The consumption of Ni powder/Ah, and of active Ni was half as great as that of a sputtered electrode.

1436. **Milov, V. A., Skalozubov, M. F., Gaivoronskaya, N. P., Dunaeva, T. I., Ereiskaya, G. P., and Osipchuk, N. Yu.**

**Effect of the Charge Time on the Life of a Silver Battery Electrode**

*Nauch. Tr. Novocherkassk. Politekh. Inst.* **1970**, No. 217, 27-31. Results are considered from establishing the dependence of the utilization factor of the Ag-electrode active mass on the number of cycles under various charge times. The utilization factor decreased most sharply during charge of the electrodes by 150% of the theoretical capacity. The electrode, which is chargeable up to the potential of termination of O liberation, maintained a high utilization factor even after a significant number of cycles. The liberation of O resulted in the formation of an additional amount of $Ag_2O$ deep in the grains of the active mass. The plot of the change in utilization factor versus the number of cycles passed through a maximum at 5 to 7 cycles.

1437. **Gaivoronskaya, N. P., Dunaeva, T. I., Ereiskaya, G. P., and Skalozubov, M. F.**

**Reduction of the Capacity of Silver Electrodes Operating in Forced Discharge Systems**

*Tr. Novocherkassk. Politekh. Inst.* **1970**, 217, 31-6. Metal-ceramic porous electrodes were studied in 10*N* KOH. The electrodes were charged with d.c. of current density 5 mA/$cm^2$, and were discharged with 500 mZ/$m^2$ to the potential -0.3 V (versus Hg/HgO electrode). The longer the charging cycles, the lower were the capacity losses as compared to the first cycle. With forced discharges, a marked increase of the electrode surface area was noted. The higher the potential to which charging was achieved and the longer the duration of charging, the higher were the capacities reached at the second anodic stage in which $Ag_2O$ forms AgO, and the more important was the part of active material participating in the oxidation process. To increase and preserve the capacity of the Ag electrode operating in forced-discharge systems, the electrodes should be charged to the potential of the oxidation stage (0.73 to 0.78 V), and, if separation is possible, charging should be allowed at the third anodic stage with O evolution. It is also possible to apply charging once per 10 cycles by using a reduced current density of 2 mA/$cm^2$ and attaining 150 to 200% of the theoretical capacity. In this case, the coefficient of active material utilization increases by 80%.

1438. **Ereiskaya, G. P., Dunaeva, T. I., and Skalozubov, M. F.**

**Effect of the Discharge Temperature on Operational and Structural Characteristics of a Silver Oxide Electrode**

*Nauch. Tr. Novocherkassk. Politekh. Inst.* **1970**, No. 271, 36-41. Tests were conducted on pressed electrodes that are chargeable with a current density of 5 $mA/cm^2$ and dischargeable in a free electrolyte volume (10*N* KOH) by a forced system (500 $mA/cm^2$) at from -10 to +90°. A decrease of the discharge temperature to -10° was accompanied by a sharp decrease in the capacitance of the electrodes. The decrease of the capacitance during cycling is less in the case of discharges conducted at +90° and then at +20°. A radiog. study showed the change of the submicrostructure of reduced Ag on forced discharge systems as compared to the initial, which led to the loss of contact between the particles of the active mass and its nonparticipation in the current-generating processes.

1439. **Ionkin, A. I., and Karavaev, V. M.**

**Erosion of Smooth Silver Anodes by High-Density Direct Current in Potassium-Hydroxide Solutions**

*Tr. Novocherkassk. Politekh. Inst.* **1972**, No. 266, 61-4. Anodic polarization of Ag was carried out in 1.0 to 10.0*N* KOH at 1 to 4 $A/cm^2$ at 25 to 90°. The erosion rate was determined by the electrode weight loss. The erosion rate of Ag increased with increase of KOH concentration and the current density did not depend on the nature of a cation. The curve of the temperature dependence of the erosion rate had a maximum near 70°. Ag is presumed to erode because of the separation of the forming AgO particles by an intensive flow of O being separated.

1440. **Fesenko, L. N., Kudryavtsev, Yu. D., and Makogon, Yu. O.**

**Behavior of Porous Nickel Substrates in Alkaline Solutions During Polarization with Asymmetrical Alternating Current**

*Tr. Novocherkassk. Politekh. Inst.* **1972**, No. 266, 67-72. Polarization with asymmetrical a.c. with cathodic current density, $i_c$, exceeding the anodic current density, $i_a$, e.g., $i_c$ = 1 $A/cm^2$ and $i_a$ = 0.56 $A/cm^2$, is suggested for preparing an active material for alkaline batteries from Ni-cermet-base NiO electrodes.

1441. Shul'gina, G. A.

**Improvement of the Production of Cermet Electrodes for Nickel-Cadmium Storage Batteries**

*Tr. Novocherkassk. Politekh. Inst.* **1972**, No. 266, 96-9. The cermet-electrode matrixes of the Ni-Cd storage batteries were treated with an alkaline solution (after saturation in a salt solution containing active metals), and the effect was determined of the chemical treatment on the $NO_3^-$ and $Cl^-$ content of the electrode. The chemical treatment should begin in solutions at $\leqslant 40°$ to maintain a low content of the above ions, and the temperature should then be increased to obtain a higher degree of conversion of the active metal salts into hydroxides. To obtain the maximum removal of $Cl^-$ from the negative electrodes, the process should be limited to one charge/discharge cycle.

1442. Antonenko, P. A., Barsukov, V. Z., Krapivnyi, N. G., and Sagoyan, L. N.

**Cermet Nickel Oxide Electrode**
**II. Modeling the Electrode Steady State**

*Vop. Khim. Khim. Tekhnol., Respub. Mezhvedom. Temat. Nauch.-Tekh. Sb.* **1972**, No. 25, 18-25. Electrical, mathematical, and physical models of the cermet NiO electrode in the steady state were studied. Steady-state current radial-distribution curves under various performance conditions were calculated. The results may be used to study the dynamics of the charge/discharge processes of the electrode.

1443. Antonenko, P. A., Barsukov, V. Z., Krapivnyi, N. G., and Sagoyan, L. N.

**Cermet Nickel Oxide Electrode**
**III. Modeling of the Discharge Process**

*Vop. Khim. Khim. Tekhnol., Respub. Mezhvedom. Temat. Nauch.-Tekh. Sb.* **1972**, No. 25, 135-41. Dependences of the specific electrical conductivity of the active material of the cermet NiO electrode on the specific degree of discharge at various temperatures were obtained and used to study the electrode discharge dynamics. An algorithm was developed that permits modeling of the discharge process of a cermet electrode by an electronic computer.

1444. **Antonenko, P. A., Barsukov, V. Z., Krapivnyi, N. G., and Sagoyan, L. N.**

**Sintered Nickel Oxide Electrode**
**IV. Effect of Temperature on the Dynamic Characteristics of the Electrode**

*Vop. Khim. Khim. Tekhnol.* **1972**, No. 26, 110-15. Using experimental data on the specific resistivity of the active mass of porous sintered NiO electrodes as a function of the depth of discharge and the algorithm of the dynamic characteristics, the discharge characteristics of the electrode were estimated by means of an electronic computer. The electrodes (80 X 40 X 1.2 mm) were divided into three sections along their thickness and were discharged amilaterally at 10 mA/cm$^2$. The current distribution as a function of discharge time was plotted for -50, +20, and +50°. The consistency of the model was checked experimentally at +20°. Analysis of the current density distribution curves showed that more and more back sections of the electrode were included in the discharge process as it proceeded. The current density distribution in a nearly discharged electrode is uniform and linear. The effect of temperature on the maximum specific discharge capacity and the degree of nonuniformity of discharge is considered and methods for its calculation and experimental evaluation are given. The internal electrode resistance $R$ was studied as a function of the depth of discharge. During discharge, $R$ was increased 2.5 to 3.5 times at $>0°$ and 4 to 8 times at $<0°$.

1445. **Antonenko, P. A., Barsukov, V. Z., Krapivnyi, N. G. and Sagoyan, L. N.**

**Sintered Nickel-Oxide Electrode**
**V. Discharge Efficiency in Depth**

*Vop. Khim. Khim. Tekhnol.* **1972**, No. 26, 115-19. On the basis of the dynamic characteristics of sintered NiO electrodes with geometrical area 32 cm$^2$ and 0.12 cm thick, discharged at 10 mA/cm$^2$, the progress of the discharge process along the electrode thickness was estimated. The criterion of the most efficient thickness is the efficiency of the NiO-Cd cell defined as the ratio of the useful to the total energy of the system. As a first approximation, the energy losses are assumed to be the heat evolved during discharge. The most efficient electrode thickness was determined by the maximum depth along which the discharge process can proceed. In the case $d > d_1$ ($d$ is the electrode thickness and $d_t$ is the limiting electrode thickness), complete discharge at the expense of the energy of the system

was impossible. The calculated values of $d_1$ at constant $\eta$ = 85 and 95% are presented as functions of current density and temperature.

1446. Antonenko, P. A., and Sagoyan, L. N.

**Description of the Process of Impregnating Sintered Nickel Oxide Electrodes for Alkaline Storage Batteries by Experiment-Planning Methods**

*Vop. Khim. Khim. Tekhnol.* **1972**, No. 27, 34-40. The statistical model of the title process was derived. The density, pH, and temperature of the $Ni(NO_3)_2$ solution exert the decisive effect on the process efficiency. Their respective values of 1.71 g/cm$^3$ and 1.5 and 90° were found to be optimum ones. When performed under the optimum conditions, duration of the process was reduced 50%, and electrical characteristics of electrodes obtained were improved by 10 to 5%.

1447. Vyal, L. F., Shuvalova, I. N., Fedorova, T. V., and Arkhangel'skaya, Z. P.

**Scanning Microscope for Studying the Structure of Porous Electrodes of Chemical Current Sources**

*Zavod. Lab.* **1972**, 38 (11), 1366-7. Scanning microscopy showed that the active material of the Ag-oxide electrode consists of fine crystalline aggregates, separated by medium-sized regularly distributed pores. During reversible electrode reactions, the aggregation of the active material and the formation of large deep pores occurs.

1448. Gamaskin, E. I., and Pozin, Yu. M.

**Improvement in the Saturation of Negative, Sintered Metal Electrodes for Nickel-Cadmium Storage Batteries**

*Zh. Prikl. Khim. (Leningrad).* **1970**, 43(3), 681-3. The impregnation of porous Ni plates, the electrodes for alkaline storage batteries, with mixtures of solutions of $CdCl_2$ and $Cd(NO_3)_2$ was studied in the case of cathode polarization. The polarization of the plates was caused by their contact with the Cd anodes. This method of impregnation shortens the time necessary for preparing the electrodes by a factor of 3 to 4 and eliminates the corrosion in Cd solutions.

1449. Arkhangel'skaya, Z. P., and Mashevich, M. N.

**Course of the Secondary Process During the Polarization of Zinc Electrodes with Dense and Porous Active Materials in Alkaline Electrolyte**

*Zh. Prikl. Khim. (Leningrad).* **1970**, 43(6), 1248-55. During the anodic polarization of Zn in a limited electrolyte volume, the change in Zn concentration is governed mainly by the rate of $OH^-$ entry into the reaction zone. Factors that promote supply of $OH^-$ to the electrode surface (higher temperature, forced circulation) lead to an accumulation of zincate complex, which increases the probability of passivation. With electrodes having spongy active material, the secondary process quickly attains a constant rate, ensuring good reliability even under unfavorable conditions. When electrodes with dense Zn deposit are polarized, the conditions of $OH^-$ entry and zincate ion removal from the surface change sharply with the initiation of the secondary process. The differences in processes observed with Zn electrodes containing structurally different active materials are displayed predominantly during intensive discharge. These differences are related to the different conditions of approach and removal of reacting substances in the reaction zone.

1450. Pozin, Yu. M., Gamaskin, E. I., and Vogman, M. Sh.

**Introduction of $Ni^{2+}$ into Negative Sintered Electrodes of Nickel-Cadmium Storage Batteries**

*Zh. Prikl. Khim. (Leningrad).* **1970**, 43(7), 1478-82. Polarization ($\eta$) measurements were made at porous Ni electrodes in neutral and alkaline solutions. In 4.2*M* solutions of $CdCl_2$, $Cd(NO_3)_2$, or mixtures, the anodic and cathodic $\eta$ showed that, in $CdCl_2$, the degree of cathodic control ($C_c$) is 99.8% and anodic control ($C_a$) 0.2%; in solution of $Cd(NO_3)_2$, $C_c$ = 67.6% and $C_a$ = 32.4%; in mixtures, $C_c$ = 93.2% and $C_a$ = 6.8%. $C_c = [(\varphi_{Ni} - \varphi_x)/(\varphi_{Ni} - \varphi_{Cd})] \times 100\%$ and $C_a = [\varphi_x - \varphi_{Cd})/(\varphi_{Ni} - \varphi_{Cd})] \times 100\%$, where $\varphi_{Ni}$ and $\varphi_{Cd}$ are the Ni and Cd potentials without external polarization, and $\varphi_x$ is the electrode potential at maximum corrosion current. Thus, in the first and last instances, the anodic process occurred principally at Cd, and the Ni plate was not dissolved. In $Cd(NO_3)_2$, however, Ni may corrode. Negative Cd plates (for use in Ni-Cd batteries) that were impregnated with $Ni^{2+}$ showed two discharge potentials—the first corresponded to Cd oxidation, the second to Cd oxidation from the Cd-Ni alloy. Only one voltage plateau was observed for negative plates that were not impregnated. Plate capacity was constant at the end of 60 charge/discharge cycles for impregnated plates but had decreased 20% for unimpregnated plates.

1451. Gaivoronskaya, N. P., Dunaeva, T. I., Ereiskaya, G. P., and Skalozubov, M. F.

**Effect of Recharge on the Capacity of the Silver Electrode of an Alkaline Battery Operating Under Forced Discharge Conditions**

*Zh. Prikl. Khim. (Leningrad).* **1971**, 44(12), 2666-9. The longer and more complete the recharge, the lower was the loss in capacity as compared with the first cycle. Thus, electrodes charged to 100% of their capacity retained 70% of their utilization factor after 10 cycles. Electrodes charged to 0.73 to 0.78 V versus an Hg/HgO reference electrode retained 64%, and those charged to 0.65 to 0.70 V versus Hg/HgO reference electrode retained only 56% of their utilization factor. The duration of recharging the utilization coefficient of the electrode mass (a metalloceramic porous Ag electrode). The drop in capacity results from enlargement of the electrode surface, dispersion of the active mass, and the exclusion of particles from the oxidizing process at potentials of the second anodic stage; the first stage proceeds to the oxidation of Ag to $Ag_2O$, the second to AgO, and the third to evolution of O.

1452. Pozin, Uy. M., and Shtertser, N. I.

**Saturation of Nickel Plates in Cadmium and Nickel Salt Solutions Suitable for the Manufacture of Alkaline Storage Cells**
**VII. Anodic Behavior of Nickel Metal in a Nickel Nitrate Solution Containing Chloride Ion Impurities**

*Zh. Prikl. Khim. (Leningrad).* **1972**, 45(8), 1724-8. The anodic behavior of smooth Ni metal in $Ni(NO_3)_2$ solutions containing $Cl^-$ impurities was studied by using a potential scan technique in solutions containing 5.4*M* $Ni(NO_3)_2$, and 0, 0.5, 10, and 40 g/l. of $Cl^-$, at 50° and various pH. The Ni anodic polarization curve depended virtually on pH and the presence of $Cl^-$. In a pure $Ni(NO_3)_2$ solution, Ni had two areas of active dissolution and passivity. In the presence of $Cl^-$, the initial passive area disappeared. Acidifying of the solution facilitated the anodic process and enhanced Ni corrosion. The presence of $Cl^-$ slowed Ni dissolution at the start of investigations, but the decrease in the corrosion rate with time was slower, resulting from a change in the alkaline-nickel salt deposits covering the metal surface. In neutral $Ni(NO_3)_2$ solution, Ni passivity in the potential range 0.9 to 1.3 V was observed only with $Cl^-$ content $\leq$0.5 g/l.

1453. **Mikhalenko, M. G., Perminov, V. I., and Flerov, V. N.**

**Change in the Characteristics of Zinc Electrodes of Alkali-Zinc Storage Batteries During Cyclic Operation**

*Zh. Prikl. Khim. (Leningrad).* **1972**, 45(9), 1953-8. The irreversible decrease in the capacity of Zn electrodes of alkali-Zn batteries after lengthy conditions of discharge was determined by the loss of their active material through diffusion as a zincate into the inner electrode region where the saturated zincate solution was subjected to accelerated aging under the interaction of the positive electrode with the precipitation of the slightly soluble oxide phase. The introduction into the battery of additives (aging retarders, stabilizers of zincate solutions) significantly decreases the loss of active material of the Zn electrodes.

1454. **Andreeva, G. P., Arkhangel'skaya, Z. P., Nikol'skii, V. A., Ivanov, E. G., and Vorob'eva, G. B.**

**Silver Oxide Electrode for an Alkaline Storage Battery**

*Zh. Prikl. Khim. (Leningrad).* **1972**, 45(10), 2333-5. The electrochemical behavior of rolled positive $Ag_2O$ electrodes for alkaline storage batteries during long-term operation in batteries was investigated, as well as the coefficient of active material utilization, $K_u$, and changes in the state of the phase and losses in capacity during storage in a charged state at 50°. The process of gas liberation during charging of the $Ag_2O$ electrodes was also investigated. All measurements were made on $Ag_2O$ electrodes and Ag electrodes produced by the metal-ceramic method. The $Ag_2O$ electrodes, as compared to the metal-ceramic ones, had a higher $K_u$ (by 15 to 20%) and a more stable capacity during long-term operation, and could be more efficiently stored in a charged state. The rate of O liberation during oxidation of Ag electrodes depended on the grain size of the initial active material.

1455. **Shuvalova, I. N., Arkhangel'skaya, Z. P., and Fedorova, T. V.**

**Anodic Process on a Silver(I) Oxide Electrode**

*Zh. Prikl. Khim. (Leningrad).* **1973**, 46(1), 68-71. The anodic process of $Ag_2O$ giving AgO was studied in detail on a $Ag_2O$ electrode. The electrodes used were prepared by rolling $Ag_2O$ powder on an Ag-plated Cu mesh grid. Investigations were made by plotting

galvanostatic and potentiostatic anodic polarization curves in 1, 4.5, and 10*N* KOH at 20°. The structure of AgO obtained as a result of the process was also examined. The oxidation process proceeded through an indirect ionic state in the solution. In view of the lowest limitations during formation and growth of crystals, the most complete and rapid oxidation of $Ag_2O$ was possible in 4.5*N* KOH, as compared to all the other solutions tested.

**1456. Pozin, Yu. M., Terent'ev, N. K.**

**Electrochemical Behavior of Electrodes from Cadmium-Nickel Alloys in Potassium Hydroxide Solutions**

*Zh. Prikl. Khim. (Leningrad).* **1973**, 46(1) 187-91. The electrochemical behavior of metal-ceramic porous negative electrodes from Ni-Cd alloys in KOH solutions was studied. The electrodes were obtained by pressing and sintering at various temperatures (300, 330, 370, 400°), 5, 11, 18, 32, and 50% (weight percent) carbonyl Ni with Cd powder according to the method previously described. The sintered electrodes were examined by chemical and X-ray phase analyses; their electrochemical behavior was studied in 5.5 and 10*N* KOH; and their potentials during anodic polarization and at the end of charging and the overvoltage of the process were determined. Studies on Ni-Cd alloy electrodes containing $Ni_5Cd_{21}$, $Ni_2Cd_5$, and NiCd in KOH solutions indicated that the extent of oxidation of the electrodes during anodic polarization depended on their phase composition, sintering temperature, and the concentration of KOH. The most active electrodes had a high $Ni_5Cd_{21}$ content and were sintered at 300 to 30° in concentrated KOH; the least active Ni-Cd electrodes were sintered at 370 to 400°.

**1457. Tarasov, E. A., Kukoz, F. I., Fateeva, V. N., and Avdeev, N. Ya.**

**Effect of Sintering Conditions on the Porosity of Nickel Substrates for Unlayered Electrodes of Storage Batteries**

*Zh. Prikl. Khim. (Leningrad).* **1973**, 46(2), 303-8. The title conditions were studied with Ni plates prepared by using a paste made from the mixture of 1 kg carbonyl Ni of specific volume 0.49 $cm^3/g$ and 1 kg 4% carboxymethyl cellulose containing 44 g of glycerol. This paste was applied in a 2.2 to 2.3-mm layer on the two sides of a perforated Ni plate, dried at 87°, and sintered for 5 to 240 minutes at 600 to 1000°. The method of forcing out one

liquid (alcohol) by another one (ether) was used for determining the distribution function of the volume of the pores with respect to their effective diameter. An equation was derived for the calculation of the dependence of the specific volume of the pores on the temperature and the duration of the sintering. The optimum sintering temperature was 1000° at 15 minutes.

**1458. Zytner, Ya. D., Maksimyuk, E. A., Nikol'skii, V. A., Alekseeva, N. I., and Berkman, E. A.**

**Effect of Additives on the Anodic Dissolution of Cadmium in a Potassium Hydroxide Solution**

*Zh. Prikl. Khim. (Leningrad).* **1973**, 46(2), 436-8. Additions of 0.1*M* ethylenediamine (I), hexamethylenediamine (II), salicyclic and cinnamic acid, Li benzoate, 2-naphtol, resorcinol, $Ba(OH)_2$, and $AlCl_3$ to the KOH electrolyte (density = 1.23) do not influence the rate of anodic dissolution of Cd because of the strong adsorption of $OH^-$ on the electrode surface. Except for I and II, all additions cause passivation of the electrode. I and II form soluble complexes with Cd and extend the time for initiation of passivation.

**1459. Pozin, Yu. M., and Golub, Yu. S.**

**Formation of Nickel-Cadmium Hermetic Storage Batteries**

*Zh. Prikl. Khim. (Leningrad).* **1973**, 46(2), 453-5. Long-time cathodic polarization of the Ni-oxide electrode of a Ni-Cd hermetic storage battery at the potentials of the evolving of H in the process of the discharge of the battery activates the surface of the Ni and causes electro-reduction of the active mass of the electrode. Some of the electricity at the Ni-oxide electrode following charging is consumed for the ionization of H, for disolution of the Ni, and for oxidation of the active mass. As a result of this process, the degree of the electrical charge at the negative electrode is greater than at the positive electrode.

## OTHER JOURNALS (JAPANESE)

**1500. Takehara, Z., and Yoshizawa, S.**

**Characteristics of Cadmium in Sealed-Type Nickel-Cadmium Battery**

*Denki Kagaku*. **1970**, 38(1), 36-9. Equations giving the relation between the rate of oxidation of Cd in sealed-type Ni Cd batteries and the activity of the Cd electrode are proposed on the basis of the assumption that the reaction between Cd and O proceeds through the formation of local cells between them. The theory agreed satisfactorily with the experimental results.

**1501. Sugita, K., and Okuma, S.**

**Discharge Characteristics of Nickel-Cadmium Batteries Charged at Constant Voltage**

*Denki Kagaku*. **1970**, 38(6), 453-6. The effect of constant-voltage charging on the capacity of Ni-Cd batteries was examined. The batteries used were of pocket-type and sintered-type. The capacity decreased with repetition of the constant-voltage charging and discharging cycles. When the discharge was deeper, the capacity dropped as low as 74%. The voltage drop was 40 to 60% when the charging was made at 1.45 V and only 5% at 1.55 V. The charging at 1.55 V was, however, impractical for a sintered battery because of high current.

**1502. Takehara, Z., Yamasaki, M., and Yoshizawa, S.**

**Problems on the Life of Sealed Nickel-Cadmium Battery**

*Denki Kagaku*. **1970**, 38(12), 917-22. The time change of properties of Cd cathode in sealed Ni-Cd batteries was studied. The activity of Cd as the electrode active material decreased gradually with time. When the electrode was reduced to metallic Cd by full charging, the activity was extremely reduced because of the coalescence of the metallic Cd. The activity of $Cd(OH)_2$, formed by the reaction between metallic Cd and O, was lower than that of $Cd(OH)_2$, formed by the electrolytic oxidation in an Ar atmosphere. The catalytic activity of the pure Cd electrode for the reaction between Cd and O was higher than that of the electrode containing $Ca(OH)_2$.

1503. Iwaki, T., Kanetsuki, K., Hirai, T., and Fukuda, M.

**Sintered-Plate-Type Nickel-Cadmium Alkaline Batteries X. Effects of Additives on the Discharge Performance of Sintered-Plate Alkaline Batteries Charged at Various Rates**

*Denki Kagaku Oyobi Kogyo Butsuri Kagaku.* **1968**, 36(12), 850-7. Attention was focused on improving the capacity decrease upon charging at low rates. The investigation was carried out by applying additives to the electrolyte or positive plates prepared by new thermal decomposition methods. The discharge performance and gas volumes were examined. The discharge performance after charging at various rates and gas volume produced during charge were examined at 20 and 50°. (1) LiOH in the electrolyte: the decreasing degree of discharge capacity was somewhat reduced at 20°, and the difference in the charge potential of the positive plate and its $O_2$ evolution potential was more distinct than without additives. (2) Co and Bi ions on the positive plate: X-ray diffraction analysis suggests that the Co and Bi ions each form a solid solution with NiOH. Improvement in the charging efficiency and retardation of gas evolution at the cathode were also achieved by these ions, but the effect was smaller than with LiOH. (3) Ce ion on the positive plate: the form $CeO_2$ existed on the positive plate after it was subjected to alkaline immersion or electrolyte formation. The effect on the charge efficiency of the positive plate and the state of gas evolution appeared to be much less than in cases 1 or 2.

1504. Iwaki, T., Kanetsuki, K., Hirai, T., and Fukuda, M.

**Sintered-Plate-Type Nickel-Cadmium Alkaline Batteries XI. Discharge Performance of Sintered-Plate-Type Alkaline Batteries at Low Temperatures**

*Denki Kagaku Oyobi Kogyo Butsuri Kagaku.* **1969**, 37(7), 496-504. The effects of the concentration of KOH and of the addition of various additive solutions to the electrolyte on the discharge performance of alkaline batteries with electrodes prepared by new thermal decomposition method were studied at 20 to 40°. With increase of the KOH concentration, the anode potential decreased, but the cathode potential rose slightly at all the temperatures studied. Because the potential change of the anode was larger than that of the cathode, the terminal voltage of the cell decreased with increase of the KOH concentration. The condition of the KOH solution decreased with the lowering of the temperature. The potential drop accompanying this decrease of the condition was responsible for about half of the terminal

voltage drop. The addition of ZnO or CsOH improved the discharge performance of the anode at room temperature and the addition of $SnO_2$ or $Na_2WO_4$ had the same effect at low temperature. In the cathode, the addition of $SnO_2$ or $Na_2WO_4$ improved the discharge performance at room temperature. No additives improved the discharge performance of the cathode at low temperatures.

**1505. Yamas, D., and Ohata, I.**

**Sintered-Type Alkaline Storage Battery**
**XI. Formation of Active Material from the Nickel Plaque**

*Kogyo Kagaku Zasshi.* **1969**, 72(9), 1986-9. The surface layer of porous Ni plaque was changed to active material by repeated reductions and oxidations in KOH solution. The formation of active material increased with increase of KOH concentration and was accelerated by the reduction of Ni plaque. The mechanism for the formation of the active mass was studied by X-ray diffraction, electron diffraction, potential sweep, microscopic observation, and anodic polarization on plaque cathodized in various electrolyte solutions.

**1506. Oda, S., Ito, Z., Mukunoki, J., and Ito, A.**

**Characteristics of Sealed Nickel-Cadmium Rechargeable Battery "Pananica"**

*Nat. Tech. Rep. (Matsushita Elec. Ind. Co., Osaka).* **1970**, 16(2), 238-45. A high quality cylindrical sealed Ni-Cd battery, Pananica, which is capable of high-rate discharge with safety and high reliability, has been developed. Improvement in procedures for making electrodes, as well as in electrode structure, made possible the preparation of Pananica. The characteristics of Pananica, such as high discharge rate and temperature characteristics, are described. Newly developed rapid-charging systems, which can reduce the time required for charging from 16 to 5 hours, are also discussed.

**1507. Kanetsuki, K., Yamaga, M., and Ogawa, H.**

**Hermetically Sealed Nickel-Cadmium Battery for Use in Scientific Satellites**

*Nat. Tech. Rep. (Matsushita Elec. Ind. Co., Osaka).* **1970**, 16(2), 246-56. A hermetically glass-sealed Ni-Cd battery was developed. The cell was of cylindrical type,

25 mm in diameter and 55 mm in overall length. The cell was of the high-discharge-rate type with a sintered positive plate, a pasted negative plate, and an auxiliary electrode.

**1508. Ogawa, H., and Ohira, T.**

**Charge-Discharge Characteristics of Silver Oxide and Alkaline Storage Battery**

*Nat. Tech. Rep. (Matsushita Elec. Ind. Co., Osaka).* **1970**, 16(2), 257-68. The Ag-oxide-Zn alkaline storage battery that is used as a small, lightweight, and highly reliable power-supply unit for sounding rockets is described. Developmental work and a wide variety of performance tests were conducted for this type of battery by studying how conditions like upper cutoff voltage of charger, charging time, ambient temperature discharge rate, operating attitude, standing time after charge, and shock and/or vibration affect its characteristics. This battery can be safely operated for at least 10 cycles under very severe conditions. A power-supply unit was prepared by combining this type of battery and regulator and was used to launch a rocket.

**1509. Yamashita, D., and Yamamoto, Y.**

**Pressed-Type Alkaline Storage Battery**
**VI. Characteristics of Pressed-Type Nickel Positive Electrodes Containing Silver or Silver Oxide**

*Nippon Kagaku Kaishi.* **1974**, (3), 459-63. The effects of the addition of Ag and $Ag_2O$ (5 or 10%) on the characteristics of the positive plate ($Ni(OH)_2$ 50, graphite 35, polyethylene 15%) of a pressed-type Ni-Cd storage battery were studied by measuring the overpotential, the capacity changes with charge/discharge cycles, and the potential-current curves obtained by the potential sweep method. The availability of the active material at the initial cycle increased with the addition of Ag and $Ag_2O$. The increase exceeded 80% when $Ag_2O$ content was 10%. The addition of Ag and $Ag_2O$ decreased the overpotential in charge and discharge processes. The effect of $Ag_2O$ was greater than that of Ag. The capacity of the plates containing 10% $Ag_2O$ increased gradually with charge/discharge cycles, whereas that of the plates containing Ag decreased suddenly and shedding was observed.

## OTHER JOURNALS (GERMAN)

**1600. Drazic, D. M., Vujcic, V., and Rakin, R.**

### Effect of Preparation Conditions on the Capacity of Sintered Nickel Electrodes for Alkaline Storage Cells

*Metalloberflaeche*. **1970**, 24(3), 76-7. The electrode was prepared by admixing 4 g carbonyl Ni with 0 to 25% $H_2C_2O_4$, compressing at 850 kg/cm$^2$, and sintering at 550° in H. The electrode was impregnated with saturated $Ni(NO_3)_2$ solution, dried at 115° for 0.5 hour, and immersed in 4.6*N* KOH for 1 hour at 80° to form $Ni(OH)_2$. At 25°, the capacity of the electrode was 0.17 Ah/g Ni. To demonstrate the dependence of the electrode capacity on the amount of added NiO, a second electrode was prepared by admixing carbonyl Ni with 0 to 100% NiO and sintering at 220° or 300°. Two-thirds of the capacity results from Ni dissolution from the matrix because of corrosion during impregnation, and one-third results from impregnation with $Ni(NO_3)_2$.

**1601. Euler, K. J.**

### Impedance Measurements at Rotating Zinc Electrodes

*Metalloberflaeche*. **1971**, 25(1), 13-15. The frequency dependence of the Zn-electrode impedance has previously been shown to be representable in the resistance plane as a semicircle displaced in the inductive direction. By rotation of one of two coaxial Zn electrodes, the impedance displacement of the center of the local curve is reduced by factors of 1/3 to 1/2 that of ordinary dry cells. Of the four possible causes of the displacement, the influence from the positive electrode and induction can be completely excluded and the influence of diffusion impedance can be largely excluded. The remaining displacement (~20 mohms), corresponding to 5 to 10% electron transfer resistance, can be attributed to crystalline impedance and reaction-impedance.

**1602. Jovanovic, S. M., Rakin, P., and Vojnovic, M. V.**

### Modification of Cellulose-Based Separators by Silver-Zinc Batteries

*Metalloberflaeche*. **1971**, 25(3), 80-4. Measurements of the distribution of Ag and Zn in the individual layers of the multiple-layer separator of an Ag-Zn cell at various phases

of utilization (cycle No.), and knowledge of the degree of polymerization of the separator cellulose leads to the following conclusions: (1) Ag is deposited as the product of oxidative degradation of the cellulose, the soluble Ag compounds reacting principally on the separator layer immediately beside the position electrode. Amounts of Ag on other separators are negligible and are formed by diffusion of colloidal Ag particles from the oxidative degradation; (2) the distribution of the deposited Zn on separator layers is much more uniform, being appreciable even in the layers near the positive electrode; hence, the Zn separation is more important for the "metallization" of the separator than that of Ag; (3) degradation of the separator cellulose involved both alkaline hydrolysis and oxidation by soluble Ag salts; the former is uniform over the layers, but the latter affects only the layer closest to the positive electrode. Degradation of the cellulose during the lifetime of the cell adversely affects the physical and mechanical properties, but not so seriously as to impede its functioning.

**1603. Gossner, K., Eftychiadis, T., and Koerner, D.**

**Anodic Formation of Silver Oxides**
**I. Charging Curves and Covering Layers**

*Z. Naturforsch. A.* **1969**, 24(5), 807-13. Electron diffraction analysis of Ag surfaces galvanostatically oxidized in 0.01*N* NaOH shows the oxide formation sequence $Ag \rightarrow Ag_2O \rightarrow AgO_x \rightarrow AgO$. Potentiostatic experiments gave no oxide at <200 mV versus Standard Calomel Electrode, formation of $Ag_2O$ at 200 to 450 mV, of $AgO_x$ at 360 to 650 mV, and of AgO at 480 to 2000 mV. $Ag_2O_3$ is sometimes found in the region of beginning O evolution.

**1604. Gossner, K., Eftychiadis, T., and Koerner, D.**

**Anodic Formation of Silver Oxides**
**II. Structures and Transformations of the Oxide Phases**

*Z. Naturforsch. A.* **1969**, 24(5), 813-19. Ion etching with Ar at ~5 μamp of oxide films anodically formed at constant potential on Ag shows the absence of mixed oxides. During removal of monoclinic AgO, Ag lines appear after 30 seconds and increase in intensity. Ag lines appear after 12 seconds during removal of $AgO_x$ (face-centered cubic Ag sublattice), and $AgO_x$ lines do not appear after 140 seconds. During removal of cubic $Ag_2O$, Ag lines appear after 9 seconds, and $Ag_2O$ lines do not appear after 120 seconds.

## OTHER JOURNALS (EASTERN EUROPE)

1700. **Vertes, G., Horanyi, G., and Nagy, F.**

### Oxidation on the Nickel Hydroxide Electrode III. Determination of the Oxidation Rate by an Electrochemical Method

*Acta. Chim. (Budapest).* **1972**, 68(3), 217-28 (Eng.). The rate of oxidation of alcohol on an Ni-hydroxide electrode was indirectly determined by a method based on the principle that the reaction rate can be determined from the complete discharge time measured for different currents, the electrode having been discharged at a given rate. The rate of oxidation of EtOH on an Ni-hydroxide electrode is proportional at a given time to the amount of NiOOH present on the electrode.

1701. **Hajdu, L., and Zahoran, J.**

### Hermetically Sealed Silver-Zinc Batteries Operating in the Silver(I) Oxide ($Ag_2O$) Phase

*Acta Tech. (Budapest).* **1974**, 76(1/2), 153-75 (Eng.). Hermetically sealed cells are superior to unsealed cells in that they have a higher storage capacity per unit volume and they are immediately ready for use.

1702. **Vorkapic, I., and Despic, A. R.**

### Zinc Electrode for Primary Batteries with High Specific Power

*Hem. Ind.* **1973**, 27(11), 479-81 (Serbo-Croatian). A porous Zn electrode was obtained by pressing amalgamated electrolytic Zn powder onto an amalgamated copper grid. The Zn was first washed with a saturated $NH_4Cl$ solution. Solid $NH_4Cl$ powder (particle size 40$\mu$) was added, homogenized with the Zn, and pressed onto the Cu grid, and the $NH_4Cl$ was washed out with water. The effects of applied pressure, electrode thickness, amount of $NH_4Cl$, and concentration of NaOH in solution on the polarization characteristics and efficiency of the electrode were studied. This type of electrode could operate well above 100 mA/cm$^2$ with little polarization and with 80% consumption efficiency of Zn.

1703. **Marek, J.**

**Nickel-Cadmium Storage Batteries with Sintered Electrodes**

*Kniznice Odbornych Ved. Spisu Vys. Uceni Tech. Brne B.* **1972**, (Pub. 1973). 32, Pt. 2, 271-8 (Czech). Nickel powder prepared from Ni carbonyl is most suitable for preparing sintered electrodes for Ni-Cd batteries. This powder exhibits a low thermal contraction, a bulk density of 0.5 to 0.6 $g/cm^3$, and a specific surface of 0.5 $m^2/g$. The diameter of pores is ~15 $\mu m$. The impregnation of the negative plate is best done by decomposition of Cd formate at 320 to 350°.

1704. **Hajdu, L., and Zahoran, J.**

**Hermetically Sealed Silver-Zinc Storage Battery Operating in the Silver(I) Oxide ($Ag_2O$) Phase**

*Musz. Tud.* **1973**, 47(3/4), 279-300 (Hung). Harmful gas evolution may occur at the Ag cathode by decomposition of AgO, especially if impurities such as Co, Ni, Zr, Ce, Pd, or W are present. Ag is oxidized to $Ag_2O$ and not to a higher state, this being promoted by addition of 0.8% Pb. The Zn anode, which should not contain impurities $>10^{-3}$%, is amalgamated with 2 to 4% Hg. CdO containing 30 to 40% Ag powder is used as secondary depolarizer. The active materials are applied in excess to avoid overcharging. The separating foil is cellophane that contains no plasticizer. The cells show improved capacity and useful life.

1705. **Olga, M.**

**Hermetically Sealed Alkaline Battery Systems**

*Slaboproudy Obz.* **1968**, 29(1), 17-23 (Czech). A review with 25 references.

## BOOKS AND DISSERTATIONS

1800. **Romanov, V. V.**

**Silver-Zinc Batteries**

(Voenizdat: Moscow). **1969**, 104 pp.

1801. **Gagnon, E. G.**

**Discharge of Porous Silver/Silver Oxide Electrodes in Concentrated Potassium Hydroxide Electrolyte**

(Pennsylvania State Univ., University Park, Pa.). **1970**, 250 pp. (Eng.). Univ. Microfilms, Ann Arbor, Mich., Order No. 71-6304.

1802. **Durando, A. R.**

**Modeling, Identification and Control Optimization of a Satellite Power System**

(Univ. of California, Los Angeles). **1973**, Univ. Microfilms 73-23386.

1803. **Chua, D.**

**Relationship of Electrode Structures and Cell Performance in Sealed Sintered-Type Nickel Cadmium Cells During Cycling**

(Rensselaer Polytechnic Institute, Troy, N.Y.). **1973**, Univ. Microfilms, Ann Arbor, Mich., Order No. 74-12, 781.

## PART V

## INDEX BY AUTHOR

Page
Intentionally
Left Blank

## INDEX BY AUTHOR

*U.S. GOVERNMENT PRINTING OFFICE: 1976 - 735-004/5

*"The aeronautical and space activities of the United States shall be conducted so as to contribute . . . to the expansion of human knowledge of phenomena in the atmosphere and space. The Administration shall provide for the widest practicable and appropriate dissemination of information concerning its activities and the results thereof."*

—NATIONAL AERONAUTICS AND SPACE ACT OF 1958

# NASA SCIENTIFIC AND TECHNICAL PUBLICATIONS

TECHNICAL REPORTS: Scientific and technical information considered important, complete, and a lasting contribution to existing knowledge.

TECHNICAL NOTES: Information less broad in scope but nevertheless of importance as a contribution to existing knowledge.

TECHNICAL MEMORANDUMS: Information receiving limited distribution because of preliminary data, security classification, or other reasons. Also includes conference proceedings with either limited or unlimited distribution.

CONTRACTOR REPORTS: Scientific and technical information generated under a NASA contract or grant and considered an important contribution to existing knowledge.

TECHNICAL TRANSLATIONS: Information published in a foreign language considered to merit NASA distribution in English.

SPECIAL PUBLICATIONS: Information derived from or of value to NASA activities. Publications include final reports of major projects, monographs, data compilations, handbooks, sourcebooks, and special bibliographies.

TECHNOLOGY UTILIZATION PUBLICATIONS: Information on technology used by NASA that may be of particular interest in commercial and other non-aerospace applications. Publications include Tech Briefs, Technology Utilization Reports and Technology Surveys.

***Details on the availability of these publications may be obtained from:***

**SCIENTIFIC AND TECHNICAL INFORMATION OFFICE**

**NATIONAL AERONAUTICS AND SPACE ADMINISTRATION**

**Washington, D.C. 20546**